THE PRIMATE ECTOTYMPANIC TUBE: CORRELATES OF STRUCTURE, FUNCTION, AND DEVELOPMENT

by
Ellen Elise Irwin Fricano

A dissertation submitted to Johns Hopkins University in conformity with the requirements for the degree of Doctor of Philosophy

Baltimore, MD

Submission Date:
October 2018

ABSTRACT

The primate ectotympanic bone form is frequently used in anthropology as a discrete characteristic with strong phylogenetic signaling among primates; however, the proximate mechanism by which this variation operates has not been shown. Some primates (catarrhines and tarsiers) have been described as having an elongate bony ectotympanic tube; others (strepsirrhines and platyrrhines) maintain just a ring of bone. While some functional theories have been suggested, the present dissertation project suggests that the variation in the ectotympanic bones is more likely a morphological response to overall cranial shape.

Structural correlates were identified using geometric morphometric methods in two sets of analyses, one using large intraspecific sample sizes of two catarrhine species and the other looking across all primates. The relative length of the ectotympanic bone in both of these analyses is tested for correlations with overall cranial structure. Two fossil catarrhines are included that have been noted for their unusual ectotympanic bones: *Aegyptopithecus zeuxis* and *Pliopithecus vindobonensis.* This dissertation project also illustrates the growth of the ectotympanic bone in primates via an in-depth discussion of the human, catarrhine, tarsier, and lorisiform growth patterning. This subproject is presented using non-metric analyses and qualitative description.

Across analyses, these three subprojects show that the relative length of the ectotympanic tube is most correlated — and potentially driven by — the width of the cranium relative to the length of the cranium. Relatively wide crania and wide brains tend to present with long ectotympanic bones. Thus, while ectotympanic bone morphology is still useful in descriptions of primate phylogeny, it is more likely that it is a consequence of the shape of the cranium rather than an independent character. The ectotympanic bones of the two fossil species are shown to be abnormally short for catarrhine taxa, more similar to the platyrrhine condition. There is much more diversity in ectotympanic

morphology than previously appreciated, particularly among lorisiforms. Some of that diversity is accounted for in the way in which the ectotympanic develops across taxa; lorisiforms and tarsiiformes are born with fully developed ectotympanic rings that lengthen to variable degrees likely due to relative cranial width.

Dissertation Advisor:

Valerie B. DeLeon, Johns Hopkins University and University of Florida

Dissertation Committee:

Jonathan M. G. Perry, Johns Hopkins University

Mary T. Silcox, University of Toronto

Lauren A. Gonzales, University of South Carolina

Preface

Acknowledgments

I would like to thank my dissertation committee Drs. Valerie DeLeon, Jonathan Perry, Mary Silcox, and Lauren Gonzales. In particular, I want to thank my advisor Valerie who never gave up on me and never let me give up. She is the kind of scientist I have always wanted to be and I would never have made it through this dissertation without her.

I also want to thank Darrin Lunde and Nicole Edmison for access to primates at the NMNH. I would like to thank the KUPRI, the Digital Morphology Museum (DMM) of the Primate Research Institute (PRI) in Kyoto for access to CT scans. Thank you to University of Pennsylvania Museum of Archaeology and Anthropology, the Open Research Scan Archive at Penn, and Drs. Janet Monge and P. Thomas Schoenemann specifically for access to human CT scans. I also thank Dr. Zabiulah Ali, Office of the Chief Medical Examiner Baltimore, for his help accessing juvenile human CT scans. I also want to express my gratitude to all scientists who make their data freely accessible. These databases are an important step towards increasing the scientific impact of and access to data worldwide. In particular I thank Dr. Fred Spoor and the Natural History Museum of Vienna for access to the scans of *Pliopithecus vindobonensis*; thank you to Alan Walker and Timothy Ryan for making their scans available on Morphosource and granting permissions.

I also thank my cohort Kaya Zelazny for her scientific insights, unwavering friendship, and support. Thank you to the rest of my extended academic family, Christopher Ruff, Ken Rose, Dave Weishampel, Gabriel Bever, Adam Sylvester, and Siobhán Cooke for educating me and showing me what it means to be both an anatomist and anthropologist.

Thank you to my family as well for their love and support: Mom, Starla, Devin, and Sharif. Thank you particularly to my husband, John, for always believing in me and pushing me to go after what I want even when things get hard.

Table of Contents

LIST OF FIGURES

List of Tables

1. Introduction

The characteristics of the ectotympanic bone have been used as a phylogenetic indicator in small and large-scale studies of primate evolution over the last century (e.g., Gregory, 1920; Zapfe, 1958, 1960; Hershkovitz, 1974; Delson and Rosenberger, 1980; MacPhee and Cartmill, 1986; Szalay et al., 1987; Simons et al., 2007) but researchers still do not understand the proximate mechanism behind the described variation in the ectotympanic bone. In the fields of anthropology and paleobiology, the ectotympanic bony tube is usually coded as either present or absent to estimate the phylogenetic relationships of extinct and extant primates; meaning that the ectotympanic bone exists as either a bony ring (absent) or elongates into a tube (present) (e.g., Shoshani et al., 1996; Seiffert et al., 2009). Because the ectotympanic bone length appears to hold phylogenetic significance, it is used as a trait in reconstructing phylogenetic affinities of fossil forms (Zapfe, 1958; Rosenberger, 1985). However, while it is known that some primates ossify long ectotympanic tubes and others retain the ring, it is not known what causes this difference. This trait appears to be more-or-less bimodal in extant taxa, with very few fossils and no extant examples of so called “intermediate” ectotympanic morphologies. Several hypotheses are proposed here for this shift based on the current literature, evolutionary histories, and cranial shapes. The present dissertation will describe and analyze ectotympanic bone morphology variation across primates and place it in the context of greater cranial variation.

Literature is reviewed in this first chapter to provide a clear picture of the current understanding of the primate ectotympanic bone, highlighting the questions that still must be answered. The general anatomy of the primate auditory complex is detailed and terminology is defined. Next, the evolutionary history of the ectotympanic bone is explored by placing primate anatomy within the context of the mammalian tree. The

within-primate variation is then described as it is currently understood among strepsirrhines and haplorhines. Haplorhine ectotympanic bone morphology is of particular interest because the auditory structure arrangement was key to building some of the original phylogenies of primates and thus the interpretations of the ectotympanic bone were long debated in this taxon. The ectotympanic bone form is often cited in establishing fossil affinities for many fossil taxa, some of which are discussed here including *Aegyptopithecus, Pliopithecus, Pliobates,* and *Saadanius*.

The adult primate ectotympanic bone, as with all anatomy, is in actuality the result of many forces acting on it. Some of those potential forces are explored here, including developmental patterning, function, and structure. The study of developmental programs provides insight into evolutionary processes, especially in that the ontogenesis of a characteristic provides evidence for the primitive versus derived states and lends relative certainty to anatomical descriptions. Ontogeny can be used to understand how and why the ectotympanic bone varies among primates.

When describing anatomical variation, it is important to consider the functional implications. While the function of the external ear tube is well understood (the collection of sound waves for transmission to the middle ear, inner ear, and eventually the brain) the functional differences between a mostly bone or mostly cartilage ear tube are still something of a mystery. Some functional hypotheses are discussed here; however, functional signals will not be directly tested in this dissertation.

This dissertation argues that cranial structure correlates with relative length of the ectotympanic bone. “Structural correlates” refers broadly to the way in which the ectotympanic bone is interacting with surrounding structures. Given that the ectotympanic bone does not exist in a vacuum, it is possible and likely that cranial structure and potentially brain structure are affecting ectotympanic bone morphology in dynamic ways. For example, the bony tube could be a structural response to expansion

of brain volume relative to the auditory capsule, and bone provides a more stable channel, which is only critical beyond a given distance between the tympanic membrane and the external environment. Thus, as the brain expands, the increase in cranial base width could induce the ectotympanic tube to lengthen and ossify. This dissertation argues that ossification is a by-product of other processes in the skull, like brain growth. Structural correlates are identified and discussed in the following chapters using geometric morphometrics.

Literature Review

The bony ectotympanic tube is thought to be a derived characteristic of catarrhines and tarsiers, whereas platyrrhines and strepsirrhines maintain only a bony ectotympanic ring paired with a cartilaginous tube (Piveteau, 1957; Saban, 1963; Fleagle, 2013). This interpretation underestimates the complexity contained in this single, small bone. Within the anthropoid clade, the earliest fossils display a mix of morphologies in which some fossils have an ectotympanic tube, some have an ectotympanic ring, and some fossil taxa have been described as exhibiting an intermediate condition (Zapfe, 1960; Begun, 2002; Simons et al., 2007). The present dissertation elucidates the functional, spatial, and developmental factors associated with the ectotympanic bone among primates, and the current chapter will provide a detailed review of the literature.

Anatomy

The ectotympanic bone forms one part of the mammalian ear, all of which is contained within and/or supported by the temporal bone (Warwick et al., 1973). The temporal bone as it is seen in humans and many primates is comprised of three individual bones, squamous (plate-like bone that forms part of the lateral neurocranium),

petrous (rock-like portion that contributes to the cranial base), and tympanic (the ectotympanic bone). The primate ear also consists of three parts (external, middle, and inner) that are partly contained within the petrous portion of the temporal bone. The ectotympanic ring marks the division between the external and middle ear.

The external ear spans from the pinna to the tympanic membrane supported by the ectotympanic bone. The pinna, a roughly conch shaped, cartilaginous structure, funnels sound waves from the external environment to the ear canal. The ear canal transmits sound waves, collected at the pinna, to the middle ear beginning at the tympanic membrane. The inferior catarrhine ear canal is composed of ectotympanic bone and auricular cartilage; the ear canals of many other primates have contributions from the petrosal bone and/or the squamous. The tissues that contribute to the ear canal vary significantly among primates; it may be composed of soft tissues (most mammals) or be mostly bony derived from the ectotympanic bone (catarrhines and tarsiers). Among catarrhines and tarsiers, the ectotympanic bone elongates and consequently, the ear canal is largely bony. Such an arrangement means that the ear canal is derived from the petrous portion of the temporal bone superiorly, and the ectotympanic bone inferiorly. The lateral-most bony landmark of the external ear in all taxa is referred to as either the *external auditory meatus* or *external acoustic meatus* (EAM). Auricular cartilage then provides support and bridges the gap between the pinna and the EAM. At the medial end of the ear canal lies the tympanic membrane, surrounded and supported by the ectotympanic bone in all mammals, variably called the tympanicum or tympanic.

Once sound waves have been collected by the pinna and have traversed the ear canal, they will hit the medial boundary of the external ear, the tympanic membrane. The middle ear is mostly an open space enclosed within the petrous part of the temporal bone that is bounded by the tympanic membrane laterally, the inner ear medially, the tegmen tympani superiorly, and the pharyngotympanic tube anteroinferiorly. The

tympanic membrane, or the eardrum, is a sheet of circular thin, membranous tissue that vibrates with specific noise frequencies. Spanning the middle ear and stretching between the tympanic membrane and the inner ear are three small bones or ossicles: the malleus, incus, and stapes. The tympanic membrane receives sound waves from the ear canal, the malleus of the middle ear is tightly adhered to the deep surface of the tympanic membrane and then oscillates with that given frequency. The other ear ossicles (the incus and stapes) are connected in a chain to the malleus with tough synovial joints that allow for very little movement between bones, thus the ossicles tend to act as a single unit transferring vibrations to the inner ear. The function of these ossicles is to compensate for the impedance mismatch between air and the fluid in the inner ear (Zwislocki, 1965; Coleman and Ross, 2004).

The inner ear, the sensory center of the ear, houses the vestibulocochlear nerve, a special sensory nerve that consists of two divisions that relay auditory and angular acceleration information back to the brain. The vestibular division consists of semicircular canals, three fluid-filled, interconnected canals within the temporal bone. These canals contain a fluid-filled, membranous duct, which as the position of the head changes the fluid inside the membranous duct lags behind, bending specialized hair cells in the ampulla that elicit signals to the brain about head and neck position. In the auditory division, the cochlear nerve, as the name implies, sits in a bony cavity in the temporal bone that is shaped as a cochlea (Latin, ‘snail shell or screw’) that is nearly entirely encased in bone. Like the vestibular system, the cochlea consists of a bony encasement containing a fluid known as perilymph and within that sits the membranous ducts that contain endolymph. Vibrations transmitted through the ear ossicles enter the inner ear via the oval window, one of two openings in the bony encasement of the cochlea. At this point vibrations are converted into pressure waves in the fluid filled inner ear, the pressure waves ruffle the membranes of the cochlea which alters the positional

relationships of the hairs in the hair cells sitting on the basilar membrane. The deflection of these hairs sets up an action potential in the cochlear nerve and that is transmitted to the hearing center in the brain. Auditory processing is a complex process and mammals have unique adaptations to optimize this system, particularly in the external and middle ear.

Evolutionary Origins of the Ectotympanic Bone

Mammals and non-mammals possess an inner ear for the processing of auditory information from the external environment. Mammals, however, have developed the middle ear structures as an adaptation for increased conduction and amplification of vibrations (Turner, 1990). The external and middle ear structures are homologous with several bones in the non-mammalian jaw; importantly, the mammalian ectotympanic bone is derived from the angular bone (Figure 1.1). The transition between the non-mammalian and mammalian conditions is relatively well-understood as there is a robust fossil record supporting this interpretation. The fossil group from which mammals evolved, cynodonts, possessed an array of ear and jaw morphologies. The most advanced species' dentary bone became larger and the angular bone develops a "reflected lamina" which appears to have supported a membrane that was used to detect vibrations similar to the tympanic membrane (Klaauw, 1931; Allin, 1986; Allin and Hopson, 1992; Maier and Ruf, 2016a). The early stages of ectotympanic bone evolution can be seen in the fossil record; the beginnings of the reflected lamina of the angular can be seen in the angular concavity on the dentary in taxa such as *Sinoconodon*, *Morganucodon*, and *Hadrocodium* (Luo et al., 2016).

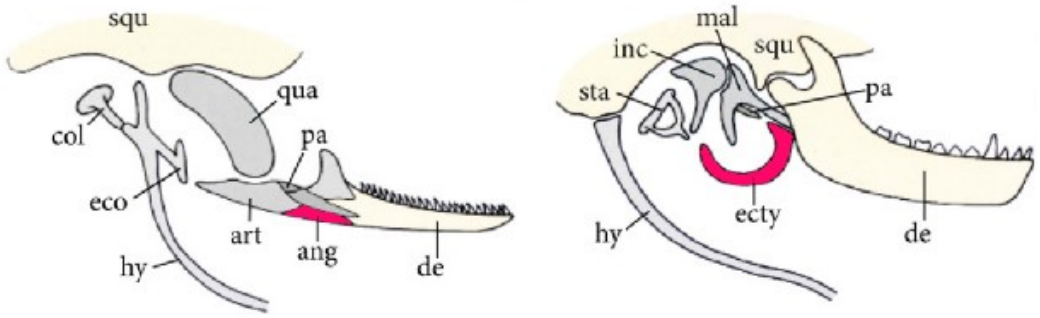

Figure 1.1: Generalized mammalian ear evolution adapted from Maier and Ruf (2016). Left shows the theorized ancestral state and right shows the mammalian ear morphology. The angular (ang) and ectotympanic (ecty) bones are homologous and are highlighted in pink. The quadrate (qua) and the articular (art) have evolved into the incus and malleus respectively in mammals. In mammals, the jaw is formed solely of the dentary bone. Other abbreviations: col=columella, squ=squamous, eco= extracolumella, hy=hyoid, art=articular, qua=quadrate, pa= processus ascendens palatoquadrati, de=dentary, mal=malleus, inc=incus, sta=stapes.

All extant mammals possess an ear canal with some contribution from the ectotympanic bone (Maier and Ruf, 2016a). In many therian mammals, the ectotympanic bone is encased in the entotympanic bone. The entotympanic comprises at least some of the auditory bulla in most mammals (Xenarthra, Macroscelidea, Hyracoidea, Pholidota, Carnivora, Perissodactyla, Chiroptera, Dermoptera, and Scandentia) (Maier, 2013). The degree to which the entotympanic bone contributes to the bulla varies; the Dermopteran bulla, for example, has only a small contribution from the entotympanic bone (Wible, 1993; Wible and Martin, 1993). An auditory bulla is a balloon of bone that in many mammals is derived from entotympanic bone (a neomorphic component of the cranial base in mammals) but it is derived from petrosal bone in extant primates. Though there has been some debate on this subject, extant primates do not possess an entotympanic bone, exhibiting instead a fully petrosal bulla (MacPhee, 1979). Other mammals that lack the entotympanic include Glires, Cetartiodactyla, and Eulipotyphla (Maier, 2013; Maier and Ruf, 2016b). Interestingly, some species in these taxa, particularly Glires and Cetartiodactyla have been shown to have relatively expanded

ectotympanic bones that contribute to the bulla (Figure 1.2; Meng et al., 2003; Maier and Ruf, 2016b).

Figure 1.2: Adult rabbit skull with ectotympanic highlighted.

Extant primates exhibit a mosaic of conditions in auditory anatomy. The extant primate bulla is petrosal derived and varies greatly in size and form; in general, it is relatively the largest in Lemuriformes where it encompasses the middle ear and some of the ear canal. The bulla is smaller and encompasses only the middle ear in Lorisiformes and higher primate taxa. Thus, the ectotympanic bone may be intra-bullar (aphaneric) or extra-bullar (phaneric) (Cartmill and MacPhee, 1980; MacPhee et al., 1988). This differentiation has received a great deal of attention in anthropological literature and is key to the present dissertation. MacPhee (1977) examined some of the ontogenetic factors that lead to the differentiation of the intra-bullar versus extra-bullar ectotympanic condition, finding key factors to be:

> "(1) the growth and positioning of the bony elements involved in the relationship, i.e., the ectotympanic and the petrosal plate; (2) the effects of the pneumatization of the middle ear on the petrosal bone and its outgrowths; and (3) the differentiation and fate of the soft tissues intervening between the petrosal plate and the ectotympanic. Other, extrinsic factors - such as the expansion of the neurocranium - may well have indirect effects" (MacPhee, 1977, p.252)

MacPhee's interpretation indicates that the factors that affect the intra- or extra-bullar condition are largely structural. Other researchers have proposed that the size of the auditory bulla may be a functional adaptation; i.e., the bulla serves as a resonating chamber that amplifies sounds, and may be larger in primates that rely heavily on auditory predation methods (Packer and Sarmiento, 1984; Lombard and Hetherington, 1993). The inflated auditory bullae lead to large middle ear volumes, which have been suggested to be an adaptation to maximize low-frequency hearing (Fleischer, 1978).

The ancestral condition of the ectotympanic bone and its relationship to the bulla may have been similar to the lemuriform, lorisiform, or tarsiiform conditions. In estimating the ancestral condition of any characteristic, an appropriate out-group must first be established. Many living mammals exhibit an entotympanic derived auditory bulla and a mostly detached ectotympanic bone, including Scandentia which has in previous years been used as the sister group to primates (e.g., Martin, 1990; Novacek, 1992). Despite the fact that the bulla is entotympanic derived the scandentian form is very lemur-like in nature with a mostly detached ectotympanic ring within a bulla. However, the living sister group to primates based on the most recent molecular data sets is Dermoptera (Perelman et al., 2011). Among dermopterans, the majority of the bulla is derived from the ectotympanic bone and the bone is elongated, similar to the modern tarsier (Wible and Martin, 1993). Turning to the extinct relatives of primates, some Plesiadapidiformes demonstrate a lemur-like condition while the majority exhibits a tubular EAM with a fused ectotympanic bone. Non-microsyopid plesiadapiforms generally have a tubular EAM, though differentiating the bones that contribute to that structure is difficult without developmental evidence; it is possible that the tubular EAM in these animals is partially or completely ectotympanic-derived (Bloch and Silcox, 2001). The earliest euprimates exhibit a myriad of morphotypes ranging from tubular (some omomyids, e.g., *Necrolemur*) to ring-like (e.g., Adapids) (See Phylogeny: Primate, Haplorhine).

Phylogeny: Primate

Among extant primates, two character states are often cited for the ectotympanic bone - either a mostly bony ectotympanic tube with a small cartilaginous tube or a mostly cartilaginous tube and an ectotympanic ring (e.g., Shoshani et al., 1996; Seiffert et al., 2009) . These may be further broken down into five morphotypes (Figure 1.3, two catarrhines are shown here: an Old World Monkey and Human).

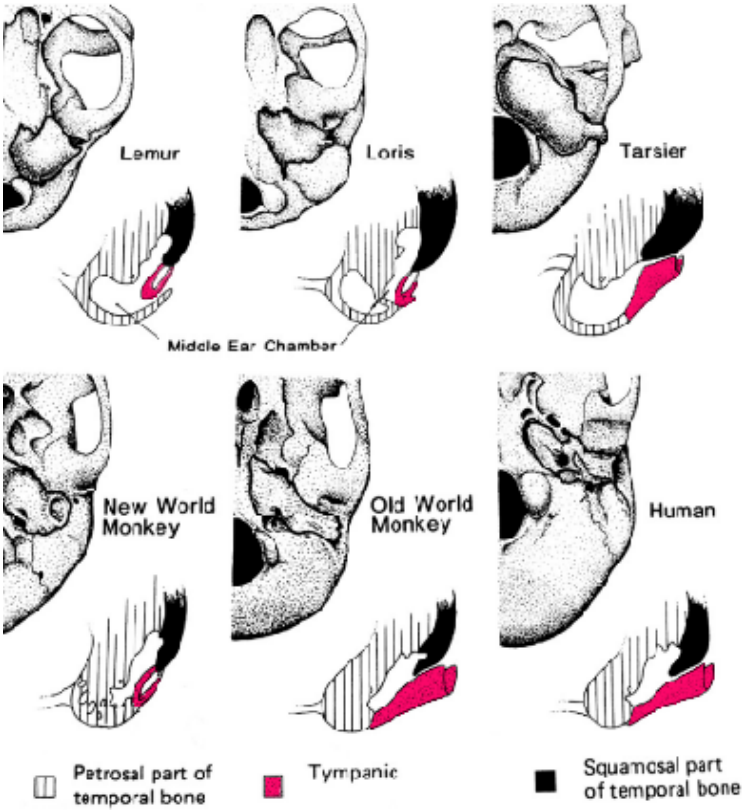

Figure 1.3: Ectotympanic ring and tube morphology. The ectotympanic (tympanic) is highlighted in pink. Adapted from Fleagle (2013). There are two examples of ectotympanic bone morphology for the catarrhine morphotype, listed as “Old World Monkey” and “Human”. Note the length of the bony tube in tarsiers is illustrated as relatively longer than the loris and shorter than the catarrhine.

Strepsirrhine

The lemur character state is the most similar to the generalized mammalian anatomy but the establishment of an ancestral state for this characteristic is complicated.

The lemuriform morphotype is a freely floating ectotympanic ring within an auditory bulla, which is derived from the petrosal bone. Among lorisiforms, the ectotympanic ring is shifted laterally relative to the otic capsule and it juxtaposes with the lateral side of the petrosal bulla. Most illustrations and discussions of the modern lorisiform condition tend to show a single-origin ear canal for lorisiforms (see Figure 1.3). Some researchers have noted potential variation in the arrangement of the lorisiform ectotympanic, arguing that the ear canal of lorisiform primates may include contributions from the other portions of the temporal bone, i.e., the petrous (the bulla), and the post-glenoid process (Saban, 1963; Conroy, 1980). Other key differences between the lorisiform and lemuriform cranial anatomy include: a reduced tympanic region (middle ear) among lorisiforms, rearrangement of vascular circulation, and relative orbit size (Piveteau, 1957).

Haplorhine

Similar to the lorisiforms, the tarsier ectotympanic ring is fused to the lateral margin of the dorsoventrally reduced auditory bulla. Although the tarsier ectotympanic tube is elongated relative to what is observed in the lemuriforms or lorisiforms, it is wider and shorter than the catarrhine tube (see Figure 1.3). The derived condition of the ectotympanic bone of the tarsier has historically been a source of complication in the primate phylogenetic tree, before DNA confirmed the phyletic affiliation of tarsiers and anthropoids (platyrrhines and catarrhines) (Packer and Sarmiento, 1984; Simons and Rasmussen, 1989; Kay et al., 1994). Hershkovitz (1974) described the tarsier ectotympanic bone as an intermediate condition between platyrrhine and catarrhine morphotypes. The platyrrhine ectotympanic bone is very short; it is a thin ring fused to a small bulla. The platyrrhine ectotympanic bone is sometimes described as “ragged”, the lateral margin of the bone is often bumpy where the catarrhine EAM is smooth (Simons et al., 2007). Finally, the catarrhine ectotympanic bone is extremely elongated, the

longest in the primate tree (Saban, 1963). The catarrhine ectotympanic tube occupies much of the width of the cranial base, reaching and fusing to the squamous portion of the temporal bone.

The bony ectotympanic ring and tube have been used as a clear phylogenetic marker. All extant strepsirrhines maintain an ectotympanic ring, similar to the majority of mammals though notably not Dermoptera, with auricular cartilage supporting much of the external ear. The evolution of the character gets a murkier among haplorhines; catarrhines and tarsiers possess a bony ectotympanic tube, but platyrrhines retain a bony ring. Thus, the bony ectotympanic tube might have evolved only once: at the split between haplorhines and strepsirrhines, and then platyrrhines subsequently reverted to the ancestral condition (Cartmill and Kay, 1978; Cartmill et al., 1981) . Another possibility is that the bony ectotympanic tube emerged convergently in both the catarrhines and tarsiers due to either direct or indirect selection on this trait (Packer and Sarmiento, 1984; Szalay et al., 1987).

The ectotympanic bone, as it relates to the origin of haplorhines/anthropoids, has been a topic of some interest for many years (Delson and Rosenberger, 1980; Rosenberger and Szalay, 1980; Cartmill et al., 1981; Packer and Sarmiento, 1984; Kay et al., 1994). Several models of anthropoid evolution exist, hinging on the relative positions of the Eocene fossils of omomyids and adapids, the earliest true primates. Omomyids and adapids each demonstrate a mosaic of characteristics; both have a postorbital bar, digits with nails, and large brains relative to their body sizes as compared to non-primates (Gingerich, 1981; Rasmussen, 1986). There are some significant morphological differences between omomyids and adapids, though; most importantly for the present study, some omomyids (e.g., *Necrolemur*) possess a tubular ectotympanic bone similar to the modern tarsier and others retain a ring (Conroy, 1980; Beard et al., 1991). The question remains, given this diversity in form among the earliest primates,

which arrangement is ancestral? Most mammals, including Scandentia, tend toward a free ectotympanic bone, but the apparent similarities between Dermopterans, *Necrolemur*, and the modern tarsier cannot be discounted.

Due to their similarities to the modern tarsier, omomyids are sometimes considered to be “tarsiiform” fossil primates and share many unique apomorphies aligning them with the modern *Tarsius* (Szalay, 1977; Kay et al., 1994). Both *Necrolemur* and *Rooneyia* are described as having tubular ectotympanic bones, with relatively inflated auditory bullae (Simons, 1961; Packer and Sarmiento, 1984; Rosenberger, 1985). When *Necrolemur* was first described, Hürzeler (1948) interpreted the ectotympanic bone to look more like a lemur; he claimed that they had a free annular ectotympanic bone like that of an extant lemur or adapid. Later correction by Simons (1961) showed that the ectotympanic bone is fused to the lateral bulla and more tarsiiform in nature. *Rooneyia viejaensis* is a highly debated fossil that has been described by various authors as stem strepsirrhine, stem tarsiiform, or stem anthropoid; recent evidence by Kirk et al. (2014) align *Rooneyia* with the haplorhine clade. In the auditory region, Kirk et al. confirmed that the tympanic cavity consists of a single large middle ear space that is undivided by major septa, similar to lemuriforms. However, they note that the ectotympanic is fully fused to the lateral bullar wall but could not delimit the extent to which the ectotympanic bone contributes to the EAM. These early primate fossils remain of great interest to anthropologists in an effort to clarify the root of the primate tree, but auditory structures of fossils at the platyrrhine-catarrhine split have received comparatively little attention.

Platyrrhine-Catarrhine Split

Some of the earliest probable catarrhines, Propliopithecoidea, are mixed in the presentation of the bony ectotympanic tube. Propliopithecoids are extinct (30-35 Ma,

North Africa) primates, thought to be stem catarrhines (Figure 1.4; Harrison, 2005). One propliopithecoid, *Aegyptopithecus zeuxis*, exhibits a suite of primitive catarrhine characteristics, including: a dental formula of 2.1.2.3, canine and cranial sexual dimorphism, small orbits (likely diurnal), big cranial crests, and bilophodont molars (Simons et al., 2007). Interestingly, whereas *Aegyptopithecus* is described as having a bony ectotympanic tube, the tube is described as unusually short (Simons, 1972; Begun, 2002). Simons et al. (2007) describe a slightly elongated ectotympanic bone with a platyrrhine-like ragged lateral margin; the ragged nature is more marked on the dorsal side where it is protected from breakage. They extend this to say that in all three known *Aegyptopithecus* crania that preserve the relevant anatomy the ventral ectotympanic bone is short and beaded or lumpy in nature but extends dorsally into a tympanic process, which suggests to those authors that the bony tubular ectotympanic started to form but did not completely ossify. Thus *Aegyptopithecus* may have an "intermediate" character state, between the crown platyrrhine and crown catarrhine conditions (Zapfe, 1960; Simons et al., 2007).

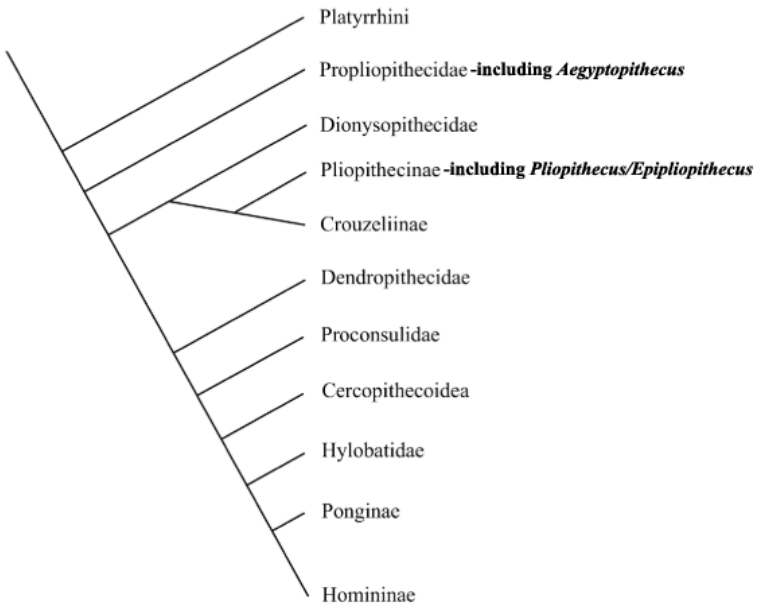

Figure 1.4: Catarrhine phylogeny adapted from Harrison (2005) with fossil taxa highlighted that are included in the present study. Both *Aegyptopithecus* and *Pliopithecus* are stem catarrhines.

Aegyptopithecus is comparatively well understood because of the rich fossil record of Fayum propliopithecoids. Many of these fossils are remarkably preserved and this density of fossil data has allowed researchers to make inferences about the degree of sexual dimorphism likely present in these animals. In an analysis of a subadult *Aegyptopithecus*, Simons et al. (2007) described pronounced craniodental, brain size, and body size sexual dimorphism among *A. zeuxis*. The best-preserved specimen, CGM 85785, is much smaller than other accepted specimens of *Aegyptopithecus*, and it is most likely a female rather than a representative of a new species. Simons and colleagues further posit that the degree of dental variation within the *A. zeuxis* cluster is more similar than neighboring well-established single species assemblages and the dental variation is most pronounced in the canine and third premolars which are areas known to exhibit a high degree of sexual dimorphism among catarrhines specifically. CGM 85785 is approximately 70% the size of another specimen, CGM 40237. CGM 40237 itself was already on the small end of the fossils described as male *A. zeuxis*.

Further, a probable female cranium of the same species, DPC 5401, exhibits intermediate facial proportions between CGM 40237 and CGM 85785. This type of extreme sexual dimorphism is seen in many lineages of catarrhines and may in fact provide support for the supposition that *A. zeuxis* is a stem catarrhine (Kelley and Xu, 1991; Kelley and Plavcan, 1998).

Much more recently in the fossil record, one pliopithecoid primate (7-17 Ma, Eurasia) has also been described as "intermediate" in the condition of the ectotympanic tube (Harrison, 2005; Seiffert et al., 2010). Pliopithecoids at large have mixed presentation of primitive and derived features; for example, they retain relatively narrow molars and incisors but look fairly ape-like in their body proportions and functional adaptations, so their position in the primate tree has been problematic. These "ape-like" adaptations refer to a suite of characteristics that include adaptations for suspensory locomotion and a more orthograde body plan which have long been associated with crown hominoids (e.g., Keith, 1903, 1923). Pliopithecoids in general have been reported to have the modern catarrhine morphology of a fully developed ectotympanic tube, e.g., proconsulids and dendropithecids (Harrison, 2005). Interestingly, the relatively well known genus *Pliopithecus* has been described as having an incompletely ossified ectotympanic tube (Zapfe, 1960; Andrews et al., 1996; Begun, 2002). Arguably, the best known of these pliopithecoids is *Pliopithecus (Epipliopithecus) vindobonensis*. *P. vindobonensis* has a classic example of an intermediate ectotympanic tube. Zapfe (1960), who originally described the fossil, described it as retaining the morphology of very young catarrhines noting the short ectotympanic bone.

A third fossil that has been noted for its relatively intermediate ectotympanic tube length is *Pliobates cataloniae*. *P. cataloniae*, a Miocene small-bodied ape discovered in Europe, dated to approximately 11.6 Ma. Images of *P. cataloniae* show an ectotympanic bone without a ragged lateral margin, but with developed anterior and posterior crura

and a deep V-shaped tympanic plate (Alba et al., 2015). Similar to the *A. zeuxis* and *P. vindobonensis,* Alba et al. (2015) describe a “tubular ectotympanic [that] is short and incompletely ossified—i.e., less developed than in *Saadanius* and extant crown catarrhines” (p. aab2625-6). *Saadanius* is described as having a tubular ectotympanic bone (Zalmout et al., 2010). Images provided by Zalmout et al. (2010) show a full tube that is narrow in the anterior-posterior direction as expected for an advanced stem catarrhine. Zalmout further describes the ectotympanic tube as both “short” and “complete”. Without a better understanding of the catarrhine ectotympanic tube and within-taxon variation, it is impossible to say whether the two fossils examined in the present dissertation, *A. zeuxis* and *P. vindobonensis*, fall into or outside of the range of catarrhine variation.

Development of the Ectotympanic Tube

One way to gain an understanding of these types of fossils is to look at the developmental programs of extant species, following the theories of evolutionary developmental biology. Even before Darwin's (1859) *Origin of Species*, scientists have noted the apparent relationship between ontogeny and phylogeny. Through the study of embryology, it is apparent that species look similarly early in development and then diverge to produce the variety of life seen in adulthood. German biologist Ernst Haeckel, following the work of Charles Darwin, wrote “ontogenesis is the short and fast recapitulation of phylogenesis, controlled through the physiological functions of inheritance (reproduction) and adaptation (nutrition)” (Haeckel, 1866, p.300). While the field of evolutionary developmental biology has evolved quite a bit, particularly with the advent of the study of genetics and more study of the earliest developmental stages (Kalinka et al., 2010), it remains true that through the study of embryology and ontogeny we can inform the study of extinct and extant species.

As stated previously, the ectotympanic bone is homologous to the angular bone among non-mammals (see Figure 1.1) (Allin and Hopson, 1992; Gilbert, 2000). From a developmental perspective, the ectotympanic bone fuses to the petrous and thus it is deeply embedded in growth processes that occur across the cranial base. As Haeckel stated, development can be a key to unpacking some of these cases of complicated morphological variation. The head overall is formed via mixed origin mesenchymal tissues, surrounding the developing brain. The vertebrate brain is an ectoderm-derived rostral enlargement of the neural tube. As the neural plate closes off dorsally to form the neural tube, loose neural crest cells are released. Neural crest cells (NCC) then migrate ventrally, and they will form much of the developing facial bones via the growth of the pharyngeal arches. Pharyngeal arches are bars of tissue that arise lateral to the presumptive foregut of the chordate that reach ventrally and eventually join at in the ventral midline of the embryo. Each arch is largely composed of loosely organized mesoderm-derived mesenchyme surrounding a core of NCCs; arches are lined internally with endoderm and externally with ectoderm. The sensory portion of the ear is formed very early in embryological development as a thickening of ectoderm on the external surface of the embryo, the otic placode. The otic placode migrates deep into the embryo's head, and will give rise to the inner ear and the vestibulocochlear nerve (Sai and Ladher, 2015).

There are five pharyngeal arches in the human embryo, two of which contribute significantly to the cranial base and auditory complex (Larsen et al., 1993). Many bones of the face are derived from the NCCs contained within the first arch: maxilla, zygomatic, squamous temporal, palatine, vomer, mandible, malleus, incus, and the ectotympanic bones. Two portions of the temporal bone are derived from the first arch, but from different prominences within this arch: the squamous is derived from the maxillary prominence and the ectotympanic is derived from the mandibular prominence. The

second pharyngeal arch gives rise to Reichert's cartilage, from which several bony elements arise including the stapes, styloid process, and portions of the hyoid. NCCs within the second pharyngeal arch give rise to much of the petrous portion of the temporal bone. The space between the first two pharyngeal arches is called the first pharyngeal cleft externally and the first pharyngeal pouch internally.

The presumptive ear forms at the first pharyngeal cleft and pouch. The first pharyngeal pouch gives rise to the middle ear and pharyngotympanic tube. The ear canal is derived from the first pharyngeal cleft. Through development, the first pouch and the first cleft expand toward one another, where they will eventually appose. At the intersection of the first cleft and pouch, the tympanic membrane forms and eventually is surrounded by the ectotympanic ring. The ectotympanic detaches from the future mandible and arches backward to form a ring within which the tympanic membrane resides (Lombard and Bolt, 1979). Lateral to the tympanic membrane is the ear canal, which early in development is a cartilaginous tube that contains contributions from the mesoderm of both the first and second pharyngeal arches. The plates of cartilage surrounding and supporting the ear canal are likely formed via mixed contributions of Meckel's and Reichert's cartilage internally and extensions of the developing pinna externally (Rodríguez-Vázquez et al., 2006; Rodriguez-Vazquez et al., 2011). The pinna is also formed from contributions of the first two pharyngeal arches. Six mesoderm derived outgrowths of the first two pharyngeal arches, or hillocks, expand and merge to form the pinna.

The temporal bone, which contributes to the auditory system among other things, is formed through a combination of endochondral and intramembranous ossification, with 21 separate ossification centers in humans (Scheuer and Black, 2000). The squamous, petrous, and tympanic bones that comprise the human temporal bone are derived from the pharyngeal arches and NCCs. The squamous bone (the plate-like bone

that makes up part of the lateral neurocranium, including the zygomatic process) is formed via intramembranous or membranous ossification. Intramembranous ossification involves the direct secretion of bone matrix by osteoblasts and subsequent mineralization (Kawasaki and Richtsmeier, 2017). Similarly the tympanic bone (ectotympanic bone) forms as intramembranous bone (Shapiro and Robinson, 1981; Sperber, 1989). Conversely, the petrous region is an endochondrally-ossified bone. Endochondral ossification involves the ossification of a cartilaginous morphogenic model. Ossification of the petrous part begins by surrounding the soft tissues of the cochlea and labyrinth of the inner ear. The bone surrounding the inner ear structures does not undergo remodeling, meaning the bone first formed in utero does not grow or change through post-natal development (Bast, 1930; Anson and Donaldson, 1981; Spoor, 1993).

Due to the developmental and evolutionary origin of the ear ossicles and ectotympanic tube, the positions of these structures are relatively constrained. The ear ossicles form a chain to allow transmission of sound waves from the tympanic membrane to the inner ear, and the ectotympanic cartilage or bone has to span the gap from the pinna externally to the tympanic membrane. Thus, the ectotympanic position in the cranium is possibly constrained by the relative positions of the middle ear and the pinna of the ear. It cannot just be displaced laterally during growth; it must connect the ear ossicles to the outside with either bone or cartilage.

Postnatal growth

The postnatal development of the ectotympanic tube in humans is relatively well understood (Weaver, 1979; Reinhard and Rösing, 1985; Ars, 1989) but has not been thoroughly described in other species of catarrhines. At birth, humans have an ectotympanic ring that later lengthens into a tube. Among humans, the ectotympanic ring

develops anterior and posterior crura at the superior aspect of the ectotympanic ring where it is adhered to the petrous portion of the temporal bone. In the first year of life, the anterior and posterior crura hypertrophy into anterior and posterior tympanic tubercles that enlarge and grow inferiorly and laterally (Figure 1.5). In humans, the anterior and posterior tubercles enlarge until they fuse in the inferior midline of the presumptive external auditory meatus, creating a second opening, the foramen of Huschke (Reinhard and Rösing, 1985; Ars, 1989). The foramen of Huschke fills in and largely closes and completes growth by five years of age (Krogman, 1932; Wunderly and Wood-Jones, 1933; Laughlin and Jørgensen, 1956; Anderson, 1960; Hashimoto et al., 2011; Rezaian et al., 2015; See also Figure 5.3 for full age sequence).

Figure 1.5: The postnatal development of the human ectotympanic tube. Pink circles are highlighting the anterior and posterior crura (elongating into tubercles). Figure adapted from Weaver (1979). A. a bony ring, B. anterior and posterior tubercles had begun to lengthen; C. tubercles had begun to stretch inferiorly.

Postnatal development of the ectotympanic bone in other primates is less well understood. Hershkovitz (1974) described the development of the ectotympanic tube across primates. In his experience, he found “considerable variation in size, shape, orientation and degree of fusion of the crural ends of the tympanic annulus in platyrrhine monkeys” (Hershkovitz, 1974, p. 239). Additionally, Hershkovitz described the morphological variation of tarsiers; he measured the degree of ectotympanic development among tarsiers using the degree of fusion with the squamosal portion of

the temporal bone as an indication of relative ectotympanic bone length. He found that in seven of the 17 skulls he studied, the ectotympanic tube failed to fuse to the squamosal. He interpreted this to mean that ectotympanic development varies significantly among tarsiers. Hershkovitz's methodology was particularly compelling as it allowed for the interpretation of ectotympanic bone length relative to the rest of the cranium. Many studies previously had proposed that the ectotympanic bone in tarsiers was "elongate" but Hershkovitz was the first to test the within-tarsier variation. The postnatal development of the ectotympanic bone in lemuriforms and lorisiforms is assumed to be relatively static as the ring does not lengthen in any significant way (MacPhee, 1981).

Length of the ectotympanic bone, however, is only one of the ways that the ear canal can vary through development. MacPhee (1981) suggested that the orientation of the ear canal may also vary through ontogeny. He remarked on the ear canal in lemuriforms and lorisiforms, stating that the ear canal rotates during ontogeny, becoming increasingly divergent from the transverse (horizontal) plane through the basicranium. Given the early development of the ectotympanic bone in all species, this rotation is referring to its orientation relative to surrounding structures and is likely describing processes external to the auditory complex. Expanding on this idea, this means if a vector were placed through the center of the cartilaginous ectotympanic tube and a second vector were placed representing the axial plane, the angle between those vectors changes through ontogeny and to different degrees across primates (Forster, 1925; MacPhee, 1981). MacPhee describes the mechanism of this rotation as due to "rotation of the otic capsule, growth of the roof of the tympanic cavity, and the expansion of the petrosal plate" (MacPhee, 1981 p. 78). What he refers to here as the "petrosal plate" is the outgrowth of the petrosal bone that forms all or part of the auditory bulla (Szalay, 1972). How the degree of rotation of the ectotympanic tube varies with phylogeny across primates has not been shown.

Spoor (1997) showed that the orientation of the petrous bone varies among hominids in complex ways that are tightly linked to brain size. He showed that among hominids that large brain sizes are correlated coronally-oreinted petrous pyramids, likely associated with the flexion of the cranial base. Humans were shown to have a less coronally-oriented petrous than would be expected and the author posits that it is possible that that modern humans reach a biological maximum and constraints on the architecture of the cranial base keeps the petrous from rotating further. The consequences of this rotation on the ectotympanic tube length and orientation are not known, but given the articulation of these two bones the angle of the petrous and basicranial flexion likely affect the ectotympanic bone in some way. Although Terhune et al. (2007) do not directly discuss the orientation of the ectotympanic tube, they do mention variation in the orientation of both the external auditory meatus and tympanic membrane within the species *Homo erectus*. This study compared potential differences in the cranial shape of Asian and African *Homo erectus* and only examined adults, but the results do allude to the presence of population-based or species-based differences in ectotympanic orientation in hominins. Some researchers note variation in the tympanic plate among hominins, citing the potential relationship between tympanic plate horizontality and brain size (Walker and Leakey, 1988). The present study will help to address this general issue.

Functional Correlates

Although the function of the ear canal is relatively well-understood (collection of sound waves), the advantages and disadvantages of ossification of (or part of) the ear tube are not. While this study will not directly test the functional implications of the ectotympanic bone, they are discussed here. There are several intriguing possibilities when considering functional correlations and selective pressures on the ectotympanic

bone including; 1) the bony tube may be an adaptation to specialize in specific target sound frequencies; 2) long cartilaginous tubes may be associated with ear mobility; 3) a bony tube may dampen the noise produced intracranially during mastication (Packer and Sarmiento, 1984).

It has been shown that the material properties of the tympanic membrane affect the quality of the sound that is conducted through the ear (Kobrak, 1948). Kobrak, however, did not test the material properties of the outer ear (skin overlying either bone or cartilage), and it is as yet unclear whether the medium of the ear canal could potentially affect the sound quality received by the tympanic membrane. It is possible that the mostly bony ectotympanic tube of catarrhines is better suited to hearing specific frequencies and the evolution of the bony tube could be an adaptation that arises from selective pressures related to hearing. Most data on auditory function are absolute thresholds: the highest and the lowest frequency detectable by an animal (Harris, 1943; Stebbins, 1975; Lonsbury-Martin and Martin, 1981; Jackson et al., 1999; Heffner, 2004).

Coleman (2009) performed a meta-analysis of audiograms for all primates that had them, and produced bivariate graphs that show absolute auditory thresholds plotted against frequency for 29 different primate species and concluded that auditory function is largely phylogenetically constrained. Coleman (2007) showed that anthropoids are more specialized for lower frequency hearing than strepsirrhines even when controlling for body mass. More recently, Ramsier (2010) collected auditory function data using an auditory brainstem response (ABR) method; she found that there is a significant relationship between sociality, as measured by average group size, and auditory function. Sociality was found to explain a significant proportion of the variance associated with auditory sensitivity, particularly to high frequencies. Ramsier et al. (2012) also found that, in many species, interaural distance was not significantly correlated with auditory function. Interaural distance refers to the distance between

ectotympanic rings, thus it does not take into account either cartilaginous or bony ectotympanic tube length but does capture one measure of cranial base width. Further work by Ramsier et al. (2012b) indicates that the Philippine tarsier (*Tarsius syrichta*) can both send and receive very high pitch signals, reaching to ultrasound frequencies. Thus, according to current literature, auditory function is largely phylogenetically constrained with some effect of sociality, and the patterns of ectotympanic ossification also fall along phylogenetic lines.

In theory, a bony ectotympanic tube could restrict movement, and a highly mobile ear might require a longer cartilaginous tube to allow for movement of the pinna. Highly mobile ears are especially beneficial for primates that hunt flying or fast-moving insects and thus are associated with several ecological factors including nocturnality, dental characteristics, and bite force (Napier and Napier, 1967). Pinna size has been shown to correlate with auditory function in primates and other mammals (Coleman, 2007; Coleman and Colbert, 2010), and pinna musculature tends to decrease in relative size with an increase in overall body size in haplorhines (Heffner, 2004; Coleman and Colbert, 2010). Notably, haplorhines do not frequently move their ears (Waller et al., 2008). There are some inherent problems with this hypothesis despite the documented differences between strepsirrhine and haplorhine pinna mobility. It has not been previously suggested that the catarrhine pinna is significantly less mobile than the platyrrhine pinna. Never the less, even the catarrhines with fully bony ectotympanic tubes maintain some cartilage lateral to the bony EAM (Figure 1.6). It is likely that the amount of cartilage varies within and between primate taxa, though this has not been specifically shown. If a functional signal associated with pinna mobility exists, it may be captured in the length of the cartilaginous portion of the ear canal.

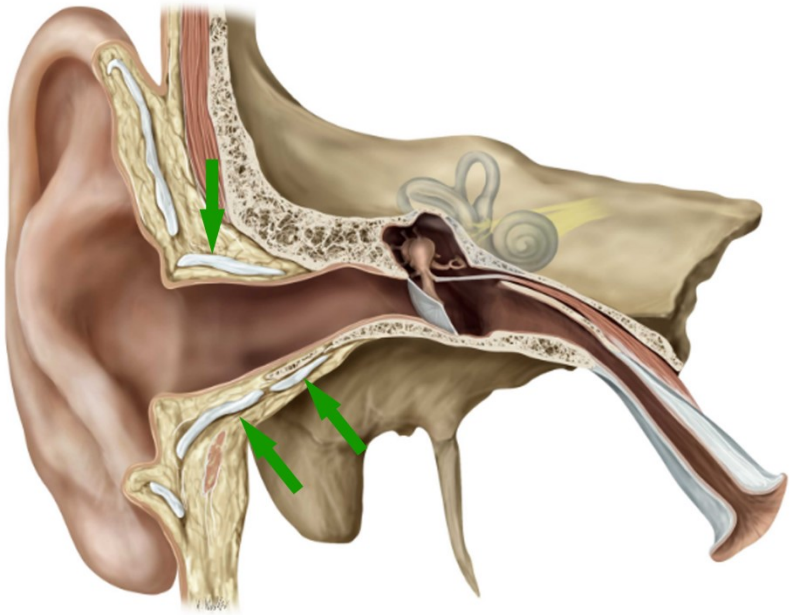

Figure 1.6: Coronal slice through the human ectotympanic tube, green arrows indicate the plates of cartilage surrounding the external ear tube. Image from Thieme Teaching Assistant (Gilroy and MacPherson, 2016). Among catarrhines, cartilaginous plates that support the remainder of the ear canal lie lateral to the bony external auditory meatus ear canal.

The final functional hypothesis to consider is that the bony ectotympanic tube may reduce intracranial noise during mastication (Packer and Sarmiento, 1984). If this last hypothesis were true, then one would expect the longest, thickest, or densest ectotympanic tube to be found among species that are extremely durophagous and/or produce a particularly powerful bite force. The most cited and well understood signal of durophagy is enamel thickness and it has not been suggested that the primates with the thickest enamel tend to have longer or thicker ectotympanic bones (Dumont, 1995; Lambert et al., 2004; Vogel et al., 2008; McGraw et al., 2012; Pampush et al., 2013). The insectivorous tarsier has never been documented to have a particularly powerful bite-force or exhibit durophagous behaviors (Perry et al., 2011). This hypothesis is

unlikely an explanation for all ectotympanic tube diversity but may contribute to the issue and further study is necessary.

Structural Correlates

It is important to consider that the ectotympanic bone is only one part of a larger system. Developmental processes that are interwoven, like the ones seen in the temporal bone, will produce patterns of covariation that persist into adulthood, a process referred to as "developmental integration." Modularity and integration, referring to the patterns of variation and covariation within and between characteristics, have been a topic of great interest in morphological studies for more than 20 years (Smith, 1996; Olson and Miller, 1999; Mitteroecker and Bookstein, 2008). More specifically, integration refers to the fact that developmentally or functionally linked characteristics are more likely to vary in similar ways often because of their proximity; because two elements have to "fit together," they must change size, shape, or orientation in a congruent way. Smith (1996) defines developmental integration as "integration that arises out of the association of events by morphogenic processes, such as regulatory genes, system-wide growth factors or hormones, or epigenetic interactions" (Smith, 1996, p. 70). Hallgrimsson et al. (2009) more simply define integration as the "tendency of a developmental system to produce covariation." Integration is often considered in a "presence/absence" way, but in reality, it exists as a continuum. In contrast, distinct functional units, or modules, can be relatively independent of each other, meaning that they vary more easily without affecting one another. Many studies have shown integration of cranial shape characteristics during primate development and evolution (e.g., Ross and Ravosa, 1993; Cheverud, 1996; Lieberman et al., 2000a, b; Marroig and Cheverud, 2001; Strait, 2001; Bookstein et al., 2003; Ackermann 2002; Bastir and Rosas 2005, 2006; Gunz and Harvati 2007; Mitterocker and Bookstein 2007, DeLeon and

Richtsmeier, 2009; Richtsmeier et al., 2009). Patterns of integration within single bones have also been demonstrated (Grabowski et al., 2011).

This dissertation proposes that ectotympanic bone morphology may be affected by many other characteristics that are under more demonstrable evolutionary selection e.g., overall brain size, regional brain scaling relationships, masticatory systems, and pneumatization of the mastoid region. Generalized encephalization is a well-documented trend across the primate tree and is largely attributed to either social (e.g., Dunbar, 1998; Marino and Marino, 2002) or ecological (e.g., Milton, 1988, 2006; Allen and Kay, 2012) selective pressures. In general, catarrhines — especially apes— have absolutely and relatively larger brains than other primates (Clutton-Brock and Harvey, 1980; Byrne and Whiten, 1989; Dunbar, 1998; Fish and Lockwood, 2003; Milton, 2006; Allen and Kay, 2012). Overall brain morphology is reflected in the endocast, or the impressions left on the internal surface of the cranium, and soft tissues have been shown to have an effect on overall skull morphology (Smith, 1928; Weidenreich, 1941; Edinger, 1948; Allen, 2014). It is possible that as the brain expands and the space between the inner ear and pinna grows, the ectotympanic bone lengthens accordingly. Another possibility is that the ectotympanic bone is lengthening with specific regions of the brain that are expanding relative to others. This type of scaling variability by brain region has been shown to exist among primates (e.g., Holloway, 1992; Semendeferi et al., 1997; Rilling and Insel, 1999; Preuss, 2000). Directly superior to the ectotympanic bone is the temporal lobe of the brain, housed in the middle cranial fossa. Therefore, it is possible that the size of the lateral brain regions (e.g., the temporal lobe) causes the middle cranial fossa to expand laterally, and that is what causes the ectotympanic bone to lengthen rather than total brain or endocranial volume.

More complicated are the potential effects of the masticatory system and pneumatization of the mastoid region on external ear morphology. Immediately anterior

to the ectotympanic bone sits the glenoid fossa and the temporomandibular joint. The spatial relationship of the auditory system and the masticatory system creates the potential need for coordinated responses to keep both systems functioning successfully, and this intimate relationship provides theoretical support for the functional correlate previously discussed, that the ectotympanic bone length may be adaptive to protect the ear from intracranial noise during mastication. Many species of primates possess a post-glenoid process that functionally divides the two regions, though this process varies greatly in its size (both total and relative size) (Lockwood et al., 2002; Terhune, 2009). Terhune (2009), however, found a distinct allometric signal in the relative size of the post-glenoid tubercle, noting that smaller taxa have small post-glenoid processes and larger bodied platyrrhines have relatively large post-glenoid processes.

This intimate relationship between the TMJ and ear canal is not the only way that the auditory and masticatory systems are potentially interacting; no muscles directly attach to the ectotympanic bone, but masticatory muscles surround it. The proximal insertion of the temporalis muscle is on the bony surface immediately superior to the EAM. Therefore, though the temporalis is not attached to the ectotympanic bone, the overall size and organization of the masticatory system has the ability to affect the lateral extension of the superior ear canal, which in turn may place pressure on the ectotympanic bone to lengthen to meet the superior boundary. Inferior to the ectotympanic bone lays neck musculature. The posterior belly of the digastric and the stylohyoid muscles glide immediately inferior and posterior to the ectotympanic tube among humans and other catarrhines.

The final potential structural influence on the anatomy of the ear canal is pneumatization of the mastoid region of the temporal bone. Among certain primates, particularly apes, the mastoid region expands and pneumatizes where musculature attaches (in humans these include the sternocleidomastoid, splenius capitis, longissimus

capitis, the digastric muscle, posterior auricularis, and occipitalis). The degree to which the mastoid process pneumatizes varies quite a bit from minimal (strepsirrhines) to profound (apes) (Himalstein, 1959; Saban, 1964; MacPhee, 1981; Kimbel, 1986; Sherwood and Ward, 1989). Relative position of elements and all of these spatial constraints and relationships have the potential to affect ectotympanic bone morphology. **This dissertation proposes that the lateral expansion of the brain relative to the auditory capsule is associated with lengthening of the bony ectotympanic tube, and that relative length of the ectotympanic tube correlates with displacement of the squamosal (including mastoid and zygomatic arch) relative to the auditory capsule.**

Conclusion

The following dissertation examines the inter- and intraspecific variation in the primate ectotympanic bone both in adults and juveniles using a combination of geometric morphometric methods, regression and correlation analyses, and qualitative descriptions. Chapter 3 examines the within-taxon variation in two samples of primates: humans and macaques. This chapter is designed to test for cranial structural correlates, consistent with the *structural hypothesis*: that the shape of the cranium as a whole, and specifically those shape variables associated with relative cranial width, correlate with the relative length of the ectotympanic tube.

Chapter 4 elaborates on findings in Chapter 3 and applies geometric morphometric methods to analyze a wider range of primates. This chapter includes a broad sample of adult primates including strepsirrhines and haplorhines. The structural hypotheses tested in Chapter 3 are applied across all primates. This chapter also includes discussion and analysis of ectotympanic bone morphology of *A. zeuxis* and *P.*

vindobonensis. This chapter is designed to corroborate or reject the inference that these fossils have “intermediate” ectotympanic bone lengths.

Finally, Chapter 5 illustrates and describes the developmental patterning of the ectotympanic bones in several taxa including catarrhines, tarsiers, and lorisiforms. Juveniles of several species of primates analyzed in Chapters 3 and 4 are illustrated and discussed in their developmental patterning. This chapter also includes a re-examination of human ectotympanic growth using a modern sample and 3D imaging to provide updated information and standards of ectotympanic human growth. Several species of non-human catarrhine ectotympanic growth is documented and compared to the relatively well-understood growth of the human ectotympanic tube. Lorisiform and tarsier ectotympanic bone development are discussed and readdressed in particular detail. The bony origins of the external auditory meatus of several species are also described and revisited in this chapter.

Chapter 6 will provide a summary of all the findings and suggest some avenues for future studies. In addition, it demonstrates that the ectotympanic bone has more nuance and research potential than previously thought. This dissertation provides insight into how and potentially why the ectotympanic bone lengthens through development and across taxa. The results presented have wide-reaching implications. Using these methods to quantify ectotympanic bone variation provides a deeper understanding of an important phylogenetic character and has implications for fossil taxon interpretation. Additionally, it expands the knowledge of the growth and development of the ectotympanic bone and places it in the context of broader evolution, which may inform clinical interpretations of pharyngeal arch deficits such as Treacher-Collins Syndrome.

2. Methods and Error Study

Structural correlates are identified and analyzed in the present dissertation using geometric morphometrics. Geometric morphometrics (GM) is a common suite of methods used when attempting to describe and compare biological shapes because it allows for the comparison of shapes while reducing the effects of size, scale, and rotation. To perform this statistical method, first “homologous” landmarks are placed on all specimens (Zelditch et al., 2012). Homology is determined using phylogeny, development, and previous literature. Landmarks may be Type I, II, or III. Type I landmarks are locations where tissues are juxtaposed such as where cranial sutures intersect (e.g., bregma); Type II landmarks are at geometric maxima that are determined using the points of greatest curvature or biological maxima (e.g., gonion); Type III landmarks are determined only in reference to other landmarks and/or biological extremes (e.g., euryon) (Bookstein, 1997). Each type has some level of error, however Type I are expected to be most reliable and Type III the least.

Traditional landmarks work well for the cranium in general as there are many discrete foramina and sutures; the ectotympanic tube, however, has very few traditional landmarks available. To include the important shape variation within the tube and its orientation, a series of constructed semi-landmarks were collected. Collection of semi-landmarks is a method of mathematically determining new landmarks in a region that does not contain the types of morphologies that lend themselves to more traditional GM methodologies (Bookstein, 1997; Andresen and Nielsen, 2001). A modified version of the method employed by Squyres and DeLeon (2015) was applied to the ectotympanic tube in this study. In that paper, the researchers were analyzing the clavicle, which similarly lacks homologous landmarks. They placed two rows of semi-landmarks along the ventral and dorsal limits of the clavicle. Control points were placed at the medial and

lateral extremities of the clavicle and a plane was aligned to pass through control points at either end. New evenly spaced planes were constructed, orthogonal to the guiding plane and semi-landmarks were placed at the centroid of those sections and the most dorsal and most ventral points. This method allows repeatable landmarks to be placed along the shaft of a mostly featureless, tubular bone. A similar method is employed in the present dissertation, giving the ectotympanic tube many more potential landmarks.

Both traditional and semi-landmarks, are recorded as a series of X, Y, and Z coordinates which are subjected to full Procrustes superimposition. Procrustes superimposition standardizes the position, rotation, and scale of the specimen using generalized least squares regression? (Rohlf and Slice, 1990). The new shape coordinates? are projected into tangent space by orthogonal projection (Dryden and Mardia, 1998). There has been much debate surrounding the benefits of using full or partial Procrustes fits, the partial Procrustes was favored for many years as it is very effective at ridding the data of allometric effects and sets all centroid sizes to a value of one. A full Procrustes fit was employed here as it is more resistant to the effects of large amounts of size variation (e.g., the difference between a mouse lemur and mountain gorilla) and has been noted to be slightly more robust to the effect of outliers (Klingenberg, 2011). Procrustes superimposition produces a new set of shape variables or adjusted coordinates that can then be subjected to a number of multivariate and univariate analyses (Rohlf, 1990). If it is suspected that there is some interesting allometric component to the shape variation, size can be reintroduced by adding the logarithmically transformed centroid size as a variable allowing for the analysis of size and shape as well as their interaction (Mitteroecker et al., 2004; Klingenberg, 2016). A common GM method is a principal components analysis (PCA); this analysis takes a covariance matrix of the Procrustes aligned coordinates and identifies the axes of greatest variation. Specific shape variables in the cranial base can be isolated and

visualized using PCA; further PC scores can be used to test for significant correlation with an independent variable. In this dissertation, PC scores were tested for significant correlation with scaled ectotympanic length in multivariate and univariate regressions.

Statistical analyses were performed using MorphoJ, SPSS, and the Geomorph package in R. Geomorph is a particularly useful tool for analyzing and visualizing shape variation. In the present dissertation, ANOVAs and MANOVAs were performed testing the effects of total shape variation. These were performed using the procD.lm function in the Geomorph R package (R Core Team, 2013; Adams et al., 2017). The procD.lm function quantifies shape variation attributable to certain factors; in this case, it asks the question: How much of the relative ectotympanic bone length can be attributed to cranial shape? It creates a multivariate linear model and tests for significance between the Procrustes shape variables and an independent factor (ectotympanic bone length) using resampling permutation analyses.

GM, while certainly useful and broadly applied, has its limitations. For one, it relies heavily on the choice of landmarks being reliable, valid, repeatable, and biologically significant. Tests can be performed to determine if the landmarks are reliable and repeatable but determining whether a landmark is biologically important enough to include is largely up to the individual scientist performing them and thus contains some degree of subjectivity. Another potential problem associated with GM, more specifically with the assumptions of the Procrustes superimposition, is the potential for over-weighting landmarks that are very different from the others; this is known as the Pinocchio effect. That being said GM is an effective and commonly used means of quantifying and comparing shapes across taxa; it allows the researcher to search for the types of structural correlates that are suspected in the ectotympanic bone.

Error Study

Intra-observer error was tested for each group of analyses (1.within-human error, 2. within-macaque error, and 3. across species error); this is to identify the repeatability of the landmarks used. The landmark protocol was repeated twice with at least a day's break between trials. For Chapter 3, four macaques and four humans were each landmarked twice. Repeatability was tested to determine whether the effect of individual remains significant despite the error that occurs during measurement. Procrustes superimposition and PCA were performed to visualize the separation (Figures 2.1 - 2.3). A Procrustes ANOVA was completed to test whether the effect of individual could be distinguished despite measurement error, and that the effect of individual was significant in both humans ($p<0.001$) and macaques ($p<0.001$). Similarly, for Chapter 4 five individuals were re-landmarked. Repeatability of these landmarks was tested and the results show that the effect of individual was significant ($p<0.001$). There was apparent error in a few individuals, mostly concentrated near the less reliable landmarks (i.e., euryon), despite this error, however, there is no overlap of specimens and the error did not obscure the across-individual variation.

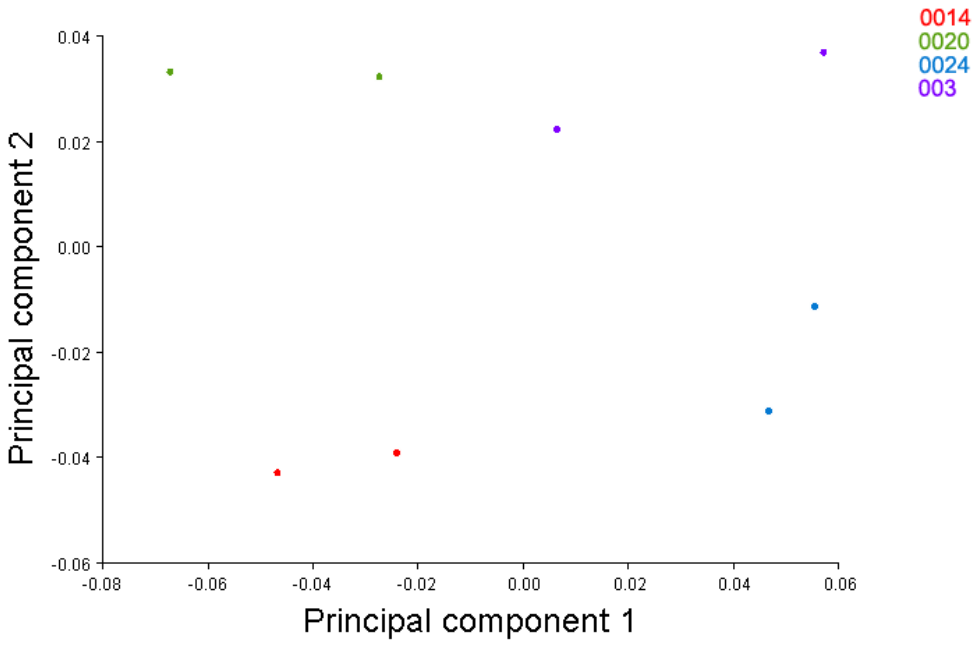

Figure 2.1: PCA analysis of intra-observer error of human sample

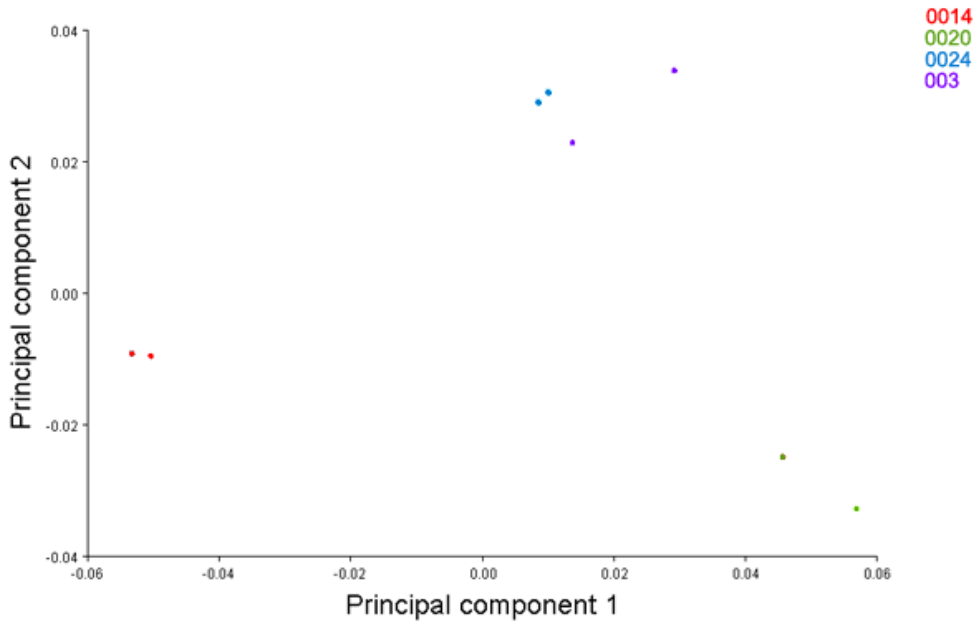

Figure 2.2: PCA analysis of intra-observer error of macaque sample

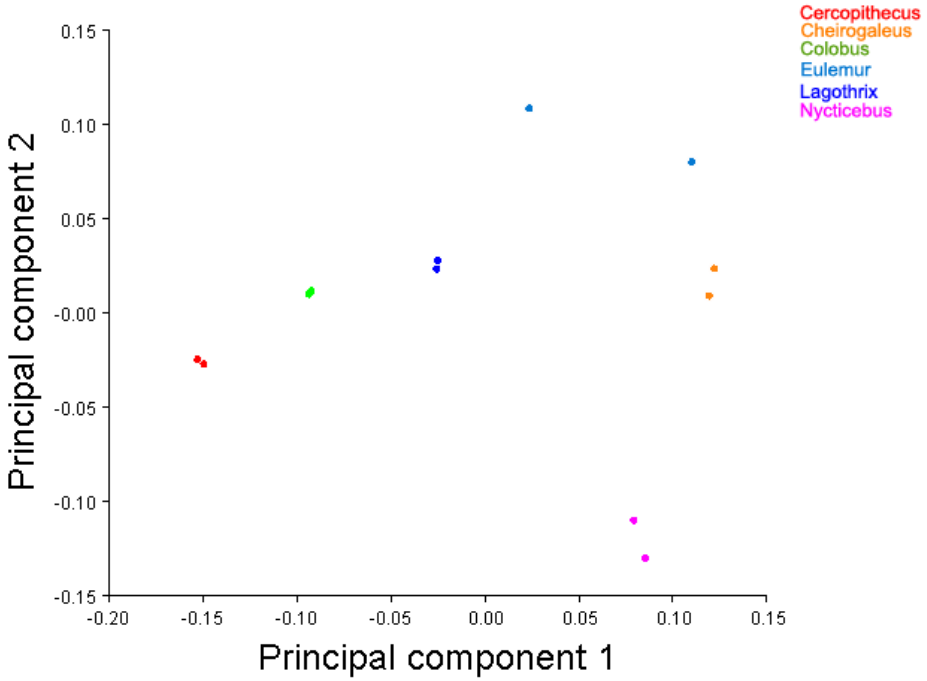

Figure 2.3: PCA analysis of intra-observer error of across primates sample

Scaling Factor

Scaling factors account for the effects of body size, and correct scaling is essential when seeking to identify real shape differences and control for the effects of allometry. Identifying an appropriate scaling factor for the ectotympanic bone length was given serious consideration prior to completion of the present dissertation and re-evaluated several times using post-hoc analyses. Bi- internal acoustic meatus distance (BiIAM) distance was chosen a priori as the location where the cranial nerves VII and VIII exit the endocranial space and roughly reflective of the width of the brain stem. It is a measure of cranial size in the lateral direction that does not include the auditory structures that were of interest in these studies. Additionally, BiIAM is measure of body size that is somewhat independent of many of the processes of encephalization and importantly does

not include the lateral aspect of the cranium, squamosal portion of the temporal bone, or brain, which are some of the most important cranial structural correlates being tested here. BilAM was tested post hoc for its correlation with centroid size (a more common measure of body size) and it was found to significantly correlate with centroid size within (Figure 2.4-2.5) and across species (Figure 2.6).

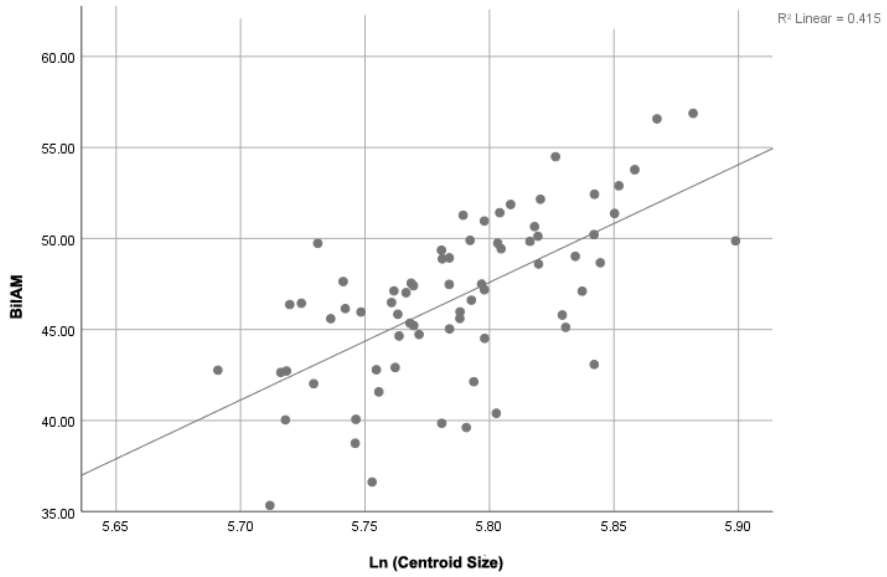

Figure 2.4: Human BilAM versus centroid size. R^2=0.42, p<0.001.

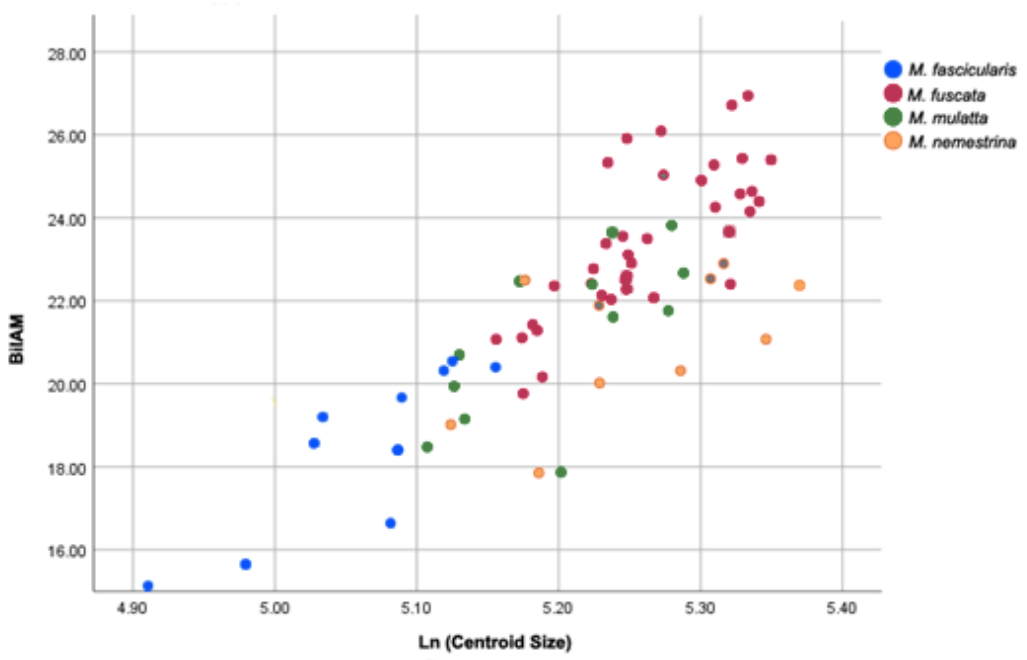

Figure 2.5: Macaque BilAM versus centroid size. R^2=0.81, p<0.001.

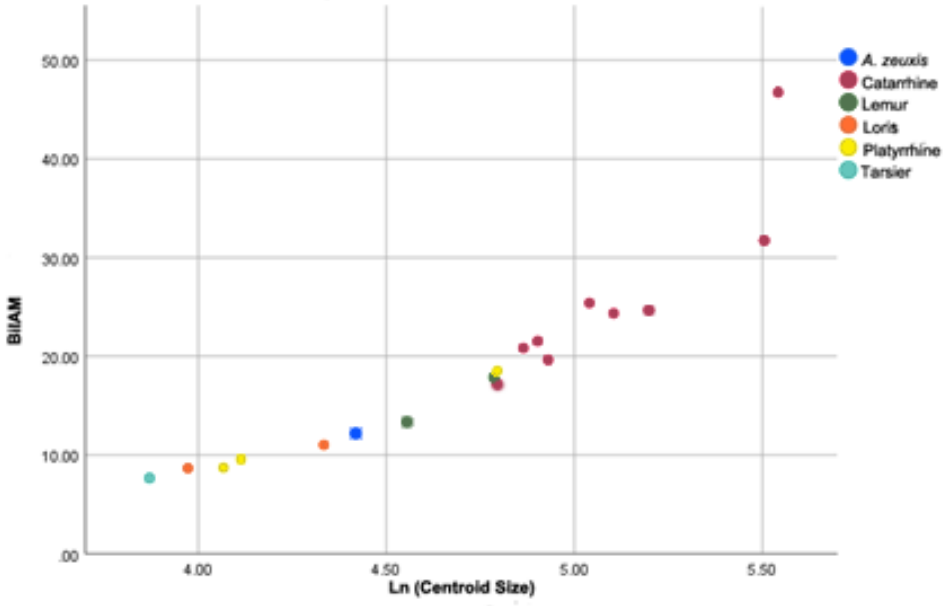

Figure 2.6: Across primates BilAM versus centroid size. R^2=0.79, p <0.01.

3. Intraspecies Variation in the Catarrhine Ectotympanic Tube among Humans and Macaques

Introduction

The primate ectotympanic tube form has been used as an important large-scale phylogenetic indicator for the last century (Gregory, 1920; Saban, 1963; Simons, 1974; Cartmill, 1982; Hershkovitz, 1974; MacPhee and Cartmill, 1986) but the within-catarrhine variation in this characteristic has largely been ignored. The ectotympanic bone is most often described in the literature as either a bony tube or a bony ring associated with a cartilaginous tube (e.g., Piveteau, 1957; Fleagle, 2013). Catarrhines and tarsiers are described as having bony ectotympanic tubes, and platyrrhines and strepsirrhines as having an ectotympanic ring. Two species of fossil catarrhine, representatives of *Aegyptopithecus* and *Pliopithecus (Epipliopithecus)*, stand out as being described as having intermediate ectotympanic tubes which are unusually short or abnormal ectotympanic tubes for catarrhines (Zapfe, 1958, 1960; Simons, 1972; Gingerich, 1973; Cartmill et al., 1981; Begun, 2002). However, the variation within extant catarrhines is not well understood and that hinders interpretation of the morphology in fossils. It may be that ectotympanic tube morphology among catarrhines is relatively uniform and scales isometrically with the size of the head. The present study tests within-taxon variation in the ectotympanic bone in two groups of catarrhines, humans and macaques.

This chapter tests a structural hypothesis: that the relative length of the ectotympanic bone within humans and macaques is heavily influenced and potentially co-varies overall cranial structure. It is suggested that cranial shape is correlated with ectotympanic bone morphology. Some of the factors that potentially affect the morphology of the ectotympanic tube are: 1) total brain volume, 2) regional brain shape, 3) the relative location of the auditory capsule, and 4) pneumatization of the mastoid region. Possibly the most obvious hypothesis as to why and how the ectotympanic tube

may vary is that it is an artifact of encephalization across the primate tree. Catarrhines, particularly hominins, are larger than other primates and have both absolutely and relatively larger brains than other primates (Weidenreich, 1941; Biegert, 1963; Gould, 1977; Holloway et al., 2005). While this hypothesis is intriguing and may certainly be true within the catarrhines, the presence of a tubular ectotympanic bone in another haplorhine, the tarsier, may potentially complicate this hypothesis as they are notably small bodied and do not possess particularly large brains for their bodies (Smith and Jungers, 1997; Fish and Lockwood, 2003).

Based on the structural hypothesis, the anatomical position of the ectotympanic tube has the potential to influence its morphology. The ectotympanic bone is a portion of the temporal bone and exists between the middle ear (specifically the tympanic membrane) and external pinna. The ectotympanic bone fuses to the petrosal portion (basicranial) of the temporal bone during development, and among catarrhines extends as far as the squamosal (neurocranial) portion. If the structure of the temporal bone in general is affecting the ectotympanic bone length, then the relative size and positions of basicranial and neurocranial elements would be correlated with relative ectotympanic bone length.

The temporal bone exists at the crux between middle and posterior cranial fossae, housing the lateral and posterior parts of the brain respectively. It is argued here that the length and orientation of the ectotympanic tube may be correlated with the specific expansion of the middle cranial fossa, the posterior cranial fossa, or both. The middle cranial fossa's main function is to house the temporal lobes of the brain; the posterior cranial fossa houses and supports the occipital lobes and cerebellum. Previous studies have shown that there are important differences that exist among species in the scaling of brain *regions*, not just in the total brain mass (Semendeferi et al., 1997; Semendeferi and Damasio, 2000; Allen, 2014). Thus, the ectotympanic tube's length

may be driven by hypertrophy of one of the regions of the brain, and its orientation may vary, at least in part, based on the volumetric relationships of the regions of the brain. For example, human brains are much larger than expected for our body size based on general primate allometric relationships (Falk, 1980; Rilling and Insel, 1999; Rilling and Seligman, 2002). However, both the visual cortex and cerebellum are smaller than expected for that brain size; conversely the prefrontal cortex and the temporal lobes are disproportionately large (Holloway, 1992; Semendeferi et al., 1997; Rilling and Insel, 1999; Preuss, 2000; Semendeferi and Damasio, 2000; Rilling and Seligman, 2002). Large temporal lobes necessitate large middle cranial fossae, which in turn may mean that the ectotympanic tubes would have to “keep up” and lengthen accordingly (Figure 3.1).

Figure 3.1: Figure adapted from Saban (1963) illustration showing a coronal slice though the human head. The image demonstrates the positional relationship between the auditory structures and the temporal lobe of the brain: 6=middle ear, 7=superior EAM/porion, 8 (orange) =floor of the ectotympanic tube/tympanic plate. Note the close relationship between the lateral aspect of the brain and the ectotympanic tube; numbers 1-5 indicate the folds of the temporal lobe. Cranial bone = green, tympanic plate = orange, brain = pink.

From a functional perspective, among catarrhines the ectotympanic tube supports the ear canal that collects sound waves and extends from the external auditory meatus (EAM) to the auditory capsule (or inner ear). Within this taxon, its length and orientation are determined by the relative locations of those two structures. The auditory capsule is phylogenetically conserved across catarrhines (Coleman and Ross, 2004; Coleman et al., 2010). The inner ear structures are locked into position early in development which suggests they are less developmentally plastic and more canalized; among humans, there is little to no postnatal change in their relative location or morphology (Scheuer and Black, 2000). Through placental mammal evolution, there have been relatively few novel innovations in the auditory capsule (Manley, 2000). In fact, the auditory capsule is so constrained that as selective pressures are placed on it, the primary adaptations seen are in the elongation of the cochlea but as there is nowhere for it to go, it winds more tightly and efficiently in on itself (West, 1985). In general, there is slightly more developmental and phylogenetic potential for adaptation at the lateral end of the external ear tube, where it can vary in location and orientation, with morphotypes laterally oriented (e.g., primate), or superiorly oriented (e.g., lagomorphs). If either of the ends of the ectotympanic tube are altered (the medial end at the tympanic membrane or the lateral end at the EAM), the tube length or orientation may change accordingly.

The present study explores the within-taxon variation in ectotympanic morphology in two well-understood extant catarrhine genera, *Macaca* and *Homo*. While the two taxa referenced in the present chapter represent only a microcosm of the potential variation within the catarrhine ectotympanic tube, they provide unique benefits. The depth of academic literature covering the shape variation, developmental patterning, cranial shape, and auditory function of these two species allows for relative certainty in the anatomical variation described here (e.g., Jackson et al., 1999; Zumpano and

Richtsmeier, 2003; Coleman and Ross, 2004; Hallgrimsson et al., 2004). These two species also bracket the shift in the cranial base associated with bipedality and encephalization between generalized cercopithecoids and hominins. Along with encephalization in the *Homo* clade, basicranial flexion affects the relationships between cranial length and craniofacial morphology. It has been argued that the flexed basicranium causes other structural changes in the cranial base, including a retracted face, a shortened oropharynx, and importantly for the current work, a relatively wider middle cranial fossa (Lieberman, 1998; Spoor et al., 1999; Lieberman et al., 2000, 2002). Less well understood, though increasingly investigated, are the consequences of this encephalization in the lateral direction (Dean and Wood, 1982; Seidler et al., 1997; Holloway et al., 2005; Bastir et al., 2008; Bastir and Rosas, 2009). There is likely some compensatory shifting in the lateral direction associated with brain flexion that would have an effect on the lateral-most points of the cranial base; in particular, the lateral border of the ectotympanic bone. Basicranial flexion could potentially alter the spatial relationships associated with ectotympanic tube morphology; looking at the variation in both species provides an excellent contrast between humans and macaques, who demonstrate less encephalization. Thus, these two taxa are ideal for identifying and analyzing structural correlates with relative ectotympanic length.

Hypotheses

Lateral expansion of the brain relative to the auditory capsule is likely associated with lengthening of the bony ectotympanic tube within and across the two catarrhine samples included here. Among primates, the morphology of the bony ectotympanic is potentially correlated with lateral displacement of the squamosal (including mastoid and zygomatic arch) relative to the auditory capsule. This will be tested in each of two well-understood taxa:

H1 Macaques: If the lateral expansion of the cranial base is determining the length of the ectotympanic tube, then the total cranial base shape should correlate with the scaled ectotympanic bone length in macaques.

H1a: Further, the PC scores associated with brachycephaly and dolichocephaly will be highly correlated with scaled ectotympanic bone length.

H2 Humans: If the lateral expansion of the cranial base is determining the length of the ectotympanic tube, then the total cranial base shape should correlate with the scaled ectotympanic bone length in humans.

H2a: Further, the PC scores associated with brachycephaly and dolichocephaly will be highly correlated with scaled ectotympanic bone length.

Materials and Methods

To identify structural correlates with the length of the catarrhine ectotympanic tube, two genera of extant catarrhines, *Homo* and *Macaca*, were analyzed using three-dimensional (3D) landmark data to estimate the shape of relevant structures.

Sample: Macaque

CT scans of macaque crania were obtained from the KUPRI database (the Digital Morphology Museum housed at the Kyoto University Primate Research Institute http://dmm3.pri.kyoto-u.ac.jp/dmm/). The macaque sample consists of several species, *M. fuscata* (37), *M. fascicularis* (13), *M. mulatta* (16), and *M. nemestrina* (14) (see table A.1 for scan parameters). Four species of macaque were included to capture the range of variation in lateral cranial expansion among macaques.

Sample: Human

The human sample was compiled from CT scans of archaeological specimens obtained from the Open Research Scan Archive (https://www.penn.museum/sites/orsa). This archive, in general, contains specimens housed at the University of Pennsylvania, Museum of Archaeology, mostly from the *Samuel George Morton Collection.* The Morton collection consists of archaeological and modern human crania, collected between the

1820s and 1851. The CT scans of crania included in this study were sampled from the Morton collection, including 40 female and 40 male crania (voxel size: 0.6x0.6x0.6mm). Demographic information available, although incomplete, indicates that the crania came from varied locales and ancestral backgrounds (Appendix Table A.2).

Data Acquisition and Preparation

Three-dimensional reconstruction, visualization, and landmark placement on the crania were performed by importing stacks of digital images into AMIRA 5.6 or 6.3 (FEI Houston, Inc.), surfaces were extracted using consistent threshold levels for each sample. A total of 78 landmarks were used to assess the shape of the human crania and 76 in the macaque sample (Table 3.1, Figure 3.2). The macaque landmarks did not include the mastoid process, because among macaques the sternocleidomastoid muscle attachment is not clearly demarcated on the bony anatomy as it is in humans. Landmarks were used to quantify both the shape of the cranium as a whole and the ectotympanic tube.

Table 3.1: Landmarks

Landmark	Region	Side	Abrev.	Type
Superior ectotympanic constructed landmarks 1-5	Auditory isolated	Bilateral	SEcto	Semilandmark
Inferior ectotympanic constructed landmarks 1-5	Auditory isolated	Bilateral	IEcto	Semilandmark
Inferior EAM	Cranial base, Auditory isolated	Bilateral	IEAM	Fixed
Superior EAM	Cranial base, Auditory isolated	Bilateral	SEAM	Fixed
Superior Tympanic Ring	Cranial base, Auditory isolated	Bilateral	STR	Fixed
Inferior Tympanic Ring	Cranial base, Auditory isolated	Bilateral	ITR	Fixed
Superior middle ear	Cranial base, Auditory isolated	Bilateral	SME	Fixed
Inferior middle ear	Cranial base, Auditory isolated	Bilateral	IME	Fixed
Internal Acoustic Meatus	Cranial base, Auditory isolated	Bilateral	IAM	Fixed
Anterior tympanic	Cranial base	Bilateral	AT	Fixed
Inferolateral tympanic	Cranial base	Bilateral	IT	Fixed
Petrous apex	Cranial base	Bilateral	PA	Fixed
Carotid canal	Cranial base	Bilateral	CC	Fixed
Styloid process	Cranial base	Bilateral	SP	Fixed
Stylomastoid foramen	Cranial base	Bilateral	SMF	Fixed
Lateral jugular fossa	Cranial base	Bilateral	JF	Fixed
Mastoid process ***	Cranial base	Bilateral	MP	Fixed
Anterior articular eminence	Cranial base	Bilateral	AAE	Fixed
Lateral articular eminence	Cranial base	Bilateral	LAE	Fixed
Inferior post-glenoid	Cranial base	Bilateral	IPG	Fixed
Temporal zygomatic arch	Cranial base	Bilateral	TZ	Fixed
Foramen ovale	Cranial base	Bilateral	FO	Fixed
Basion	Cranial base	Center	BA	Fixed
Foramen caecum point	Cranial base	Center	FC	Fixed
Sphenobasion	Cranial base	Center	SBA	Fixed
Opisthion	Cranial base	Center	OP	Fixed
Incisive canal	Total cranium	Center	IN	Fixed
Bregma	Total cranium	Center	B	Fixed
Glabella	Total cranium	Center	G	Fixed
Inion	Total cranium	Center	I	Fixed
Stephanion	Total cranium	Bilateral	ST	Fixed
Orbitale superiorus	Total cranium	Bilateral	OR	Fixed
Frontotemporale	Total cranium	Bilateral	FT	Fixed
Euryon	Total cranium	Bilateral	EU	Fixed
Alveolon	Total cranium	Bilateral	AL	Fixed

***The mastoid process landmarks were omitted in the macaque data collection.
Total cranium landmarks were taken and used to calculate interlandmark distances but were eliminated from shape analyses as they were reflecting shape variation in the face and neurocranium that were irrelevant for the current study.

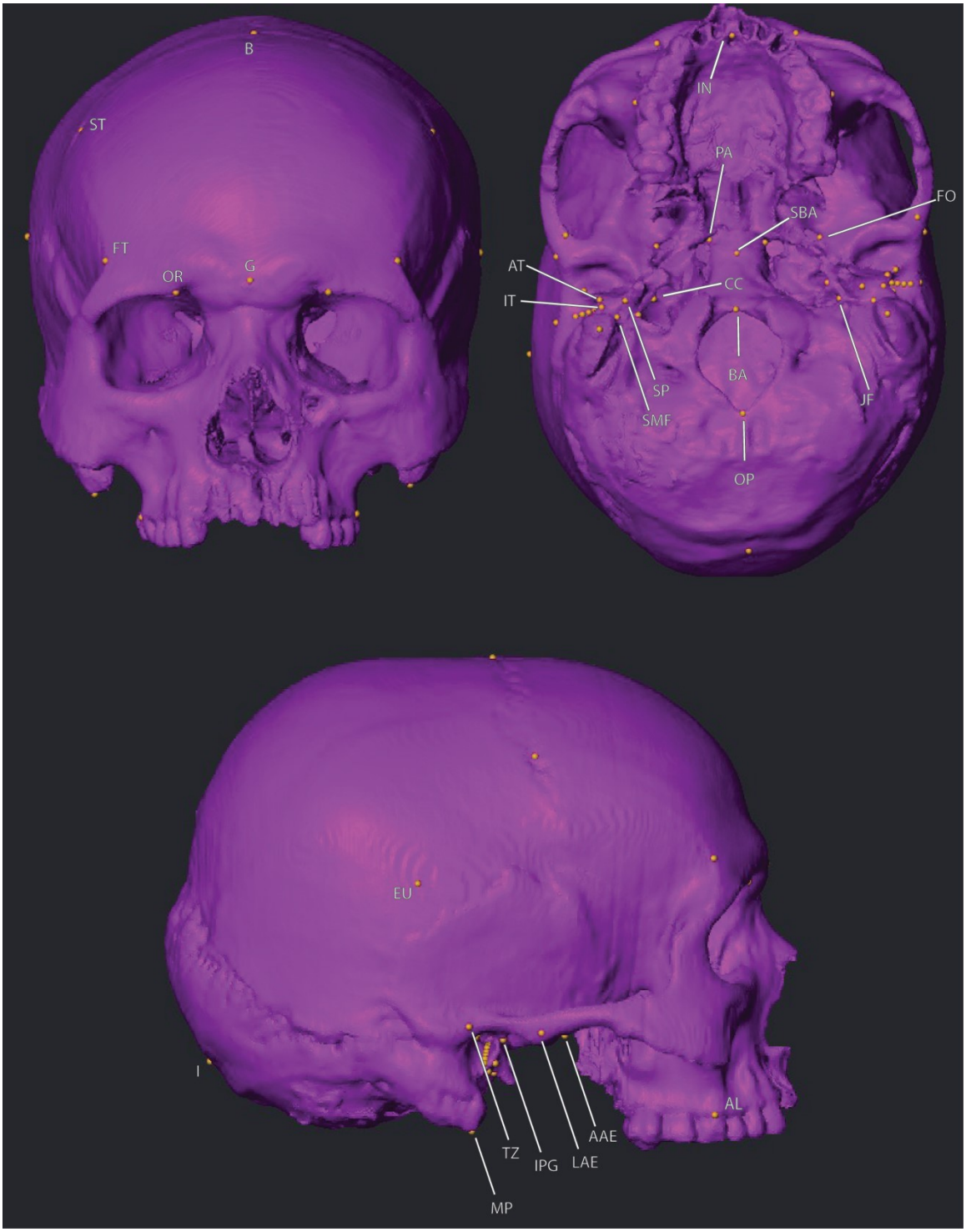

Figure 3.2: Landmarks Included. AT=Anterior Tympanic, IT=Inferolateral Tympanic, PA=Petrous Apex, CC=Carotid Canal, SP=Styloid Process, SMF=Stylomastoid Foramen, JF=Jugular Foramen, AAE=Anterior Articular Eminence, LAE=Lateral Articular Eminence, IPG=Inferior Post-Glenoid, TZ= Temporal Zygomatic Arch, MP=Mastoid Process, FO=Foramen Ovale, BA=Basion, OP=Opisthion, SBA=Sphenobasion, IN=Incisive Canal, B=Bregma, G=Glabella, I=Inion, ST=Stephanion, OR=Orbitale superiorus, FT=Frontotemporale, EU=Euryon, AL=Alveolon.

Because the ectotympanic tube is largely devoid of Type 1 landmarks, constructed landmarks were placed along the superior and inferior ectotympanic tube at evenly spaced intervals following the method of Squyres and DeLeon (2015) (Figure 3.3). First, the landmarks demarcating the tympanic ring and external auditory meatus were placed. The tympanic ring landmarks were placed at the crista tympanica, or the apex of the ridge of bone that supports the tympanic membrane, at the superior-most and inferior-most points. The inferior EAM landmarks were placed at the points of greatest curvature as the bone slopes inferiorly (Figure 3.3). The superior EAM was placed at the superior-most point on the ridge of the EAM, not including the temporal ridge. Once these two points have been defined, six evenly spaced planes were placed orthogonal to the ectotympanic tube; these planes are roughly parasagittal but account for the slight inferior angling of the ectotympanic tube. This process resulted in six slices through the ectotympanic tube and the cross-section of the tube is revealed. Constructed landmarks were placed at each of the superior and inferior-most points of the cross-sections. These constructed landmarks capture not only the shape of the ectotympanic but also the angle of the tube with respect to the cranial base.

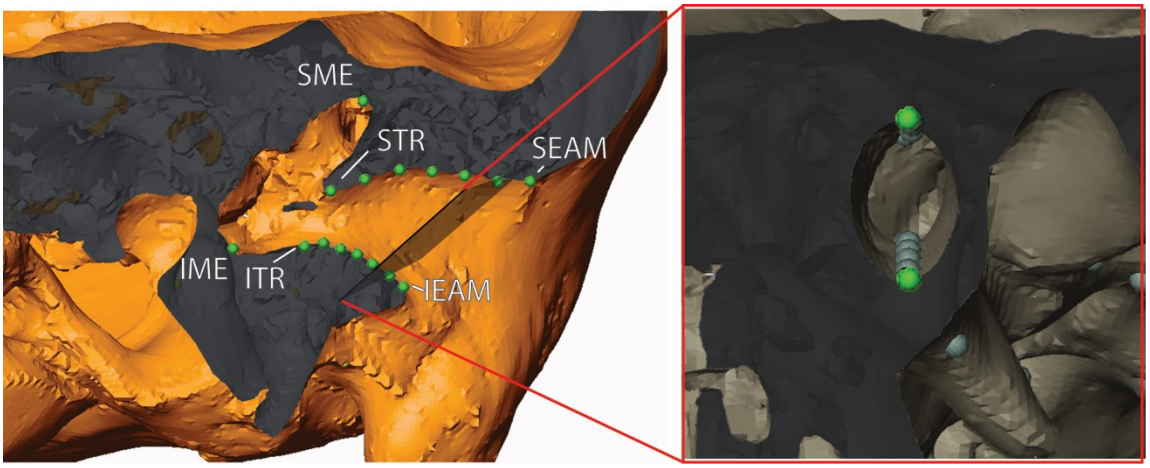

Figure 3.3: Illustration of constructed landmarks through catarrhine ectotympanic tube (anterior view of left temporal). The inset to the right shows one example of a cross-section through the catarrhine ectotympanic tube; landmarks are placed at the superior-most and inferior-most points. SME=Superior Middle Ear; IME=Inferior Middle Ear; STR= Superior Tympanic Ring; ITR=Inferior Tympanic Ring; SEAM= Superior External Auditory Meatus; IEAM= Inferior External Auditory Meatus.

In addition to shape data captured using landmarks, several inter-landmark distances were calculated (Table 3.2). Variation in the lengths of the ectotympanic tube was standardized by taking the ratio of the ectotympanic length (the distance between the ITR and IEAM landmarks) by the distance between the right and left internal acoustic meatuses (BiIAM) as an estimate of body size. The BiIAM scaling factor was chosen as it is a reliable, repeatable, and biologically relevant inter-landmark distance (see Chapter 2). It is a measure of brainstem width, which does not include the effects of lateral encephalization that are relevant to the hypotheses tested in the present chapter. BiIAM in a set of post hoc analyses was regressed on centroid-size, a more common body size scaling factor, and the correlation was strong in both analyses (see Figures 2.4 and 2.5). BiIAM was preferred, however, because it reduces the potentially confounding factor of encephalization.

Table 3.2: Linear Distances

	Name	
1	Inferior ectotympanic length	Length of the inferior ectotympanic taken from the most inferior point of the tympanic ring to the inferior external acoustic meatus
2	Superior ectotympanic length	Length of the superior ectotympanic taken from the most superior point of the tympanic ring to the inferior external acoustic meatus
3	BiEuryon	Distance between right and left euryon
4	Bi-Internal Acoustic Meatus (BiIAM)	Distance between right and left internal acoustic meatus
5	Bi-Extenal Acoustic Meatus (BiEAM)	Distance between right and left external acoustic meatus

Data Analysis

Two subsets of landmark coordinates (cranial base and isolated auditory, defined in Table 3.1) were separately subjected to full Procrustes superimposition, and resultant shape data were then visualized and analyzed using principal components analysis (PCA). The symmetric component was isolated and used for all analyses; the symmetric component is often the most informative approximation of cranial "shape" and minimizes the effects of asymmetric variation that are not directly relevant to the analyses (Klingenberg et al., 2002; Jurda et al., 2015). Neurocranial landmarks (whole crania) were collected and used for interlandmark distances but were excluded for most analyses because the large variation in neurocranial landmarks overpowered the more relevant variation in the cranial base. Constructed landmarks were excluded from cranial base analyses to avoid putting undue weight on these densely distributed landmarks in the Procrustes superimposition. These constructed landmarks are included in the "Isolated Auditory" analyses, which were designed to look for localized variations in the ectotympanic shape and orientation.

The ProcD.lm function in the geomorph package in R was used to test the correlation between relative ectotympanic length and overall cranial base shape. To test H1a and H2a, multiple regressions were used to identify the types of cranial shape

variables (PCs) that are most strongly correlated with relative ectotympanic length. Bivariate correlations were used to describe intraspecific variation in ectotympanic bone lengths. All statistical analyses were performed using MorphoJ (Klingenberg, 2011), R (R Core Team, 2013), and RStudio (RStudio, 2015).

Results

Macaque Geometric Morphometrics

Results of the macaque procD.lm analysis show that total cranial base variation is significantly correlated with relative ectotympanic bone length (Table 3.3).

Table 3.3: Macaque procD.lm results

	Df	SS	MS	Rsq	F	Z	Pr (.F)
Ectotympanic length	1	0.021	0.021	0.097	6.81	5.63	**0.001**
Ectotympanic length: Centroid size	1	0.019	0.019	0.089	6.22	5.92	**0.001**
Residuals	57	0.17	0.0030	0.81			
Total	59	0.21					

Multivariate regressions show that most of the variation in macaque ectotympanic length (75%) can be explained by the shape variance described on PC1 ($p>0.001$, $R^2=0.75$; Figure 3.4). Frequently the first principal component can be attributed to body size, and the results show that the first principal component is significantly correlated with centroid size, though the relationship is weak ($p=0.05$, $R^2=0.054$) (Figure 3.5). It captures variation related to cranial proportions, with dolichocephalic forms at the high end and brachycephalic forms at the low end (Figure 3.6).

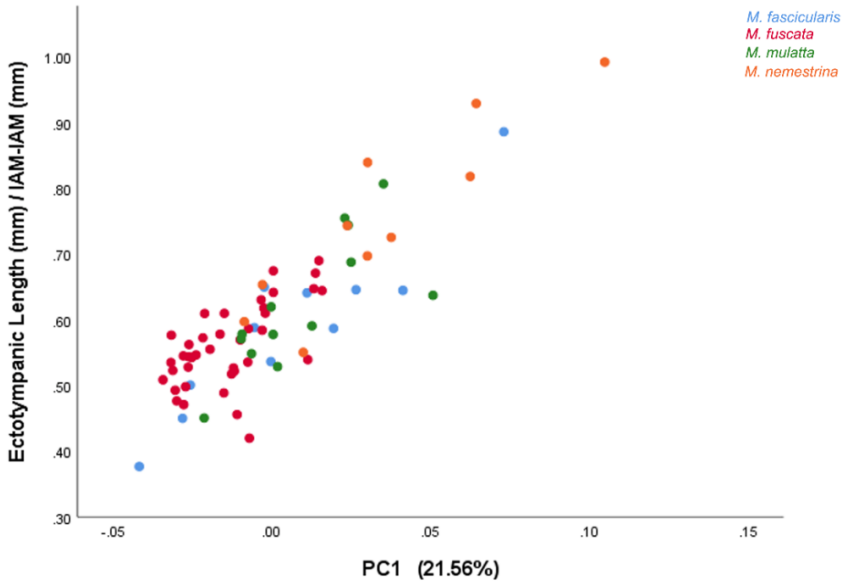

Figure 3.4: Scatterplot of the macaque PC1 and scaled ectotympanic tube length ($p<0.001$, $R^2=0.75$). PC1 is showing 21.56% of the total cranial base shape variation. Traditionally, PC1 is often assumed to reflect allometry and PC1 significantly correlates with centroid size.

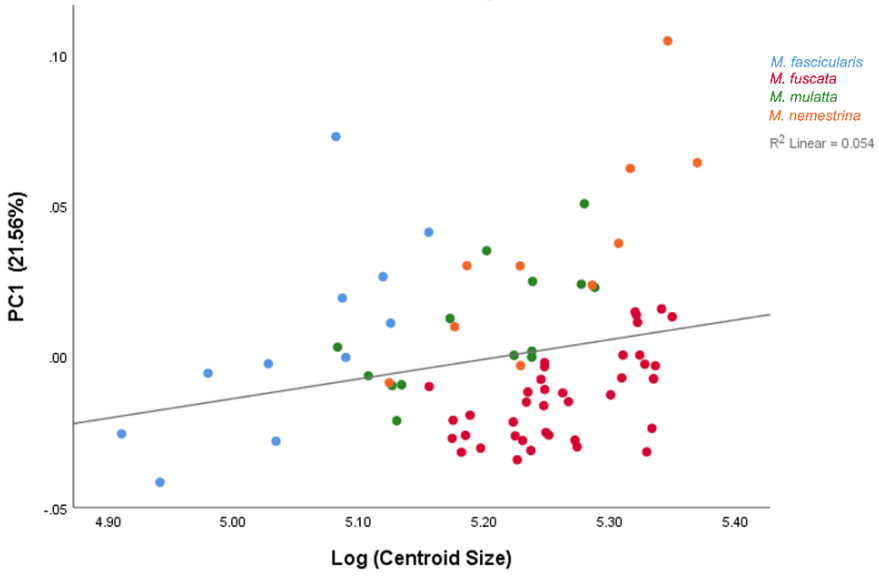

Figure 3.5: Scatterplot of macaque PC1 and centroid size ($p=0.05$, $R^2=0.054$). This result shows that while PC1 is associated with gross shape of the basicranium, the effect of size is still present and cannot be fully discounted.

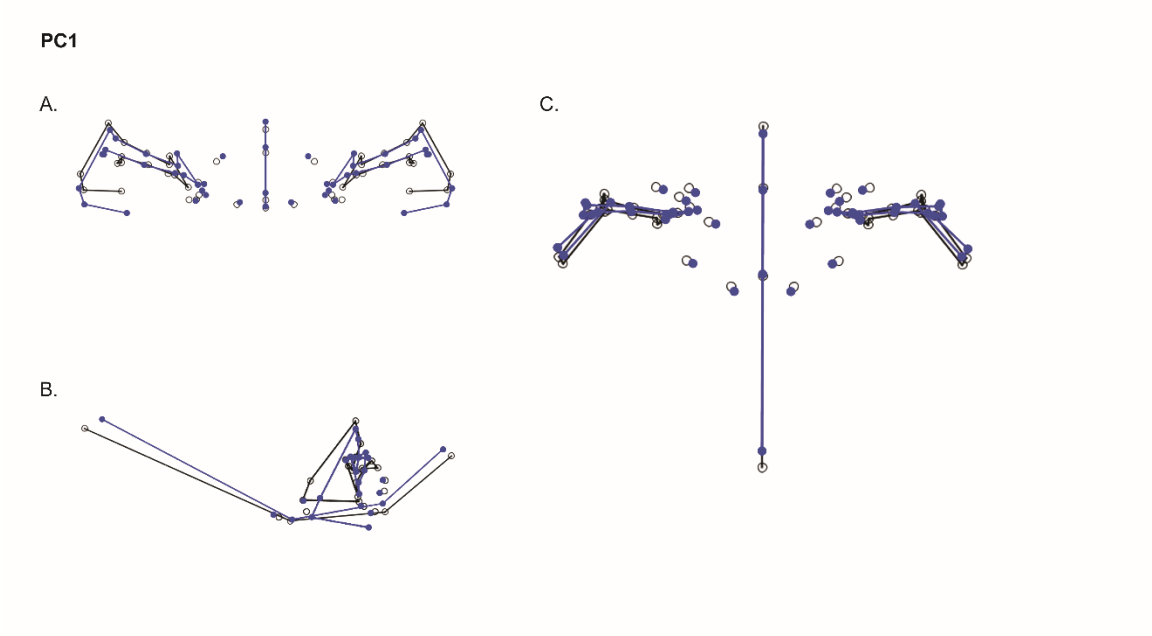

Figure 3.6: Wireframe visualization of macaque PC1. The black indicates the mean shape and blue indicates shape change that corresponds to an increase of 0.1 units of Procrustes distance (Klingenberg, 2011). PC1 is mostly describing the relative brachycephaly or dolichocephaly of the individual. A. Anterior-posterior view; B. Lateral view; C. Superior-inferior view.

There is some separation between species on PC1 (Figure 3.7). Among macaque specimens, using an ANOVA, the effect of species was found to be significant on PC1. Post hoc pairwise comparisons using a Kruskal-Wallis test and a Bonferroni correction factor show that the significant differences lie in the *M. fuscata* shape when compared to the other species (Table 3.4).

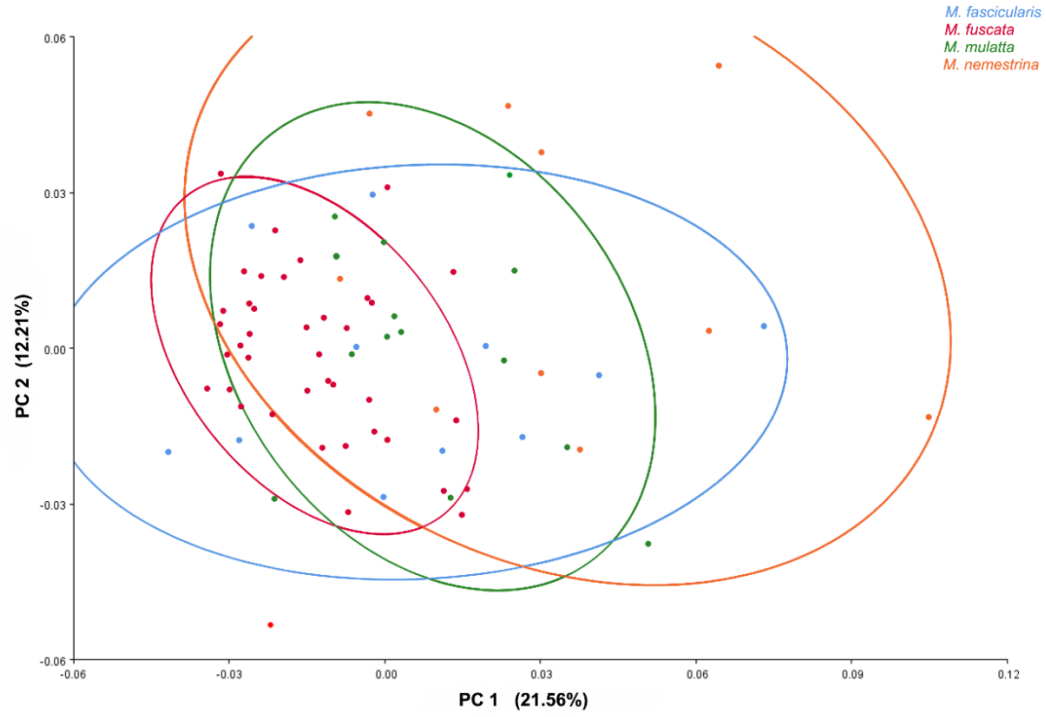

Figure 3.7: Macaque PC1 v. PC2 with 90% confidence ellipses by species. PCA results of the cranial base. The effect of species on PC1 was found to be significant but pairwise comparisons using a Kruskal-Wallis test show that it is driven by the morphological distance between *M. fuscata* and *M. nemestrina*, and *M. fuscata* and *M. mulatta*. Again, PC1 is mostly describing the relative brachycephaly or dolichocephaly of the individual with the *M. nemestrina* the most brachycephalic, and *M. fuscata* and *M. fascicularis* the most dolichocephalic.

Table 3.4: Pairwise Kruskal-Wallis tests for the effect of species on PC1 (Bonferroni corrected).

Sample	Test Statistic	Std. Error	Std. Test Statistic	Sig.	Adj. Sig.
M. fuscata v. *M. fascicularis*	15.80	7.34	2.15	0.031	0.19
M. fuscata v. *M. mulatta*	-22.33	6.70	-3.33	0.001	**0.005**
M. fuscata v. *M. nemestrina*	-33.61	7.62	-4.41	0.000	**0.000**
M. fascicularis v. *M. mulatta*	-6.53	8.67	-0.75	0.45	1.00
M. fascicularis v. *M. nemestrina*	-17.82	9.40	-1.90	0.058	0.35
M. mulatta v. *M. nemestrina*	-11.29	8.90	-1.27	0.21	1.00

Macaque Auditory Isolated Analysis

Partitioning out only the landmarks associated with the auditory complex allows for the examination of the shape and orientation of the ectotympanic tube without unduly weighting those landmarks in the Procrustes superimposition in the skull overall. The landmarks included in this analysis are only the constructed ectotympanic tube landmarks, middle ear landmarks, and IAM. The orientation of the ectotympanic varies among species. Relative ectotympanic tube length is significantly correlated with PC1 and PC2. PC1 is correlated with centroid size and is likely an allometric effect. Scaled ectotympanic length also correlates significantly with PC2 (R^2=0.15, p=0.001); however, PC2 is capturing the shape changes associated with orientation of the ectotympanic tube (Figure 3.8). Longer scaled ectotympanic tubes (like those of the *M. mulatta*) are more horizontal and posteriorly oriented.

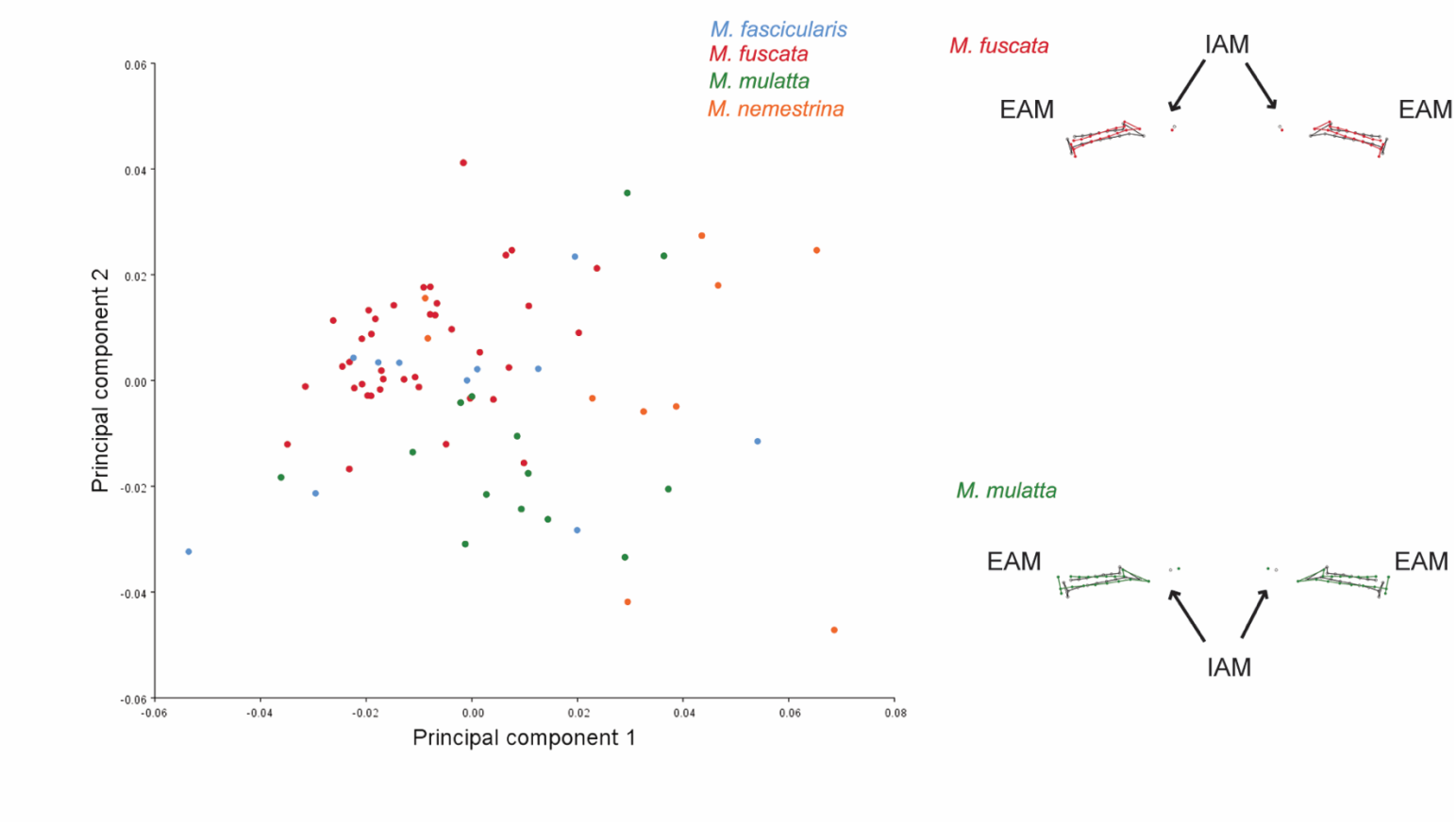

Figure 3.8: PC1 v. PC2 of only auditory landmarks and wireframe visualization of PC2 of *M. fuscata* and *M. mulatta*. The black wireframe is showing the average orientation and the green is showing an example of one extreme (*M. mulatta*) and the red shows a *M. fuscata* with a particularly inferiorly oriented tube. Relative ectotympanic tube length among macaques is most correlated with PC2. PC2 is describing the degree of horizontality in the tube. More horizontally oriented ectotympanic tubes, like those seen in the *M. mulatta* example, are longer.

Human Geometric Morphometrics

Among humans, shape variation in the cranial base also correlates significantly with scaled ectotympanic bone length (Table 3.5). This supports the structural hypothesis (H2).

Table 3.5: Human procD.lm

	Df	SS	MS	Rsq	F	Z	Pr (.F)
Ectotympanic Bone Length	1	0.015	0.015	0.041	3.08	3.86	**0.001****
Ectotympanic Bone Length: Centroid size	1	0.008	0.008	0.022	1.68	2.01	**0.032****
Residuals	70	0.33	0.0048	0.93			
Total	72	0.36					

PCA analyses show that among humans, like the macaques, the first principal component is associated with cranial proportions (relative dolichocephaly or brachycephaly). PC1 among humans is correlated with centroid size ($p<0.01$), therefore size cannot be ignored. Relative ectotympanic tube length correlates significantly with the first principal component; however, it correlates *best* with the fourth principal component. The variation described by PC4 explains much of ectotympanic tube length (32%, Figure 3.9). PC4 does not have a significant relationship with centroid size (Figure 3.10); therefore, the shape variation seen in this PC is not affected by total cranial base size. The shape variation captured in the fourth principal component is showing a broadening of the superior cranial base, as well as flexion of the cranial base (Figure 3.11).

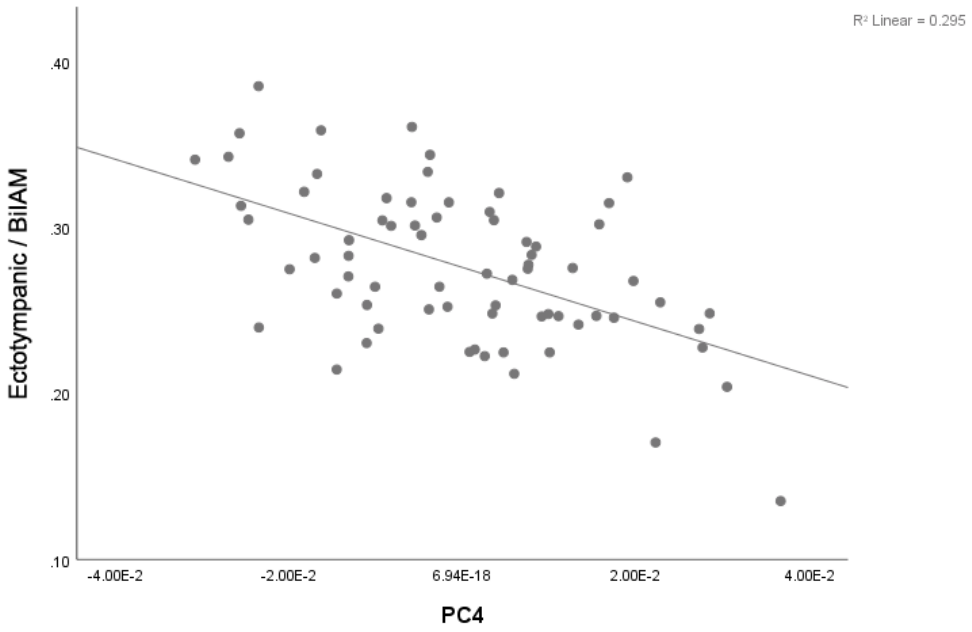

Figure 3.9: Human PC4 versus scaled ectotympanic length ($p<0.01$, $R^2=0.30$). Most of the variation in ectotympanic tube length is accounted for by PC4, which appears to be mostly describing flexion at the cranial base.

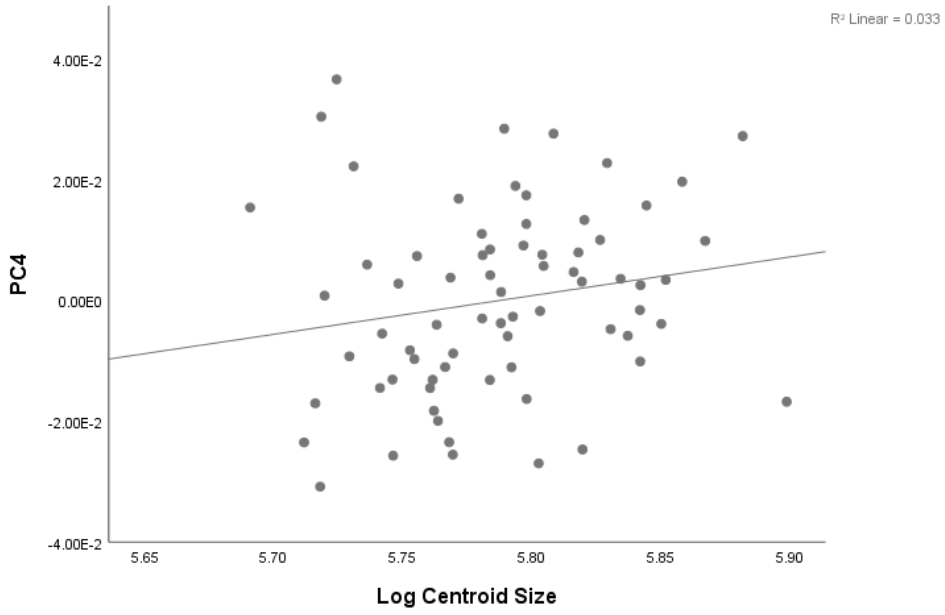

Figure 3.10: Human centroid size versus PC4, showing an insignificant correlation (p=0.13, R2=0.03). Therefore the relationship between PC4 and ectotympanic length is uncomplicated by overall body size.

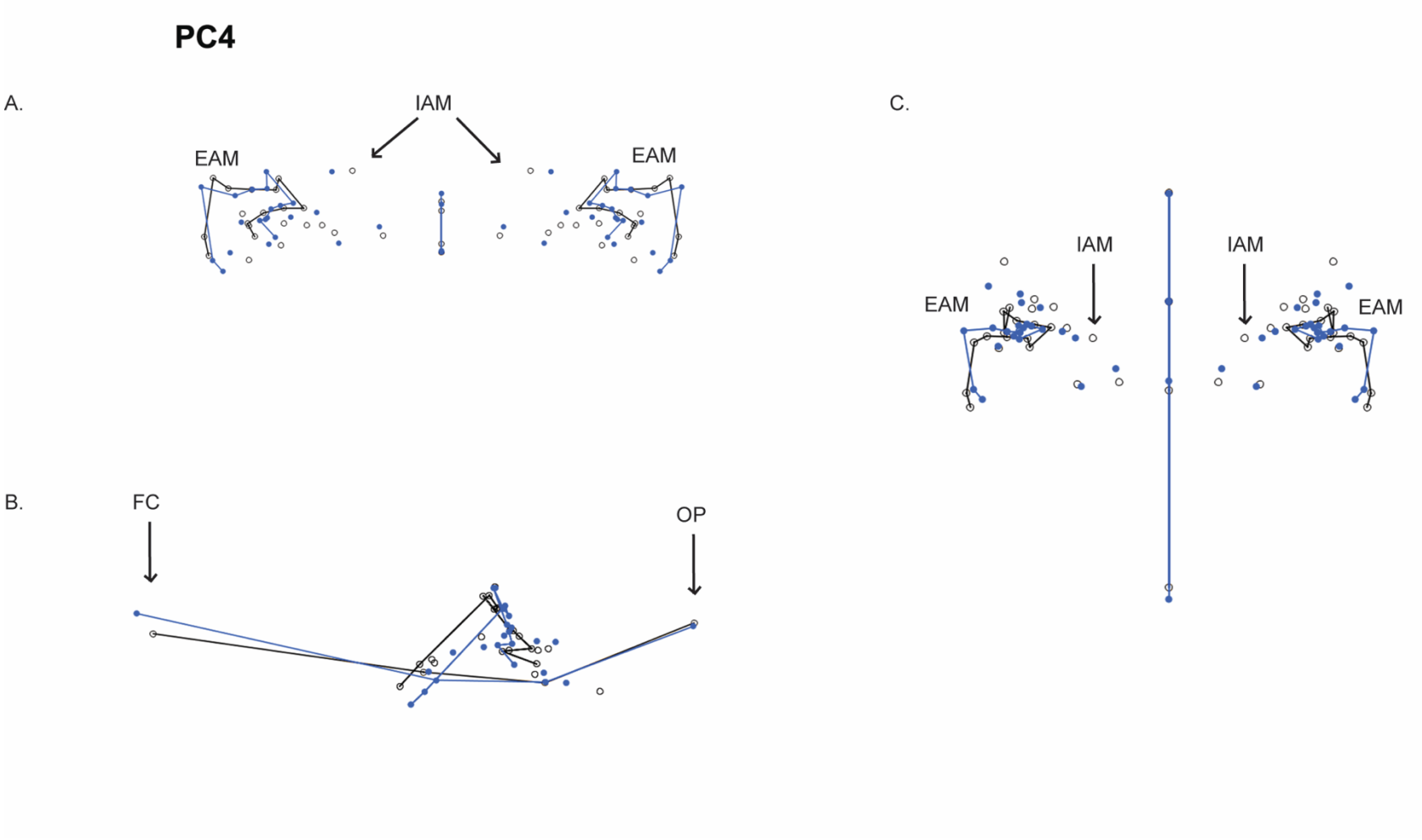

Figure 3.11: Wireframe visualization of human PC4, A) anterior, B) lateral, and C) inferior views. Black indicates the mean shape and blue indicates shape change that corresponds to an increase of 0.1 units of Procrustes distance. The shape variation captured in the fourth principal component is describing the relative width and flexion of the cranial base, indicating there is a relationship between relatively wide and less-flexed crania and long ectotympanic tubes.

Human Auditory Isolated Analysis

Analyses including only the auditory landmarks show that length of the ectotympanic tube in humans is correlated with a shift in orientation (Figure 3.12). Human relative ectotympanic tube length is significantly correlated with PC1. PC1 in humans, like in the macaques, is correlated with centroid size and thus includes some size related shape change. PC1 is visualized here, and is associated with an orientation shift, from horizontal to more inferiorly angled.

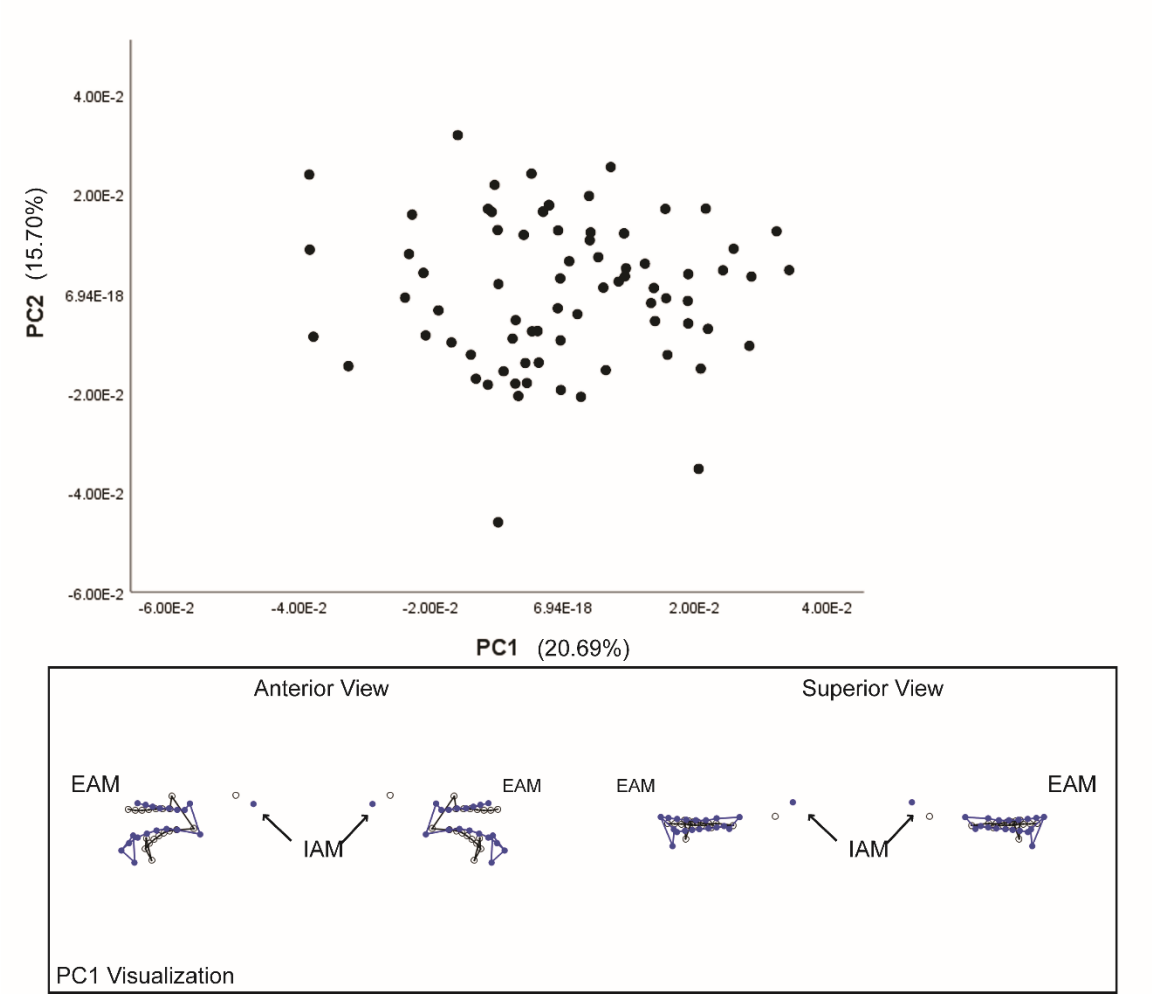

Figure 3.12: Results of PCA on human auditory landmarks only, PC1 v. PC 2 and a wireframe visualization of PC 1. PC1 shows the orientation shift from sloping to horizontal, long ectotympanic tubes are correlated with a more horizontal orientation. PC1 also correlates with centroid size and BiIAM distance, therefore is most likely describing shape changes associated with cranial base width and possibly brain volume.

Intraspecific Variation in Ectotympanic Bone Length

Results of ANOVA tests show that relative ectotympanic length (scaled by internal acoustic meatus distance), varies significantly among species of macaques. Pairwise comparisons show that the source of this significant variation between groups is mostly the difference in relative ectotympanic length between *M. fuscata* and *M. nemestrina*. *M. nemestrina* possesses the greatest relative ectotympanic tube length of all macaque species included in this study (Figure 3.13).

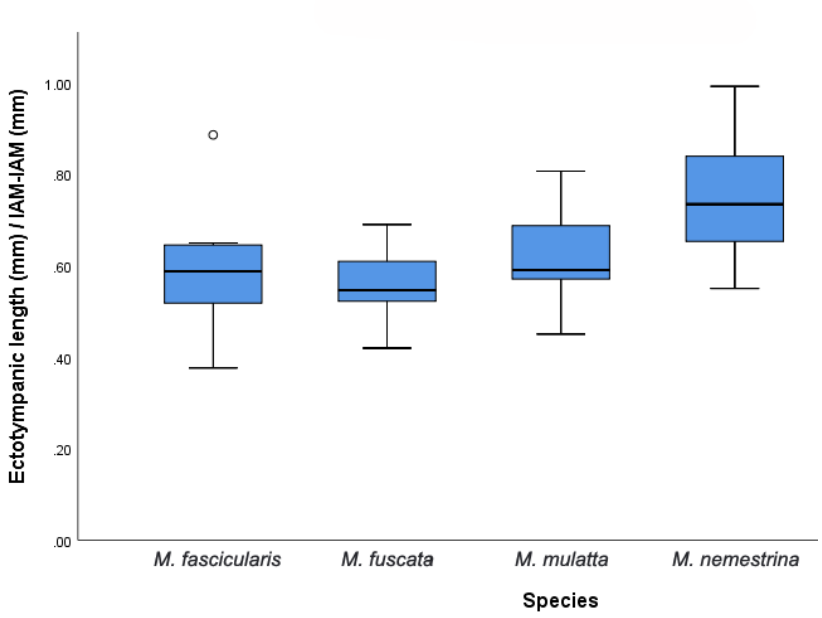

Figure 3.13: Box-plot showing the relative ectotympanic lengths of macaques by species. *M. fuscata* and *M. nemestrina* significantly differ in relative ectotympanic length. **Post hoc analyses show that there is a significant effect of species on scaled ectotympanic bone length ($p<0.001$), and Tukey HSD indicate that the differences are driven by each species being significantly different from *M. nemestrina* (*M. fascicularis* $p=0.001$; *M. fuscata* $p<0.001$; *M. mulatta* $p=0.009$)

Bivariate analyses show that within macaques, although ectotympanic tube length significantly correlates with both internal and external acoustic meatus distances, the stronger relationship by far is with the distance between EAM (IAM: $p<0.001$, $R^2=0.16$; EAM: $p<0.001$, $R^2=0.67$) (Figures 3.14-3.15). Scaled ectotympanic tube length among macaques also correlates with BiEAM significantly (Figure 3.16; $R^2=0.16$, $p<0.01$).

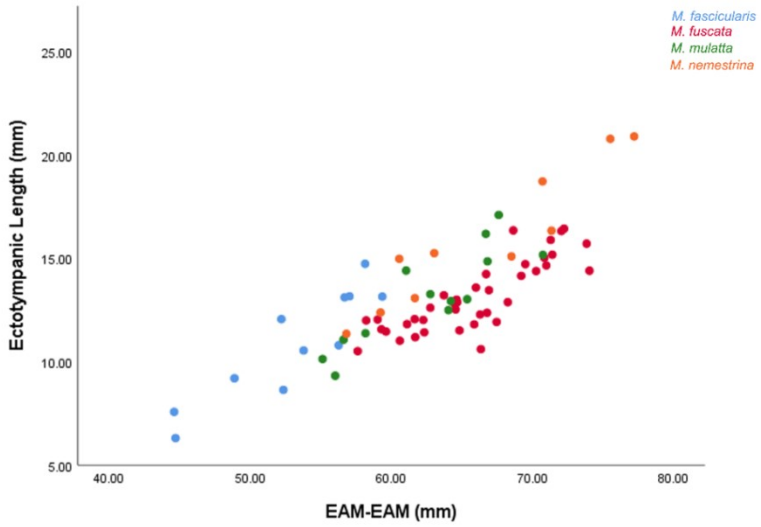

Figure 3.14: Scatterplot showing the linear relationship between macaque ectotympanic length and the inter-EAM difference ($p<0.001$, $R^2=0.67$). This significant relationship was expected and likely a result of overall body size variation.

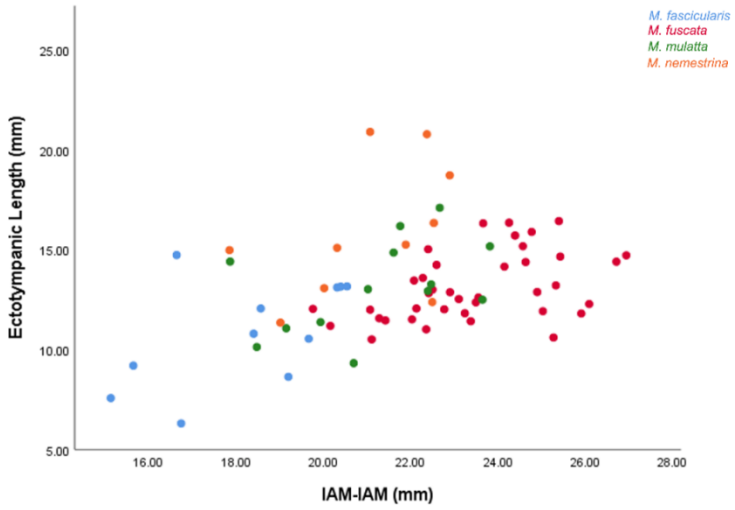

Figure 3.15: Scatterplot showing the poor but significant relationship between macaque ectotympanic length and the distance between internal acoustic meatus ($p<0.001$, $R^2=0.16$). As with Figure 3.14, this was expected and is likely an allometric effect. However, although the correlations with EAM and IAM are both significant, the correlation with EAM is much stronger.

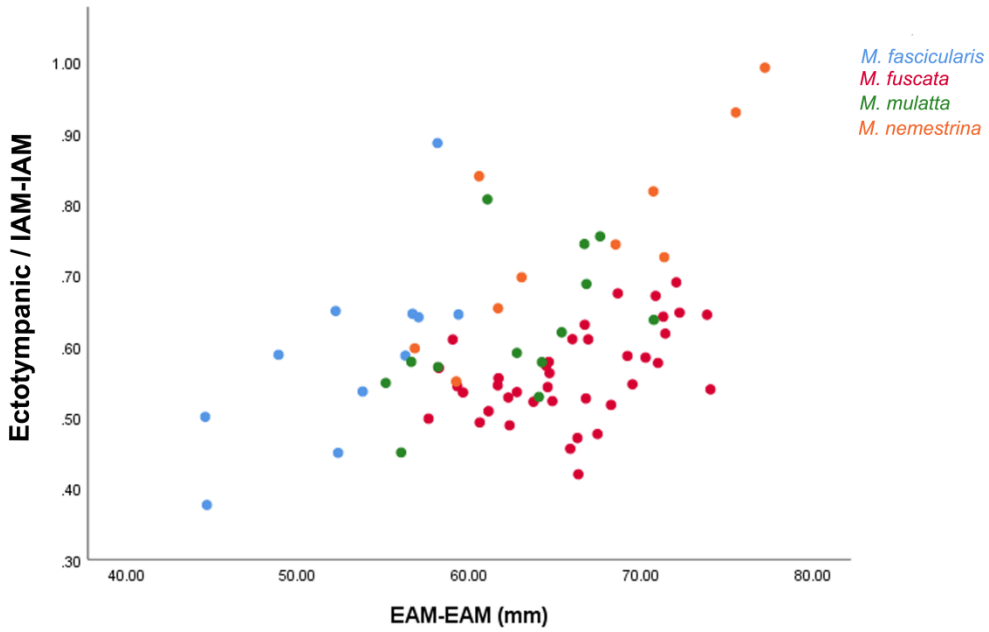

Figure 3.16: Scatterplot showing a significant relationship between the scaled ectotympanic length and the distance between external acoustic meatus (R^2=0.16, p<0.01).

Bivariate analyses show that among humans, while the ectotympanic tube length significantly correlates with cranial base width (BiIAM) and even when scaled for brain size as estimated by the internal acoustic meatus distance the significant relationship with cranial base width remains (EAM: p<0.001, R^2=0.56; IAM: R^2 =0.02, p=0.21; Scaled for IAM: p=0.007, R^2=0.10) (Figures 3.17-3.19).

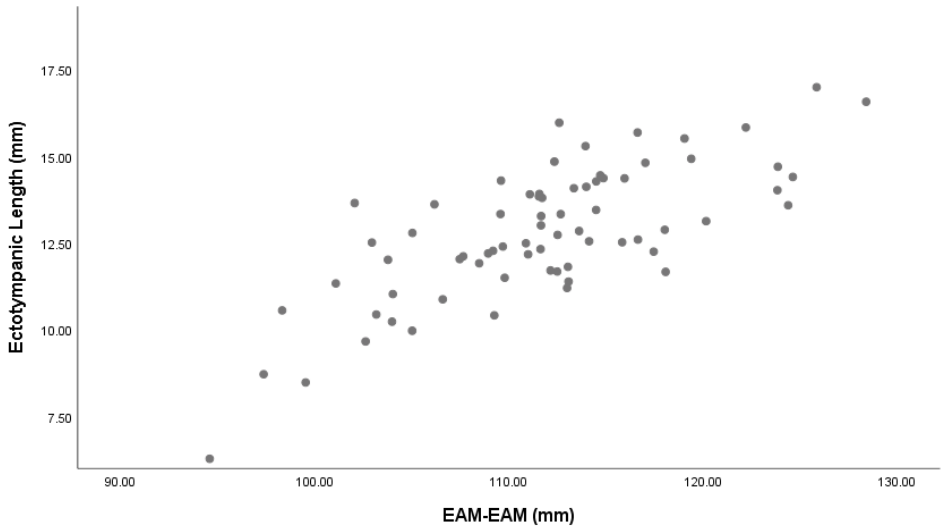

Figure 3.17: Scatterplot showing the significant linear relationship between human ectotympanic length and external acoustic meatus. Much like what is seen among the macaques, the human ectotympanic tube length is strongly correlated with the external measures of cranial base width (R^2=0.56, p<0.01).

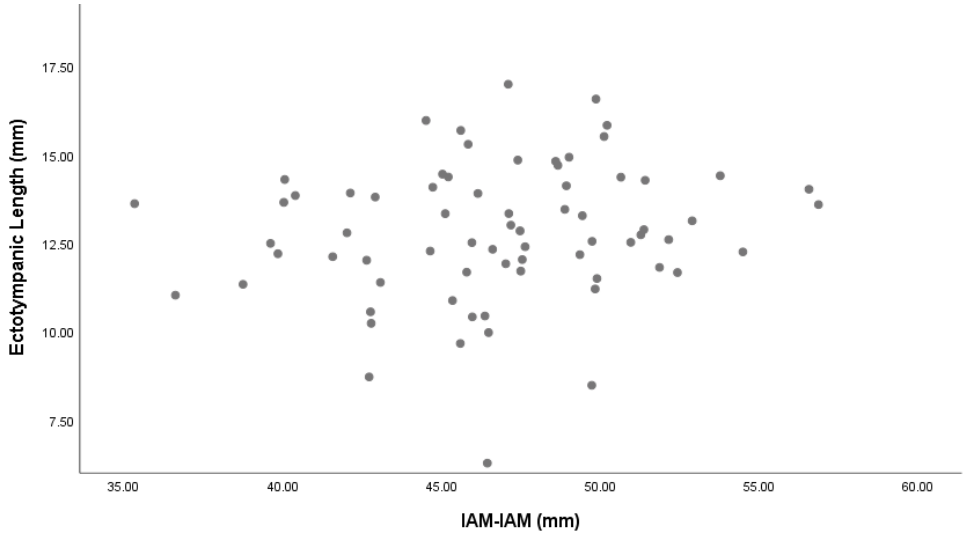

Figure 3.18: Scatterplot showing the insignificant linear relationship between human ectotympanic length and internal acoustic meatus (R^2 =0.02, p=0.21).

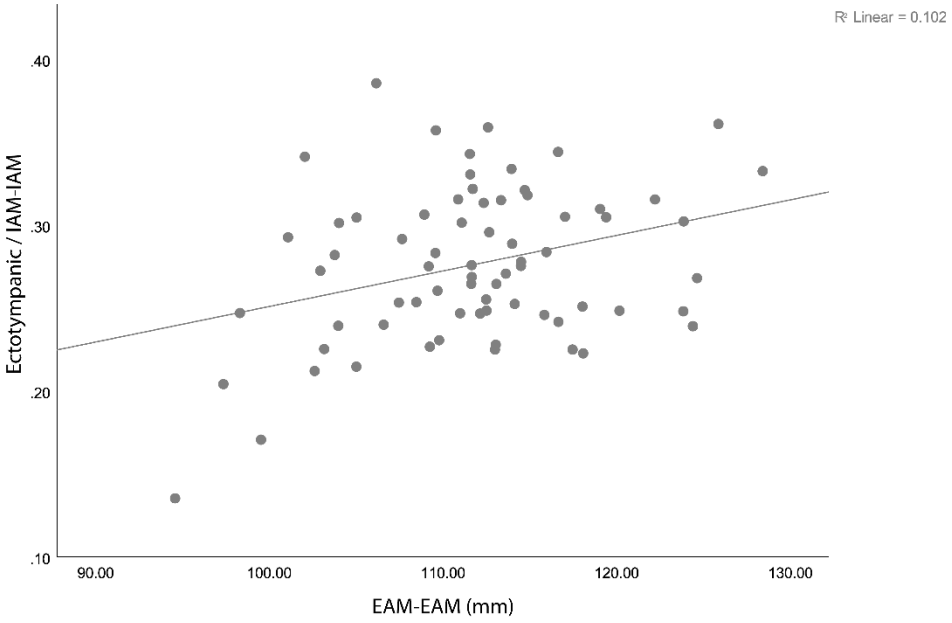

Figure 3.19: Scatterplot showing a significant relationship between the scaled ectotympanic length and the distance between external acoustic meatus. This indicates that even when controlled for size (as approximated via BiIAM distance), the length of the ectotympanic tube is significantly correlated with measure of lateral expansion.

.

Results indicate that ratios of ectotympanic tube length scaled for internal acoustic meatus distance are consistently higher among macaques than humans (Figure 3.20). The macaque sample has twice the degree of variability as the humans, although this was expected because there are four species of macaque and only one species of human.

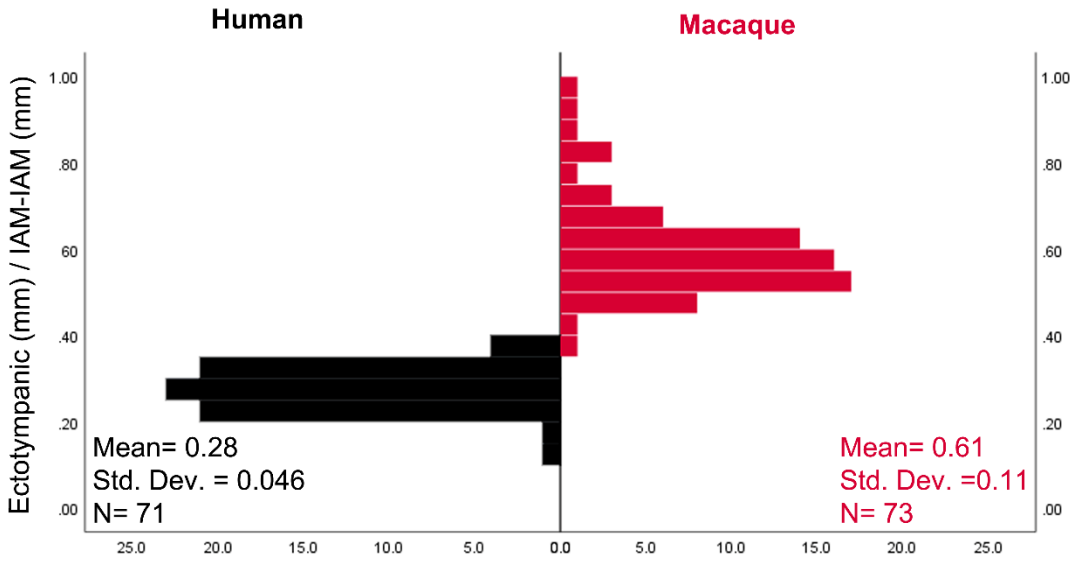

Figure 3.20: Histogram of relative ectotympanic length of humans and macaques. After ectotympanic tube length has been scaled for body size, macaques have longer ectotympanic tubes. Note that the macaque sample actually consists of four species.

Discussion

The results here provide support for the original structural hypotheses which predicted that the ectotympanic lengths in these two taxa are correlated with the lateral expansion of the cranium and brain. While this may seem intuitive or circular, it has not been shown previously that the ectotympanic bone length correlates with these types of global shape changes in any species. Further, the structural hypothesis and results presented here may have implication for the interpretation of ectotympanic bone morphology in extant and extinct primates.

Among macaques, the total cranial base variation did correlate with scaled ectotympanic bone length. When shape was broken out into directional variation (PC scores), geometric morphometric results show that the relative width of the basicranium explains almost all of the variation in ectotympanic tube length. In short, relatively wide macaque crania have relatively long ectotympanic tubes. This result also indicates that

there is important variation in ectotympanic tube length among catarrhines, or at least among macaques, that should be explored and it does not simply scale with body size. These results have broad reaching implications, for example it may be possible to use not only the presence of the ectotympanic tube but also the length of it relative to the basicranial width in identification of phylogenetic signals. In order for this to be useful, however, it will be necessary to measure a wider range of primates.

One of the most intriguing results of this analysis is that the relative length of the ectotympanic tube is greater in macaques than in humans. This result was unexpected as, based on the lateral encephalization hypothesis, the humans should have relatively longer ectotympanic tubes. Humans are frequently cited in the literature as having absolutely and relatively larger brains than other primates, with very large temporal lobes. Additionally, humans and closely related taxa are notably brachycephalic, in other words the brain is expanding in the lateral direction much more than other primates. Given all of these facts, it is surprising that in this chapter it has been shown that the human ectotympanic tube is relatively shorter than that of the macaques. Using gross observation, it is evident that the macaque ectotympanic tube spans a larger portion of the cranial base than those of humans; the macaques' inferior ectotympanic length nearly equals the superior ectotympanic tube length. In other words, the landmarks demarcating the superior and inferior EAM are more-or-less equidistant from the mid-sagittal plane. Among humans, however, the inferior EAM lies grossly medial to the superior EAM.

Inextricably entwined with the shape of the basicranium, are the biological needs of the masticatory system. Among macaques, and many other catarrhines, the inferior part of the origin of the temporalis muscle is immediately superior to the EAM; this also demarcates the lateral edge of the basicranium. A large muscular attachment at the EAM creates a "shelf" in some species, particularly among catarrhines. The temporalis

muscular attachment widens the boundaries of the cranial base, as it has been defined here, in ways that have little to do with endocranial processes. At least among the macaques in the present study, the ectotympanic tube nearly comes to meet the lateral boundary of the bony shelf supporting the temporalis. Though the functional implications are still being debated in the literature, the jaw musculature of humans appears to be reduced in cross-sectional area compared to that of closely related species (Groves, 1970; Daegling, 1989, 2001, Taylor, 2002, 2005, 2006; Taylor and Vinyard, 2013). This reduction in the gross size of the temporalis muscle may be one further reason for the apparent reduction in length of the catarrhine ectotympanic tube between macaques and humans.

Overall shape of the cranial base of humans does vary significantly with relative ectotympanic length, as suggested by the structural hypothesis. This is an important finding, suggesting that total cranial base shape predicts relative ectotympanic length. Further, relative ectotympanic bone length correlates with the specific variation associated with relative brachycephaly and dolichocephaly. The first principal component among humans, like in macaques, is capturing the relative brachycephaly or dolichocephaly of the individual. Human scaled ectotympanic bone morphology significantly correlates with PC1, which describes the same cranial structure as the PC1 of the macaque head (brachycephaly or dolichocephaly). Therefore, the human ectotympanic tube is certainly affected by relative cranial width in a similar way as the macaques. However, the relative ectotympanic bone length in humans correlated best with PC4. PC4 is showing some broadening of the cranial base and more importantly flexion of the basicranium. Thus, the length of the ectotympanic tube in humans is also related to the degree of flexion in basicranium. Basicranial flexion has been well studied as a hominin adaptation that is associated with a variety of other biological processes, most importantly encephalization and the transition to bipedality. As the brain grows

long, in order to maximize endocranial space, the basicranium creates a hinge at the middle cranial fossa. However, like most characteristics, basicranial flexion is not simply a presence/absence issue but instead exists on a continuum (Ross and Ravosa, 1993).

The spatial packing hypothesis suggests that the basicranium flexes to accommodate the expanding brain in the anterior-posterior direction (i.e., Moss, 1958; Gould, 1977; Strait, 1999; McCarthy, 2001); it is possible that the human brain "outgrows" its basicranial capacity in the lateral direction, which is one potential explanation for their relatively short ectotympanic tubes. While the soft tissues are not tested here, it is tempting to suggest that the unique lateral rounding out of the brain in humans may reduce the constraint on the ectotympanic bone length. Lateral rounding, or lateral "globularization" of the human brain, may be one reason the expected relationship between lateral encephalization and ectotympanic tube length is not as strong in humans as in macaques. That being said, total cranial base variation in humans is still predicting the relative ectotympanic length.

Thus, while the human ectotympanic tube length is certainly affected by the general width of the cranium, there is a modulating effect of basicranial flexion that is *stronger* than those of the width of the cranium. This goes counter to the expectation set forth in this chapter but is not entirely surprising if we look to the history of literature concerning the uniqueness of human cranial structure. Some paleoanthropologists have noted the reduction of the inferior ectotympanic tube (often referred to as the tympanic plate in hominins) length and shifted orientation among hominins. For example, between the robust and gracile australopiths, the tympanic plate is described as being shorter and more vertically oriented among the australopiths that have larger brains and more flexed crania(Walker and Leakey, 1988). This orientation shift was also seen within humans in the present study, the relative ectotympanic length in humans was correlated with orientation of the ectotympanic tube. Humans and macaques with relatively long

ectotympanic bones tend to have horizontally oriented tubes. Among humans, more pronounced basicranial flexion is associated with shorter, more inferiorly angled ectotympanic bones.

Some limitations are important to acknowledge here; including that only macaques and humans have been examined. This was intentional to allow for an in depth analysis and high statistical power, but these are two distinct lineages and that always presents problems when making direct comparisons. Additionally, four species of macaque were lumped into one analysis and then compared to one species of *Homo*. Therefore, the assumption of equal variance in the two taxa is violated and thus all direct comparisons of these two lines of inquiry should be taken with a grain of salt. The analyses for humans and macaques are mostly kept separate, as the direct comparison of two such disparate species would be uninformative without a broader evolutionary history. The results of these two studies in conjunction are qualitatively discussed, however, which presents a potential problem. Chapter 4 may be consulted for a broader evolutionary picture that includes many species of primates.

Conclusion

This study presents evidence that there is significant variation in the ectotympanic bone among catarrhines, both among macaques, and between macaques and humans. The relative ectotympanic length can be predicted from the cranial structure, particularly the relative width of the cranium, in these two groups. Therefore, lateral expansion in the brain is key to understanding how and why the ectotympanic tube lengthens within taxa. The human ectotympanic tube is certainly affected by the width of the brain and the skull but the flexion of the basicranium likely modulates the direct effects of brain growth on the ectotympanic tube. It is also shown here that within the human basicranium, large basicrania tend to have short, inferiorly angled

ectotympanic tubes, supporting anecdotal evidence from the human fossil record. In order to understand better the true meaning of the differences seen between macaques and humans, more species must be included.

4. Geometric Morphometric Analysis of the Primate Ectotympanic Bone with Special Reference to the Fossil Record

Introduction

The form of the ectotympanic bone has been an important phylogenetic marker among primates for the last century but the proximate mechanism by which it varies across primates has yet to be shown (Gregory, 1920; Saban, 1963; Hershkovitz, 1974; Simons, 1974; Cartmill, 1982; MacPhee and Cartmill, 1986). As applied to primate phylogenetic studies, the ectotympanic tube is generally coded as an independent cranial characteristic that can either be present or absent, when a tube is absent it takes the form of an ectotympanic ring which may or may not be encased in a petrosal bulla (e.g., Gingerich, 1981b; Szalay et al., 1987; Simons and Rasmussen, 1989). An auditory bulla is an inflated bubble of petrosal bone that encases the middle ear and in some species part of the ear canal. Among primates the bulla is derived from the petrosal ossification center (MacPhee, 1979). Taken in the context of the surrounding structures, there are five morphotypes of ectotympanic bone that fall along taxonomic lines. Those morphotypes include: 1) a free-floating bony ectotympanic ring within an auditory bulla (lemuriform); 2) a bony ectotympanic ring fused to the lateral side of an inflated petrosal bulla (lorisiform); 3) an ectotympanic bone that is elongated and fused to the lateral side of an inflated petrosal bulla (tarsiiform); 4) a bony ectotympanic ring fused to the lateral petrosal-derived middle ear cavity that is not inflated (platyrrhine); 5) fully bony ectotympanic tube that extends from the tympanic membrane to meet the squamosal portion of the temporal bone (catarrhine) (Figure 1.1; e.g.. Piveteau, 1957; Fleagle, 2013). These morphotypes are undoubtedly phylogenetically constrained as they follow strict taxonomic lines in extant species, but the precise nature of how they vary and the evolutionary forces at work are not well understood. The present study will investigate how cranial structure potentially influences the ectotympanic bone across primates.

This chapter suggests that the changes we see in ectotympanic bone morphology across the primate tree are likely evolutionary by-products of other structural changes in the cranium that are under selection, such as brain size and shape, relative orbit size, and auditory function. The results of Chapter 3 indicated that ectotympanic bone length in humans and macaques has strong correlations with cranial base shape variables — particularly those variables associated with relative cranial base width. The present study identifies structural correlates and provides spatial and functional context for this important phylogenetic marker, which can then be used in the interpretation of fossil remains.

The ectotympanic bone is one portion of the temporal bone complex within the primate cranium. It is a C or U-shaped bone that is fused to the inferior aspect of the petrous (Saban, 1963). All mammals possess an ectotympanic bone in some form that supports the tympanic membrane (Maier and Ruf, 2016a). At the base of the primate tree, omomyids and adapids each demonstrate a mosaic of character states seen in extant primates; importantly for the present study, they vary in their auditory regions. Adapids are often described as lemuriform, and omomyids are tarsiiform in several respects, specifically some, though not all, omomyids are described as possessing a tubular ectotympanic bone similar to that of the modern tarsier (Luckett, 1976; Szalay, 1977; Conroy, 1980; Gingerich, 1980; Cartmill, 1982; Szalay et al., 1987; Miller et al., 2005; Rossie et al., 2006); notable exceptions to this are *Shoshonius* (Beard and MacPhee, 1994) and *Omomys* (Burger, 2010). The precise relationships of early anthropoids have been debated for many years (e.g, Cartmill et al., 1981; Rasmussen, 1986; Kay et al., 2004), and the ancestral state of the ectotympanic bone is central to that argument. The ancestral state may have been lemuriform, lorisiform, or tarsiiform. Many non-primate mammals are similar to the lemuriform arrangement with a ring instead of a tube but notably the current molecular phylogenies place the sister taxon of

primates as Dermoptera (Perelman et al., 2011) which possess a fused ectotympanic ring similar to modern lorisiforms and tarsiers (Wible and Martin, 1993).

Lorisiforms also possess an auditory bulla but among lorisiforms, the ectotympanic bone fuses to the lateral side of the bulla thus making it extra-bullar (phaneric). An additional lorisiform characteristic is the “aditus”, a bony and soft tissue ridge that divides the bulla into two chambers. The functions of many of these auditory adaptations are still debated (Packer and Sarmiento, 1984; Coleman, 2007; Ramsier, 2010). It has been argued that this lorisiform aditus and two-chambered system optimizes the lorisiform ear for both low and high-frequency hearing that is particularly important for the lorisiforms (Lombard and Hetherington, 1993; Ross, 2000). More recent auditory functional analyses, however, have shown that anthropoids have better low-frequency sensitivity than strepsirrhines as a whole (Coleman and Ross, 2004; Coleman, 2009). Coleman and Colbert (2010) further found that lorises and lemurs have the best high-frequency hearing among the extant primates and Ramsier et al. (2012a) has shown that tarsiers, who also have a second chamber, have some of the best high frequency hearing. Thus, overall, expanded middle ear chambers like those seen in animals with inflated bullae, appear to be correlated with high-frequency auditory sensitivity. The reduction of the auditory bulla, and selection for better low frequency hearing, is one potential explanation for the elongation of the ectotympanic bone. In other words, it is possible that as the middle ear is reduced across phylogeny, the ear canal grows in response.

Tarsiers maintain an expanded middle ear despite their phylogenetic position aligning them with anthropoids. The tarsiers’ mix of primitive and derived morphologies are complicated, and the relative position of the tarsier in this evolutionary story has been the subject of great debate (Cartmill, 1982; Rosenberger, 1985; Kay et al., 2004) but has recently been resolved using molecular evidence (Shoshani et al., 1996;

Perelman et al., 2011). The phylogenetic position of modern tarsiers is now known, but their specific suite of unusual adaptations are still of great interest to anthropologists (e.g., Ramsier et al., 2012; Smith et al., 2013; DeLeon et al., 2016). The tarsier ectotympanic bone has been described as tubular and elongate when compared to the lorisiform morphology but is not as long as in catarrhines (Hershkovitz, 1974).

The three extant haplorhine ectotympanic bone morphotypes include tarsier (tube), platyrrhine (ring), and catarrhine (tube). This diversity in ectotympanic morphology within haplorhines has never been well reconciled and it is suggested here that the similarities between tarsiers and catarrhines may be structural. Do catarrhines and tarsiiformes have cranial structures that make it more likely for the ectotympanic bone to elongate in a similar way to the exclusion of platyrrhines? The striking difference between platyrrhine and catarrhine ectotympanic bone morphologies has received comparatively little attention. The lengths of the anthropoid ectotympanic bones are the most divergent of any closely related groups, but shockingly few examples of intermediate conditions. Two fossil catarrhines that have been described exhibiting "intermediate" ectotympanic bone condition are *Aegyptopithecus zeuxis* and *Pliopithecus vindobonensis* (Zapfe, 1958, 1960; Begun, 2002).

The ear tube of *A. zeuxis* (30-35 Ma, North Africa) has been controversial in its interpretation since its discovery. Simons (1972) described the ectotympanic tube of *Aegyptopithecus* as "narrow" and indicated that the ectotympanic tube is abnormally shortened; he further drew cranial morphological comparisons between *Aegyptopithecus* and ceboids. Gingerich (1973), in a survey of Fayum catarrhines, described *Aegyptopithecus* (as well as *Apidium*) as much more similar to lemur morphology with a possible intra-bullar (apharenic) ectotympanic ring. Reassessment by Cartmill et al. (1981) found that "either end of the ectotympanic, as we identify it on the Fayum fossils, differs significantly from the equivalent parts of the ectotympanic in platyrrhines" (Cartmill

et al., 1981, p. 13). Some descriptions assess *Aegyptopithecus* as having a bony ectotympanic tube, though the tube is described as unusually short (Begun, 2002). Later, based on a new and relatively complete cranium, Simons et al. (2007) describe the ectotympanic as having a ragged lateral margin, a primitive characteristic for an early catarrhine, which is more marked on the dorsal side where it is protected from breakage. Ragged margins are often associated with the platyrrhine-like conditions, referring to the bumpy lateral margins of the ectotympanic bone. In contrast, the catarrhine lateral margin is generally smooth (Saban, 1963; Starck, 1967) .

Much more recently in the fossil record, some pliopithecoid primates (7-17 Ma, Eurasia) have also been described as “intermediate” in the condition of the ectotympanic tube (Zapfe, 1958; Andrews et al., 1996; Harrison, 2005). In Zapfe’s original description of *Pliopithecus vindobonensis*, he described the ectotympanic condition as an “extremely short external auditory meatus which is deeply notched on the lower side so that it is divided into two granular projections…representative of a primitive stage of development of the bony auditory meatus of the catarrhines” (Zapfe, 1958 p. 445). The intermediate ectotympanic bone of *P. vindobonensis* requires further analysis to understand how unusual the ectotympanic bone morphology is from a quantitative perspective. The present study will place ectotympanic bone morphology, including *P. vindobonensis* and *A. zeuxis*, in the context of greater cranial base shape variation among primates including the relative positions of lateral cranial structures.

Hypotheses

H1: If the lateral expansion of the cranial base drives the length of the ectotympanic tube, then cranial base shape should be correlated with scaled ectotympanic bone length across primates.

H1a: Further, the PC scores associated with brachycephaly and dolichocephaly will be the shape variables most correlated with scaled ectotympanic bone length.

H2: If the lengthening of the ectotympanic bone is a response to reduction of the middle ear, then ectotympanic length will be negatively correlated with the dorsoventral height (the amount that the bulla projects below the cranial base) of the middle ear.

H2a: This relationship will remain significant when scaled for head size.

H3: If ectotympanic morphology is correlated with cranial shape, then in all analyses, *A. zeuxis* and *P. vindobonensis* will fall within catarrhines and measures of ectotympanic length for both species will be lower than modern catarrhines.

Materials and Methods

Sample

This study examines the relationship between the ectotympanic bone and other related structures in basicranial shape variation. Using three-dimensional (3D) geometric morphometrics to understand the ectotympanic as it relates to general cranial structure in a wide sample of primates. A total of 56 individuals representing 20 extant genera of primates were included in this study (Table 4.1). This includes 3 genera of platyrrhine, 6 genera of catarrhines, 4 genera of hominoids, 2 species of lorises, 4 genera of lemurs and 1 genus of tarsier. Additionally, the two fossil taxa (*A. zeuxis* and *P. vindobonensis*) were included wherever possible.

Data Acquisition and Preparation

Three-dimensional surfaces were created based on stacks of digital CT images (either TIF or DICOM) in Amira 5.6 or 6.3 (FEI Houston, Inc.) and measurements were taken from those models. All analyses on extant primates were performed using micro-CT scans from the Digital Morphology Museum of the Kyoto University Primate Research Institute (KUPRI, dmm.pri.kyoto-u.ac.jp) and Morphosource housed at Duke

University (https://www.morphosource.org/). For illustration, the ectotympanic bone was segmented out as an individual surface using Amira software; this was done by first identifying the crista tympanica, or the ridge of bone that supports the tympanic membrane, and working laterally until a suture, or the free surface was reached. Scans of *A. zeuxis* were obtained via Morphosource, and permissions were granted by the scans owners Alan Walker and Timothy Ryan. Scans of *P. vindobonensis* were graciously loaned by Dr. Fred Spoor and the Natural History Museum of Vienna.

Table 4.1: Species included

Genus	Species	Taxon	N	Location	Voxel size (mm)
Aegyptopithecus	*zeuxis*	Fossil Catarrhine	2	CGM; DLC	0.056x0.056x0.064; 0.041x0.041x0.41
Pliopithecus	*vindobonensis*	Fossil Catarrhine	1	NHMV	XXX
Callimico	*goeldii*	Platyrrhine	2	AMNH	0.041x0.041x0.041; 0.036x0.036x0.036
Callithrix	*argentata*	Platyrrhine	3	MCZ	0.041x0.041x0.041; 0.041x0.041x0.041; 0.041x0.041x0.041
Lagothrix	*lagotricha*	Platyrrhine	2	NMNH	0.060x0.060x0.060; 0.058x0.058x0.058
Cercocebus	*torquatus*	Catarrhine	2	KUPRI	0.21x0.21x0.2; 0.23x0.23x0.23
Cercopithecus	*petaurista*	Catarrhine	2	KUPRI	0.2x0.2x0.2; 0.2x0.2x0.2
Colobus	*guereza*	Catarrhine	2	KUPRI	0.2x0.2x0.5; 0.2x0.2x0.5
	polykomos	Catarrhine	3	KUPRI	0.2x0.2x0.2 0.2x0.2x0.2 0.25x0.25x0.5
Macaca	*fuscata*	Catarrhine	4	KUPRI	0.26x0.26x0.20; 0.31x0.31x0.2; 0.26x0.26x0.20 0.26x0.26x0.20
Papio	*hamadryas*	Catarrhine	3	KUPRI	0.2x0.2x0.2; 0.25x0.25x0.2; 0.25x0.25x0.2
Presbytis	*femoralis*	Catarrhine	2	KUPRI	0.2x0.2x0.2; 0.2x0.2x0.2;
	melalophos	Catarrhine	1		0.2x0.2x0.2
Theropithecus	*gelada*	Catarrhine	3	KUPRI	0.31x0.31x0.31; 0.25x0.25x0.2; 0.25x0.25x0.2
Gorilla	*gorilla*	Hominoid	3	KUPRI	0.50x0.50x0.50; 0.38x0.38x0.50; 0.35x0.35x0.2
Homo	*sapiens*	Hominoid	3	ORSA	0.6x0.6x0.6; 0.6x0.6x0.6; 0.6x0.6x0.6;
Pongo	*pygmaeus*	Hominoid	3	KUPRI; MCZ; MCZ	0.40x0.40x0.30; 0.13x0.13x0.13; 0.10x0.10x0.10
Symphalangus	*syndactylus*	Hominoid	3	AMNH; MCZ; MCZ	0.062x0.062x0.062; 0.075x0.075x0.075; 0.074x0.074x0.074
Galago	*senegalensis*	Loris	2	AMNH; DLC	0.025x0.025x0.025; 0.028x0.028x0.028
	alleni		1	AMNH	0.024x0.024x0.0.024
Nycticebus	*coucang*	Loris	2	AMNH; DLC	0.04x0.04x0.04; 0.043x0.043x0.043
Daubentonia	*madagascariensis*	Lemur	1	AMNH	0.072x0.072x0.072
Eulemur	*macaco*	Lemur	2	AMNH	0.07x0.07x0.07; 0.058x0.058x0.058
Indri	*indri*	Lemur	1	AMNH	0.12x0.12x0.12

Cheirogaleus	*major*	Lemur	1	AMNH	0.033x0.033x0.033
Tarsius	*tarsier*	Tarsier	1	NMNH	0.023x0.023x0.023
	bancanus	Tarsier	1	AMNH	0.045x0.045x0.045
	spectrum	Tarsier	1	AMNH	0.033x0.033x0.033

DLC= Duke Lemur Center, AMNH= American Museum of Natural History, NMNH=National Museum of Natural History, KUPRI=Kyoto University Primate Research Institute Digital Morphology Museum, MCZ=Museum of Comparative Zoology, CGM= Cairo Geological Museum, NHVM=Natural History Museum of Vienna, ORSA=Open Research Scan Archive

Fossil reconstruction

Fossils by nature are often fragmentary and can be deformed. Two crania of the species *Aegyptopithecus zeuxis* were examined for the present study (CGM-85785 and DPC-5401). CGM-85785 is a remarkably intact whole cranium of a suspected female; it is only slightly plastically deformed. The minor deformation was corrected by retro-deforming the fossil surface to regain a more normal shape. Plastic deformation was reduced using algorithmic symmetrization (Wiley et al., 2005) in Landmark Editor using the retrodeformation plug-in (Tallman et al., 2014). A similar protocol was employed for the DPC-5401 fossil, with the added step of reassembling three fragments using Geomagic studio software (3D Systems®, Cary, NC). CGM-85785 is a good deal smaller than DPC-5401 and has been suggested to be a female while DPC-5401 is slightly larger and its sex is less obvious (Simons et al., 2007). For inclusion of *A. zeuxis* in the 3D GM analyses, only CGM-85785 was used, as it had almost all of the relevant loci for landmark placement. DPC-5401 was examined qualitatively.

P. vindobonensis fragments are not complete enough to be included reliably in 3D GM analyses. An additional limitation is that the distance between internal acoustic meatus (BIAM distance), the chosen scaling factor for this dissertation (see below) was not preserved in this species. The gross ectotympanic morphology is qualitatively compared to that of platyrrhines and catarrhines to either corroborate or reject the conclusion that the ectotympanic tube is “incompletely ossified” (Zapfe, 1958, 1960; Andrews et al., 1996; Begun, 2002). It is expected that both fossil crania will fall to the

low end of catarrhines and the ectotympanic bone length will be somewhat intermediate between the catarrhine and platyrrhine forms.

Data Acquisition and Preparation

To identify structural correlates and put ectotympanic variation in the context of general cranial anatomy, a 3D geometric morphometric study was undertaken. A total of 50 homologous landmarks were placed across the crania using Amira Software and analyzed using MorphoJ (Klingenberg, 2011), R (R Core Team, 2013), and RStudio (RStudio, 2015) (Table 3.2).

Table 4.2: Landmarks

Landmark (Fixed)	Side	Region
Inferior external acoustic meatus	Bilateral	Cranial base
Superior external acoustic meatus	Bilateral	Cranial base
Superior Tympanic Ring	Bilateral	Cranial base
Inferior Tympanic Ring	Bilateral	Cranial base
Petrous apex	Bilateral	Cranial base
Carotid canal	Bilateral	Cranial base
Stylomastoid foramen	Bilateral	Cranial base
Lateral jugular fossa	Bilateral	Cranial base
Superior middle ear	Bilateral	Cranial base
Inferior middle ear	Bilateral	Cranial base
Anterior articular eminence	Bilateral	Cranial base
Lateral articular eminence	Bilateral	Cranial base
Inferior post-glenoid process	Bilateral	Cranial base
Temporal zygomatic arch	Bilateral	Cranial base
Basion	Center	Cranial base
Foramen caecum point	Center	Cranial base
Sphenobasion	Center	Cranial base
Opisthion	Center	Cranial base
Euryon	Bilateral	Whole cranium
Stephanion	Bilateral	Whole cranium
Internal acoustic meatus	Bilateral	Whole cranium
Alveolon	Bilateral	Whole cranium
Bregma	Center	Whole cranium
Glabella	Center	Whole cranium
Inion	Center	Whole cranium
Incisive canal	Center	Whole cranium

Whole cranium landmarks were taken and used to calculate interlandmark distances but were eliminated from shape analyses as they were reflecting shape variation in the face and neurocranium that were irrelevant for the current study.

Table 4.3: Linear Distances

1	Length of the inferior ectotympanic taken from the most inferior point of the tympanic ring to the inferior external acoustic meatus
2	Length of the superior ectotympanic taken from the most superior point of the tympanic ring to the inferior external acoustic meatus
3	Distance between right and left euryon
4	Distance between right and left internal acoustic meatus
5	Distance between right and left external acoustic meatus
6	Height of the middle ear, the distance landmarks placed at the superiormost and ineriormost extensions of the middle ear at the mid-ectotympanic plane.
7	Lateral encephalization quotient: (BiEuryon-BiEAM)/BiIAM

Interlandmark distances were calculated to extract several important linear variables, including superior and inferior ectotympanic length (Table 4.3). Ectotympanic bone lengths were calculated on both the right and left, and then averaged to reduce the effects of bilateral asymmetry not relevant to this chapter. Cranial width was analyzed in two ways here; an internal measurement (BiIAM) and an external measurement (BiEAM). In this way, cranial width could be understood with and without the auditory structures. In general, ectotympanic bone length was scaled by BiIAM distance. BiIAM was chosen as the size scaling factor because it accounts for the cranial width without including the lateral most basicranium, which potentially captures variation that is highly dependent on the location of the auditory structures (see Chapter 2). Middle ear height was calculated as a proxy for middle ear volume. Ectotympanic bone lengths were also scaled by body mass in one analysis in order to visualize the relative position of the fossils as BiIAM was not preserved in the *P. vindobonensis* fossil. Body masses were estimated using the area of the first maxillary molar for extant taxa (Gingerich and Smith, 1982).

A second ratio calculated in this chapter is the Lateral Encephalization Quotient (LEQ). In Chapter 3, it was suggested that one reason the human ectotympanic tube is shorter than expected given our overall cranial structure, is the degree of “globularity” in the genus *Homo*. This hypothesis is tested here using the wide range of primates analyzed in this chapter. Globularity refers to the “rounding out” of the human brain in

such a way that it maximizes the surface area and brain volume. In order to test whether the degree of globularity affects the length of the ectotympanic tube, particularly among humans, LEQ was derived from the interlandmark distances in these primates. The LEQ was designed to describe how much the superior brain is “outgrowing” the cranial base by taking the widest point of the neurocranium (BiEuryon), subtracting the width of the basicranium (BiEAM) and then scaling by dividing by BiIAM.

Data analysis

A full Procrustes superimposition fit was performed in MorphoJ and RStudio, reducing the effects of size, rotation, and translation. Full Procrustes fit was employed here as it is more resistant to the effects of large amounts of size variation and has been noted to be slightly more robust to the effect of outliers (Klingenberg, 2011). Genus averages were calculated by performing a Procrustes fit on each genus, all across species analyses were performed using these genus means.

Hypothesis 1 was tested using a procD.lm analysis, in the Geomorph R package (R Core Team, 2013; Adams et al., 2017); this tests for the significance of a relationship using between an independent variable (scaled ectotympanic length) and cranial shape. PC scores were used to test for significant correlation with scaled ectotympanic bone length using multivariate regression.

Hypotheses 2 and 3 were tested using correlation analysis between height of the middle ear and the ectotympanic bone length and using partial correlations to control for the effects of head size using both the chosen scaling factor (BiIAM) and centroid size. The LEQ was tested for correlation with scaled ectotympanic length.

Results

3D Visualizations of the Ectotympanic Bone across Taxa

Visual representations of the positions of the ectotympanic bones in several sample species are provided in Figures 4.1-4.5. The ectotympanic bones are highlighted in color. *P. vindobonensis* (Figure 4.6) and *A. zeuxis* (Figure 4.7) ectotympanic images are provided as well.

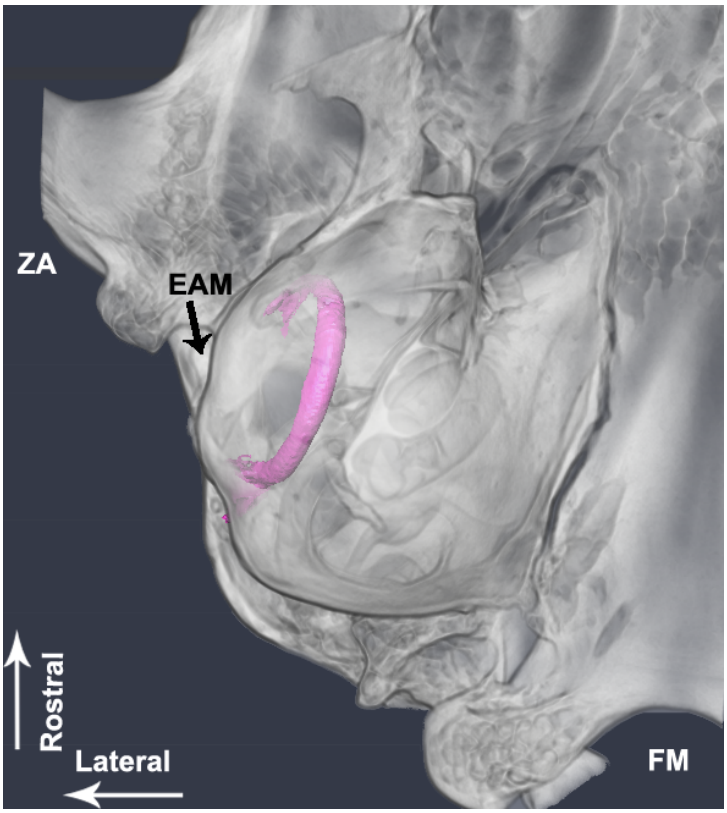

Figure 4.1: Lemuriform ectotympanic bone, *Eulemur macaco*. The lemur ectotympanic ring is seen here in pink ghosted through the auditory bulla. The lemuriform ectotympanic bone is a ring, attached only at the superior crura, with the rest freely floating within the auditory bulla. ZA= Zygomatic Arch, FM=Foramen Magnum, EAM=External Auditory Meatus.

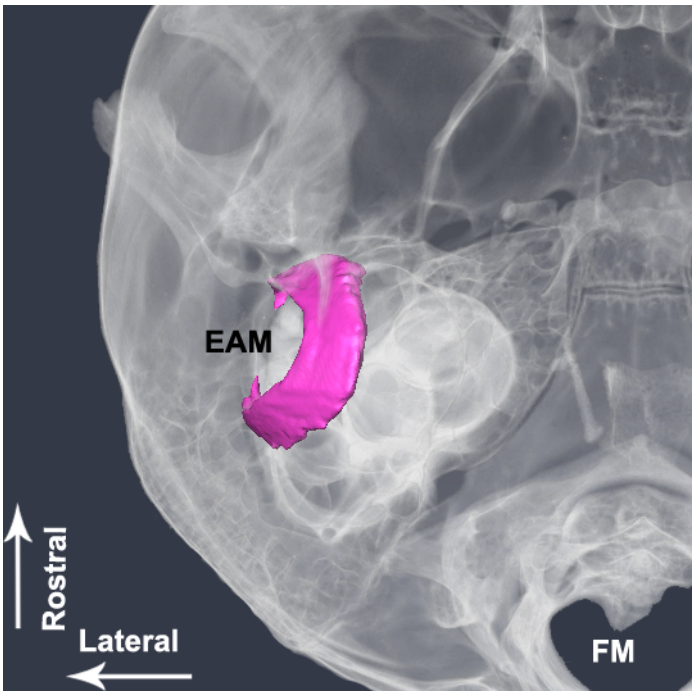

Figure 4.2: Lorisiform ectotympanic bone, *Galago senegalensis*. The lorisiform ectotympanic ring is seen here in pink, it is fused to the lateral side of the slightly deflated auditory bulla. The ectotympanic-petrosal suture is visible in this example, a *Galago*. The lorisiform ectotympanic bone is grossly longer than the lemuriform condition. FM=Foramen Magnum, EAM=External Auditory Meatus.

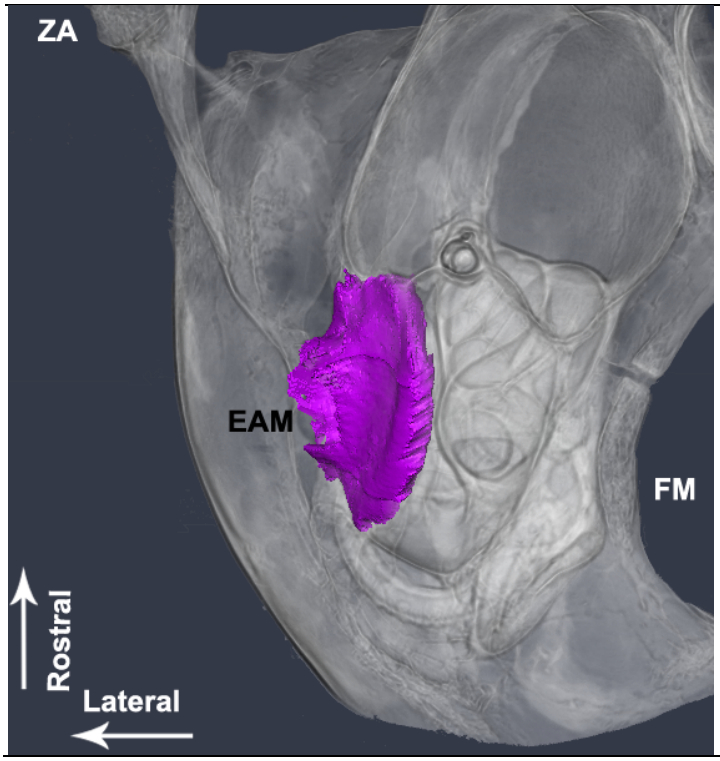

Figure 4.3: Tarsier ectotympanic bone, *Tarsius tarsier*. The tarsier ectotympanic tube is seen here in purple. The lateral edge is "ragged" and poorly defined. It is certainly longer than those seen in the lorisiforms and lemuriforms. Additionally, comparing the lorisiform and tarsiiform conditions, the tarsiiform exhibits a constriction laterally in the ear canal diameter. ZA= Zygomatic Arch, FM=Foramen Magnum, EAM=External Auditory Meatus.

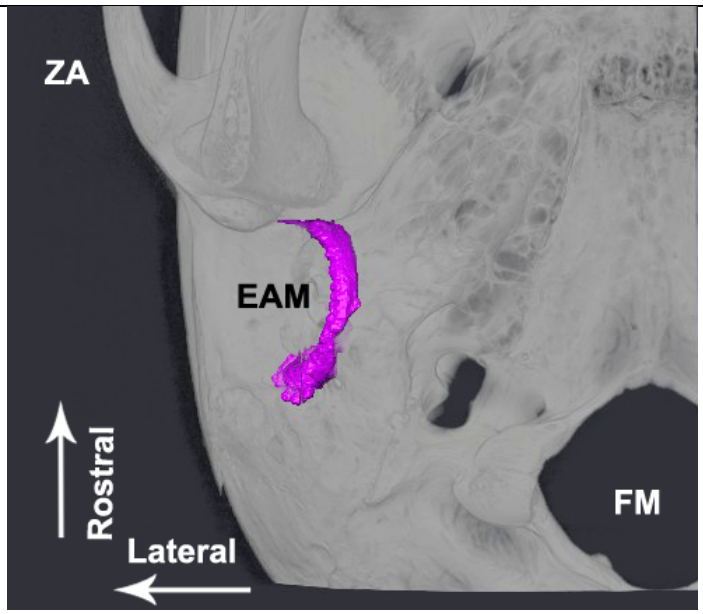

Figure 4.4: Platyrrhine ectotympanic bone, *Lagothrix lagotricha*. The platyrrhine ectotympanic bone is relatively shorter than the tarsier or the lorisiforms. The external auditory meatus (EAM) is relatively wider when compared to surrounding structures than observed in the catarrhine EAM. Note the beaded condition of the EAM, this was seen in all included platyrrhines. ZA= Zygomatic Arch, FM=Foramen Magnum, EAM=External Auditory Meatus.

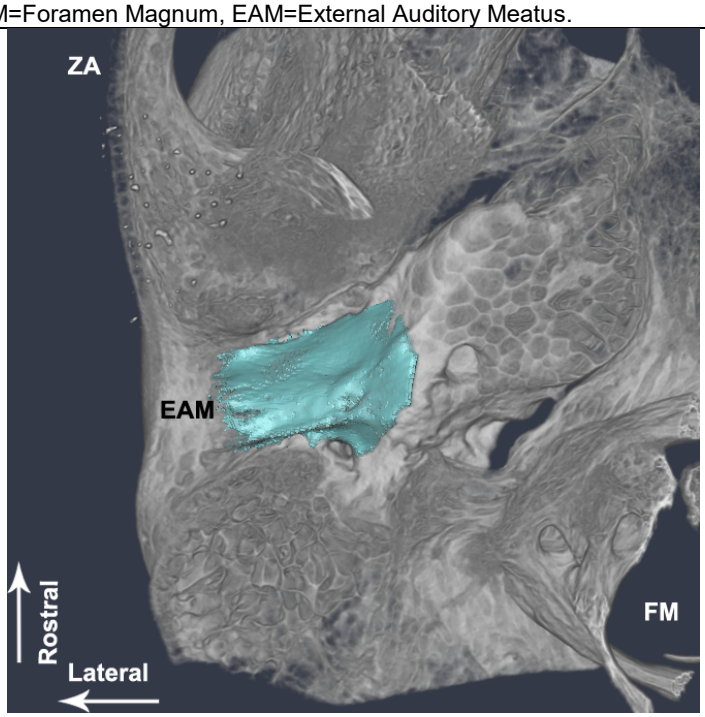

Figure 4.5: Catarrhine ectotympanic bone, *Macaca fuscata*. The catarrhine ectotympanic tube is seen here in blue. The lateral edge of the EAM is more clearly defined; most of the "ragged" edge seen in other taxa has filled in. It is relatively narrow when compared to surrounding structures. ZA= Zygomatic Arch, FM=Foramen Magnum, EAM=External Auditory Meatus.

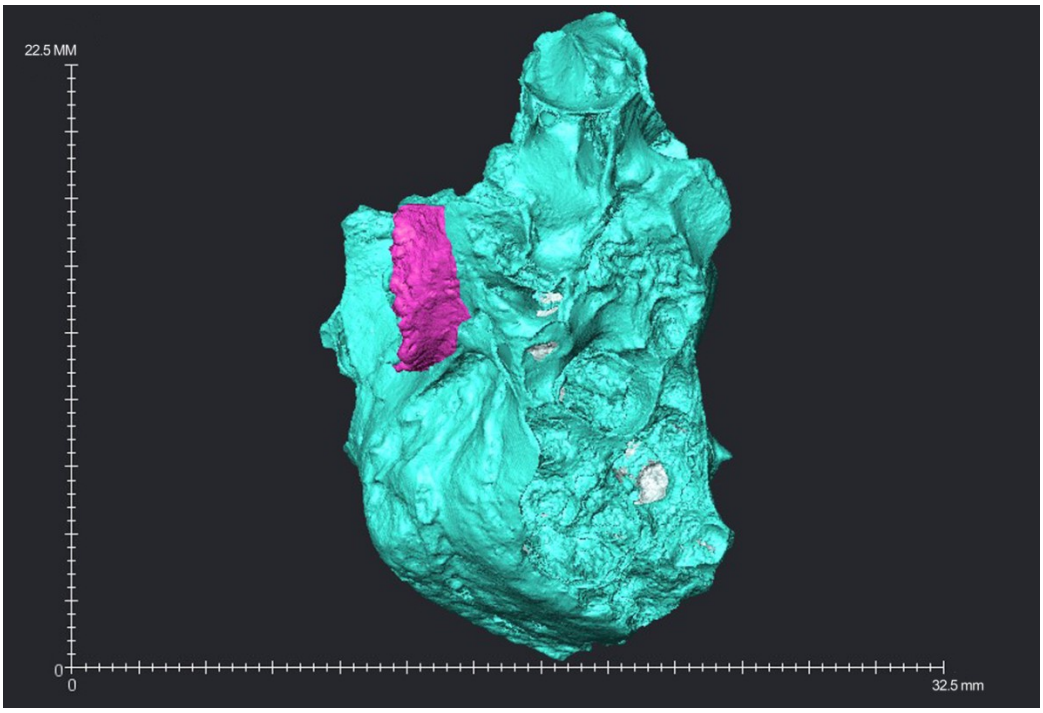

Figure 4.6: *P. vindobonensis* right temporal bone with ectotympanic highlighted in pink. Note the wide EAM diameter and beaded lateral edge.

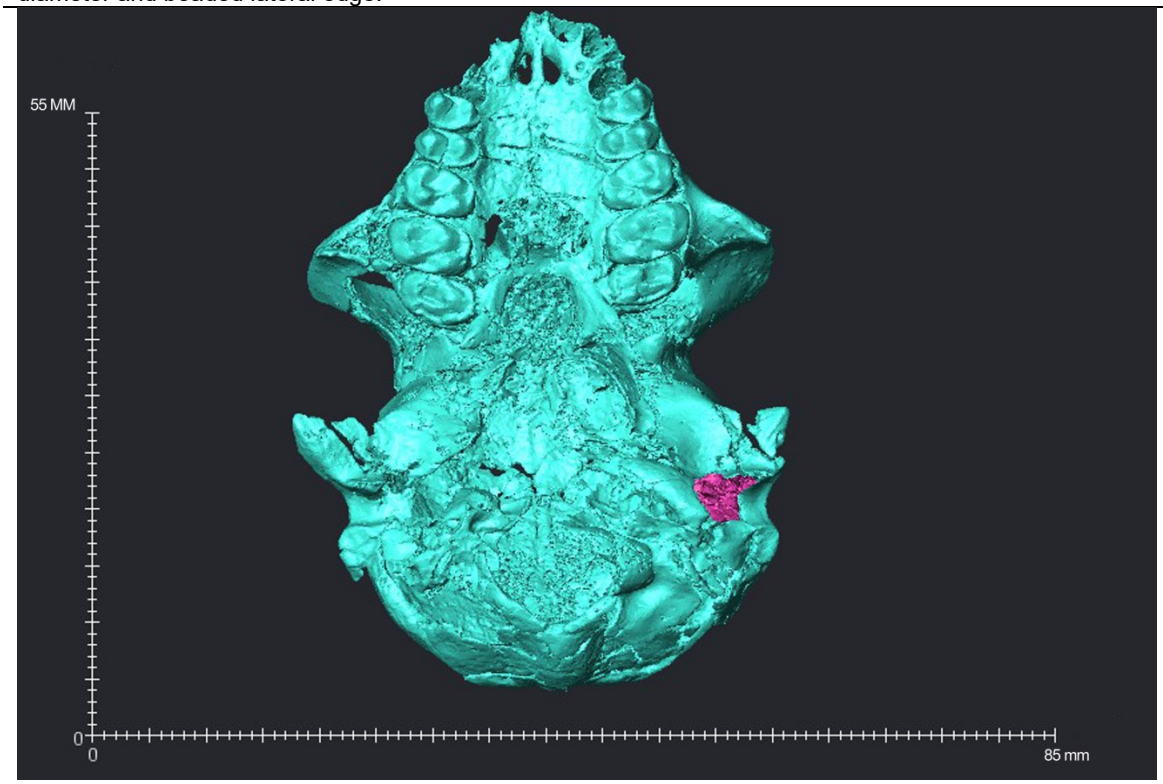

Figure 4.7: *A. zeuxis* basicranium with left ectotympanic highlighted in pink. The ectotympanic bone is less beaded than *P. vindobonensis* and the gestalt impression is slightly longer relative to the crista tympanica than that of *P. vindobonensis.*

Based on the results of Chapter 3, and hypotheses set out a priori, it was predicted that the relative ectotympanic length would be correlated with cranial widths, particularly those including the lateral-most basicranial elements. Ectotympanic bone length correlates with cranial width both with and without the auditory structures, but the correlation is much stronger in the BiEAM measurement that includes the lateral cranial structures. This is somewhat circular but it is important to note because this scaling relationship has not been shown previously. Additionally, the ectotympanic length is taken at the inferior aspect of the ectotympanic bone, so the measure of ectotympanic length is not included in the BiEAM metric. Humans stand out as an outlier when considering cranial width using either BiIAM or BiEAM distances as a metric (Figure 4.12 and 4.13). Relative ectotympanic lengths (ectotympanic length/IAM-IAM distance) are shown in Figure 4.14.

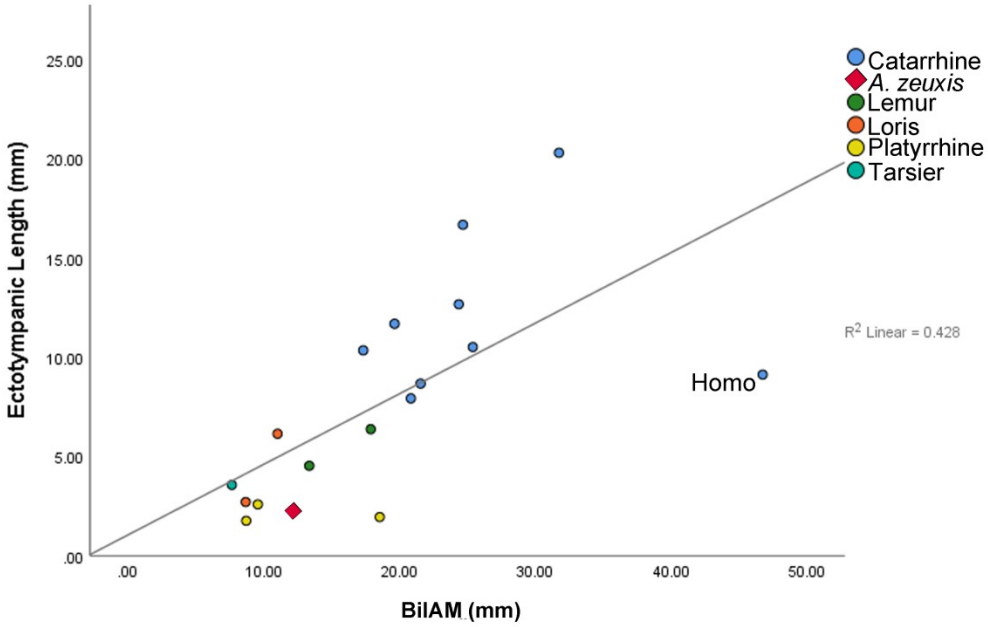

Figure 4.8: Species averages of ectotympanic bone length v. BilAM distance. The outlier in this figure is the human average, this indicates that the human ectotympanic length is unusually short for their BilAM distance.

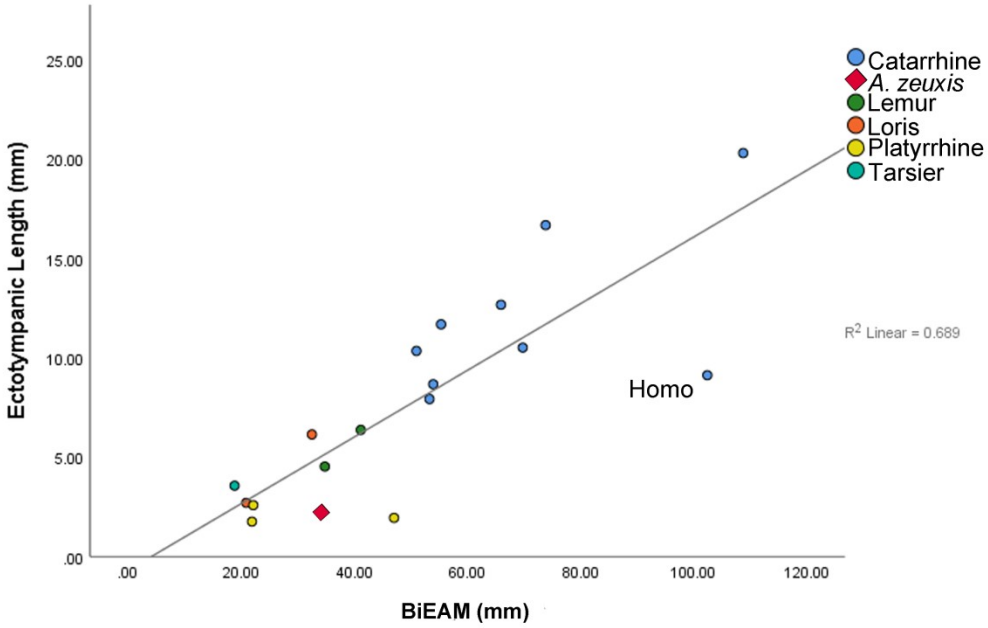

Figure 4.9: Species averages of ectotympanic bone length v. BiEAM distance. Again, the outlier on this graph is the human group.

Scaled ectotympanic length shows that, as expected, the catarrhines have the longest ectotympanic bones. Interestingly, however, the tarsier ectotympanic is not nearly as long as expected given that tarsiers are generally considered to share the elongate tube morphology with catarrhines. In fact, tarsiers fall well within the range of loris variation. Platyrrhines and lemuriforms have significantly shorter ectotympanic bones than the other taxa. *A. zeuxis* has a scaled ectotympanic tube that is certainly shorter than expected for the generalized catarrhine morphology, almost resembling the platyrrhine condition.

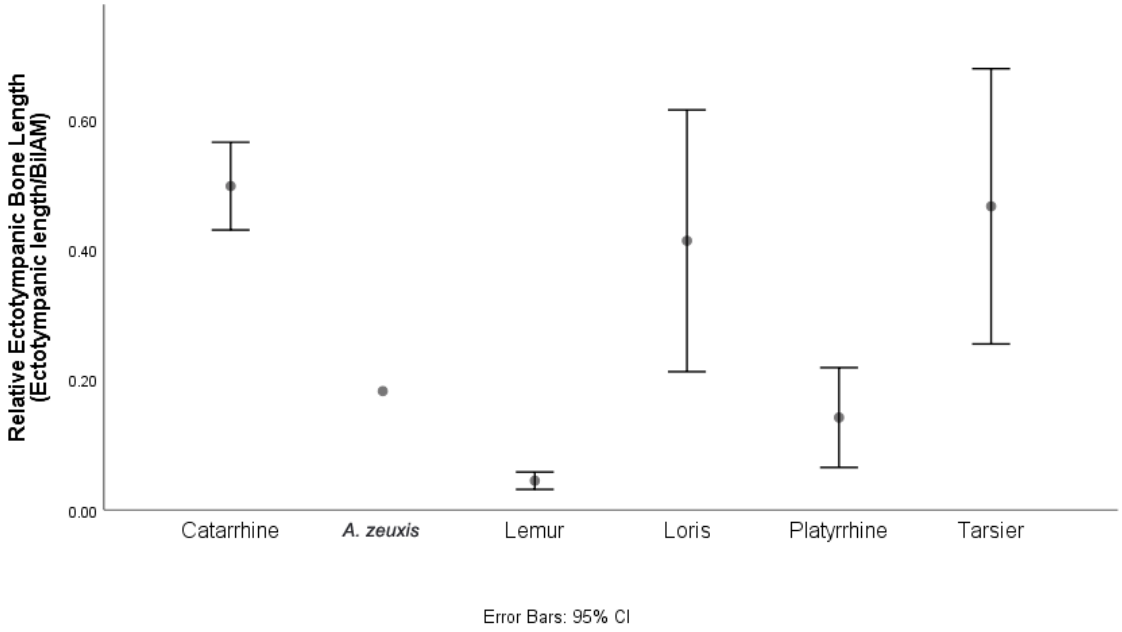

Figure 4.10: Bar chart of relative ectotympanic length by taxon. The relative ectotympanic length for catarrhine, loris, and tarsiers are all very similar. *A. zeuxis* falls into the range of platyrrhines.

Geometric Morphometric Analyses

The results of the procD.lm analysis show that total cranial base variation is not significantly correlated with relative ectotympanic bone length (Table 4.4). This result does not support the original hypothesis, that the shape of the cranial base is correlated with scaled ectotympanic length. However, given the degree of cranial base variation across taxa, it is possible that the gross anatomical differences are so great that it is

overpowering the kinds of shape variation with which ectotympanic length would be correlated (brachycephaly/dolichocephaly). For example, landmarks placed at foramina like the carotid canal and stylomastoid vary significantly in their relative locations between strepsirrhines and catarrhines; this type of anatomical variation may swamp out the effects of brachycephaly and dolichocephaly.

Table 4.4: ProcD Results

	Df	SS	MS	Rsq	F	Z	Pr (.F)
Ectotympanic Bone Length	1	0.057	0.057	0.13	1.99	1.26	0.08
Ectotympanic Bone Length: Centroid Size	1	0.054	0.054	0.12	2.17	1.79	0.05
Residuals	13	0.33	0.02	0.74			
Total	15	0.44					

Relative ectotympanic length (scaled by BilAM) is correlated with PCs 1 and 2 (PC1: R^2=0.45; PC2: R^2=0.14; Figure 4.8). PC1 (Figure 4.8) is largely describing the brachycephaly/dolichocephaly continuum. Relatively brachycephalic genera are on the high end of PC1 and dolichocephalic are on the low end (Figure 4.9). PC describes 46% of the variation in ectotympanic tube length is accounted. This result provides support for H2a, that those animals with relatively wide crania and brains have longer scaled ectotympanic bones across primates. The first principal component is often assumed to reflect the effect of allometry. That is the case here as well; the first PC is significantly correlated with centroid size. Interestingly, however, both tarsiers and *A. zeuxis* fall near the catarrhine range of variation on PC1. Lemurs, lorises and platyrrhines all cluster to the other end of the spectrum. Thus, while there is certainly an effect of body size here, PC1 is mostly describing an overall cranial shape; long narrow crania among the lemurs, platyrrhines, and lorises as compared to the wide crania of catarrhines and tarsiers.

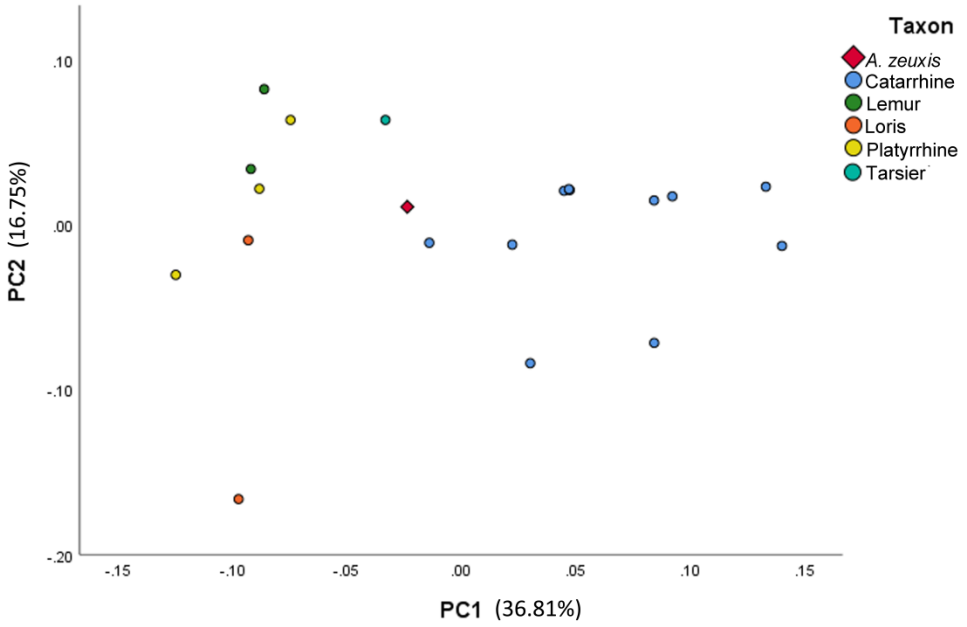

Figure 4.11: PC1 v. PC2

Principal component 2 had the next most bearing on the scaled length of the ectotympanic bone (14%). PC2 is illustrating the shifting of the anterior cranial base landmarks anteriorly (Figures 4.13). In other words, long scaled ectotympanic bone length is correlated with large middle cranial fossae.

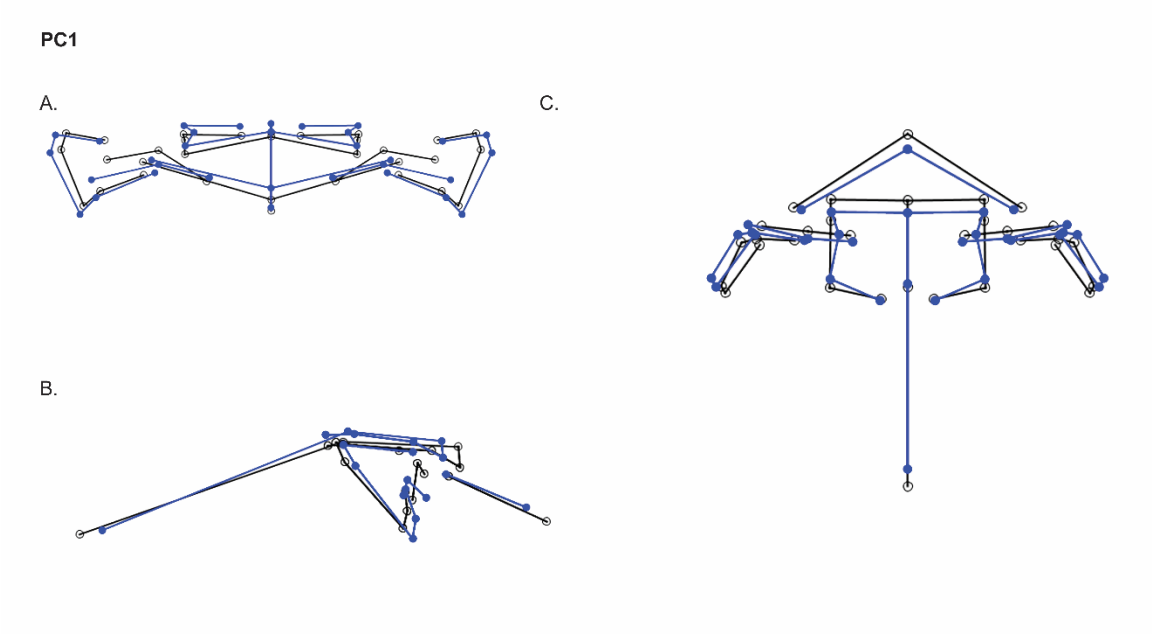

Figure 4.12: PC1 visualization. PC1 displays 32.65% of the total variation in cranial base shape and explains 46% of the variation in relative ectotympanic length. This is showing the dolichocephaly-brachycephaly continuum, A. Anterior-posterior view; B. Lateral view; C. Superior-inferior view.

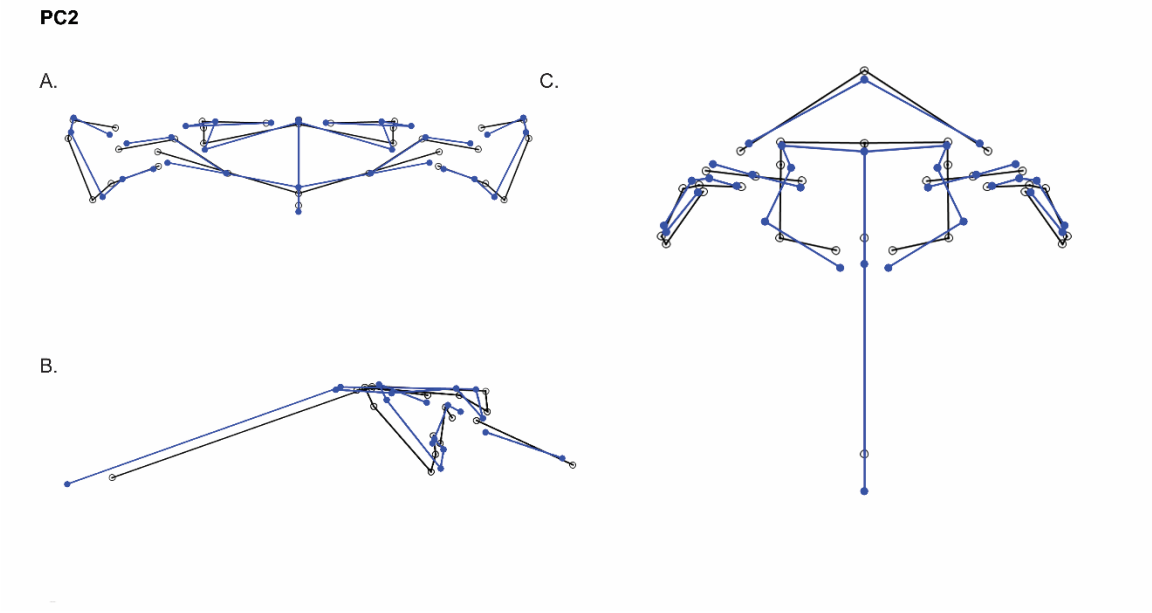

Figure 4.13: PC2 visualization. PC2 displays 13.43% of the total variation in cranial base shape and explains 13% of the variation in relative ectotympanic length. PC2 is illustrating the shifting of the anterior cranial base landmarks anteriorly, showing the long and short middle and anterior cranial fossae relative to the posterior.

Middle Ear Correlates

Based on hypothesis 2, it was expected that the ectotympanic bone length would be inversely correlated with middle ear height. As the middle ear reduces in the higher taxa of primates, the ectotympanic length was expected to increase in response. Whether controlled for either body size metric (centroid size or IAM), there is no significant relationship (centroid size: R=-0.05, p=0.81; BiIAM: R=0.24, p=0.20).

Lateral Encephalization Quotient

For visualization of the lateral globularity of the cranium in each taxon, the LEQ is presented in Figure 4.15. In this analysis, as it was expected that the human LEQ might diverge sharply from the generalized catarrhine pattern, the human taxon was isolated from general catarrhines and analyzed separately. Tarsiers are also high in LEQ but do not significantly differ from most taxa of primates. Unsurprisingly, the results of the Tukey HSD showed that the human LEQ quotient was significantly higher than any other taxa. There were no significant differences among the non-human primates.

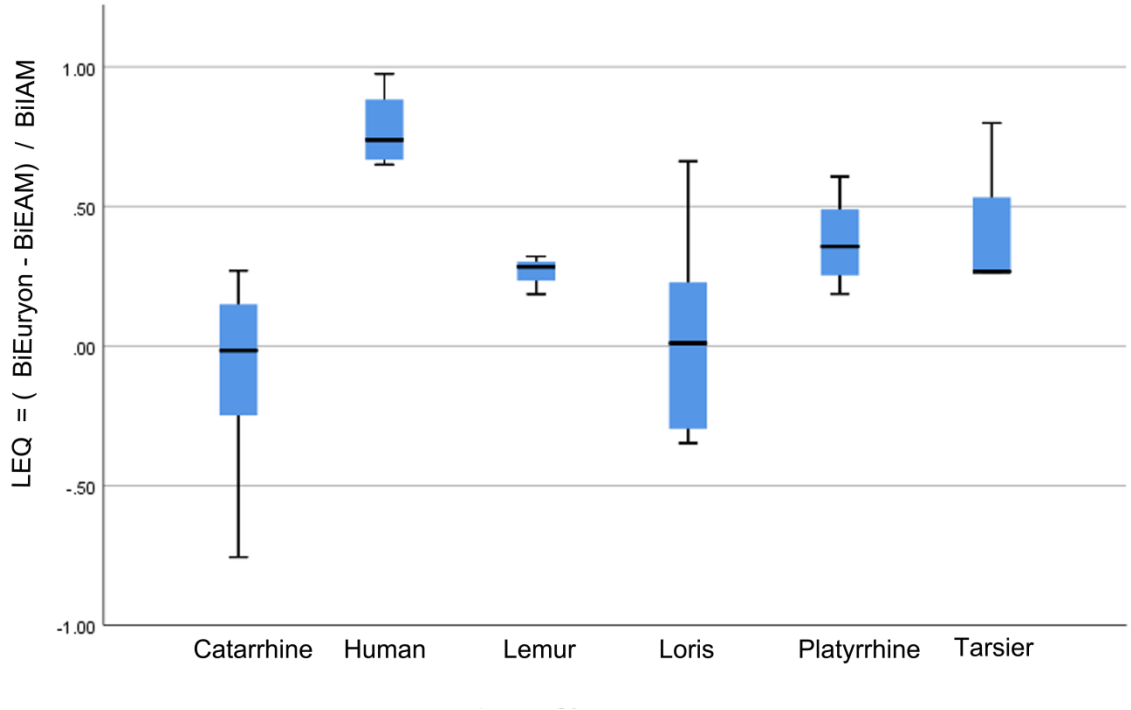

Figure 4.14: Boxplot showing the relative degrees of Lateral Encephalization (LEQ) by taxon. The human LEQ is significantly higher than any of the other taxa.

Fossils

Because the *A. zeuxis* cranium is nearly intact, it was included in many of the shape analyses based on morphometric data. As was expected, *A. zeuxis* in general falls between platyrrhines and catarrhines in cranial base variation (see Figure 4.8). The ectotympanic bone is extremely short for a catarrhine, as previous literature has indicated. The scaled ectotympanic bone length for *A. zeuxis* falls well within the platyrrhine range (Figure 4.14). While more quantitative analyses are not possible given the fragmentary nature of the *P. vindobonensis* (Figure 4.6), the ectotympanic bone does appear most similar to platyrrhine primates. The raw length of the ectotympanic bone in *P. vindobonensis* is grossly similar to the *A. zeuxis* (2.13 mm and 1.59 mm respectively). These numbers cannot be scaled using the BiIAM distance. They can, however, be scaled by body masses estimated using postcranial elements presented in

Arias-Martorell et al. (2015) (Figure 4.16). When scaled for body mass, *A. zeuxis* has a relative ectotympanic length of 1.05 mm/ (kg) $^{1/3}$ and *P. vindobonensis* has a relative length of 0.77 mm/ (kg) $^{1/3}$. Both of these numbers fall well within the platyrrhine ectotympanic range of variation.

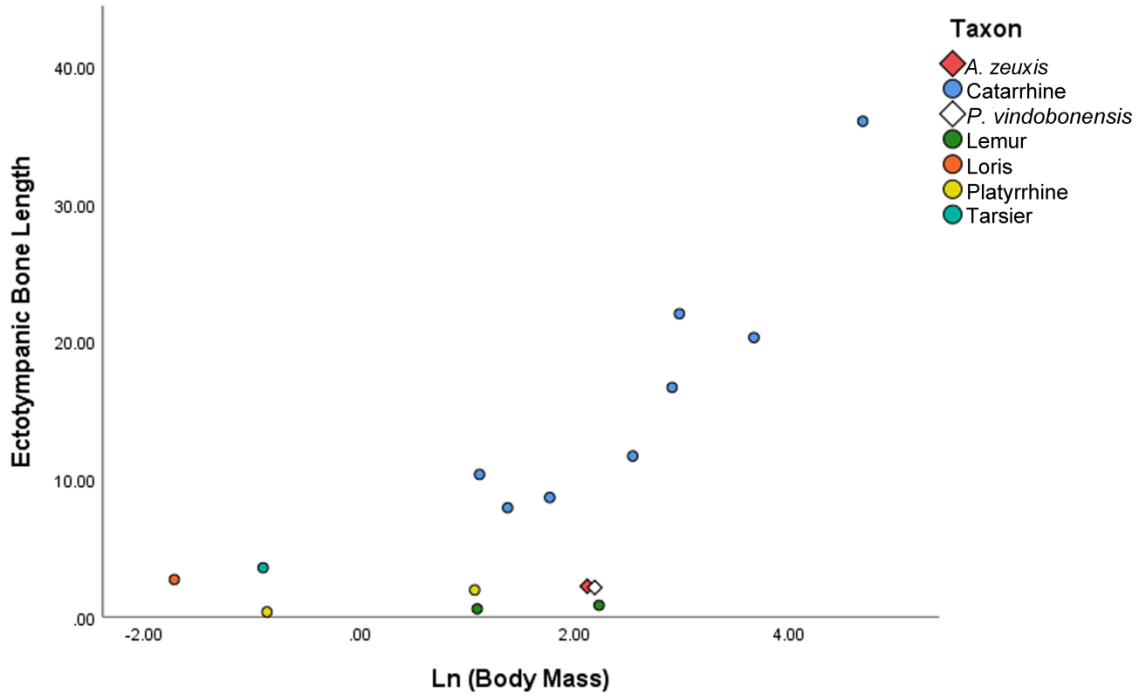

Figure 4.15: Ectotympanic bone length v. estimated body mass with fossils highlighted.

Discussion

Across taxa and analyses, the best predicting factor of the ectotympanic tube length is the relative width from the otic capsule to the pinna. While this seems relatively circular, it is very significant for interpretation of this important phylogenetic characteristic. The effects of phylogeny cannot be ruled out in any of these analyses. There is a strong phylogenetic effect on measures of brain size, cranial shape, and ectotympanic bone form; so removing phylogenic effects would remove much of the relevant variation.

Platyrrhines and catarrhines are closely related taxa, certainly more closely related than either one is related to tarsiers; however, their ectotympanic bones are the most disparate in length among haplorhines. It is clear that the ectotympanic length is not just a result of global volume increases in body size, brain size, or cranial base size; rather it is the result of lateral shifting and proportion changes in the cranial base. Consistent with previous results, the length of the ectotympanic has several influencing factors corresponding to the PCA results including cranial shape and middle cranial fossa size.

The first principal component accounts for much of the variation in ectotympanic tube morphology. While it is not independent from body size, it is showing that relatively wide crania tend to have long ectotympanic distances; this result indicates that relative ectotympanic bone length not only correlates with relative shape of the head but also the organization of the brain. Across broad scale evolution, the degree of brachycephaly/dolichocephaly likely reflects brain shape differences that are reflective of regional brain scaling. For example, Rilling and Seligman (2002) found that absolute and relative temporal lobe volumes differ between monkeys (combined platyrrhines and catarrhines) and apes; the authors note that *Cebus* has particularly small temporal lobes for their brain size, and *Macaca* and *Papio* have particularly large superior temporal gyri for their brain size. While Rilling and Seligman have small samples and do not intentionally separate platyrrhines from catarrhines, in their analyses platyrrhines have the lowest relative temporal lobe volumes. In short, among their platyrrhines, the temporal lobes are generally smaller than expected for their brain size and catarrhines have large temporal lobes and large middle cranial fossae.

As predicted, the two fossil, *A. zeuxis* and *P. vindobonensis*, taxa tend to fall intermediately between catarrhines and platyrrhines in their cranial morphology. The cranial base shape of *A. zeuxis* falls between catarrhines and platyrrhines, and the scaled ectotympanic bone is extremely unusual for a catarrhine. A whole cranium of *P.*

vindobonensis has not yet been found, thus it could not be included in many of the shape analyses. However, gross observation of the ectotympanic bone of *P. vindobonensis* supports the previous literature indicating that the ectotympanic bone of this species is short. It has been confirmed that the ectotympanic bone of *P. vindobonensis* has a beaded lateral surface and resembles a primitive condition. Therefore, it is suggested here that these two catarrhines may not have undergone the lateral encephalization that extant catarrhines do, which may be related to the temporal effect on brain size.

The middle ear

Middle ear structures are of great interest in basicranial anatomy, and variation in the middle ear between strepsirrhines and haplorhines was suggested as one of the potential factors in lengthening of the ectotympanic bone. Middle ear volume has been shown to be phylogenetically constrained (Coleman, 2007; Coleman and Colbert, 2010). It was predicted that the larger the middle ear is, the less space the external ear has to occupy and there would be a significant negative correlation. Results show that this is not the case, and in fact, when they are controlled for either centroid size (of the cranial base) or BiIAM distance the significant relationship disappears and the correlation remains positive. Therefore, the hypothesis that the reduction of the middle ear cavity is one of the reasons behind the altered position of the ectotympanic ring/tube is not supported.

LEQ

Analyses here support that the degrees of human lateral encephalization is highly unusual among primates. Humans have been found to have disproportionately large temporal lobes (Holloway, 1992; Semendeferi et al., 1997; Rilling and Insel, 1999;

Preuss, 2000; Semendeferi and Damasio, 2000; Rilling and Seligman, 2002). Their scaled ectotympanic tube lengths, however, are well below what would be expected of them given their large brains and large temporal lobes. Humans have been noted to be unusual in many respects in cranial morphology, surrounding brain size and postural differences associated with bipedalism. One such spatial packing adaptation that is also tested here is the "globular" nature of the human brain. "Globular" is often used to describe the way in which the brain expands much like a balloon to achieve the maximum brain size, and the globularity of the primate crania in the lateral direction was tested here (LEQ). Neubauer et al. (2010), point out that there is a marked "globularization" phase in human brain growth that is not seen in even our closest relatives, chimpanzees. LEQ analyses show that humans stand out starkly, possessing the highest LEQ and are the only group that significantly diverges from the other taxa in this measure. The results of the LEQ analyses (see Figure 4.15) and bivariate analyses of the ectotympanic length and cranial base widths (see Figures 4.12 and 4.13) highlight the unusual nature of the human ectotympanic tube and show that the morphology of the brain is crucially important when interpreting ectotympanic tube morphology.

The smallest LEQs are seen in the catarrhines. This was somewhat surprising as catarrhines have large brains and temporal lobes for their body sizes but perhaps the reason for this result is the organization of the masticatory muscles. The zygomatic process of the temporal bone blends into the temporal lines/ridges for the temporalis muscle inferiorly, just above the EAM. This LEQ metric bears out some of the suggestions presented in Chapter 3, that the size of the temporalis ridge superior to the EAM may be covarying with ectotympanic tube length and may be indirectly affecting the length of the ectotympanic tube in catarrhines. However, more study is necessary to parse out the complicated relationships between mastication and the ear canal.

Additional observations on phylogeny, tarsiers, and lorisiforms

The tarsier ectotympanic bone has historically been a source of confusion for the primate phylogenetic tree. One startling finding is that tarsier ectotympanic length is not unusual for their cranial width. In a recent reappraisal of the tarsier brain morphology, Allen (2014) found that tarsier brain proportions closely resemble those of other haplorhines, with such shared characteristics as an enlarged neocortex, visual cortex, and lateral geniculate body. She also notes that tarsiers have unusually short and extremely broad crania and brains. Therefore, it is unsurprising given the other evidence presented in this chapter that the tarsier ectotympanic bone is longer than that of the loris and the scaled ectotympanic tube length falls well within the catarrhine range of variation.

The lorisiform ectotympanic has been described as a “ring” fused to the lateral side of the petrosal bulla. Results presented here show that the ectotympanic ring in lorises is actually more elongate than the literature generally noted. The lorisiform ectotympanic bone length follows the same general trend, that wider crania are associated with longer scaled ectotympanic bones. An important caveat to consider is that the landmarks from which the interlandmark distances are calculated representing the “external auditory meatus” are placed on the lateral most point of the cranial base surrounding the external auditory structure. Among most taxa studied, the EAM is composed of the zygomatic portion of the temporal bone superiorly and ectotympanic bone inferiorly. Among lemuriforms, however, the inferior point of the external auditory meatus is placed on the lateral petrosal bulla, so for these specimens the “ectotympanic bone length” was taken as a linear distance from the surface models for comparison as opposed to interlandmark distances like the rest of the primates. For the GM comparisons, however, the location of the inferior EAM landmark of lemuriforms violates one of the assumptions of homology, that the locus is derived from the same tissues.

The homogeneity of the bone composing the EAM of lorisiforms is also somewhat in question. Some previous literature has suggested that among lorisiforms, not all taxa have inferior EAM's comprised entirely of the ectotympanic bone (Saban, 1963). Reappraisal of the bony contributors to the EAM of lorisiforms is required to ascertain whether the EAM landmarks of these animals are entirely homologous to those of catarrhines and tarsiers.

Future Directions

In the future, the variation in the cartilaginous ectotympanic tube will be examined in detail. Two hypotheses that will be tested specifically are: 1) the cartilaginous tube may be relatively longer in individuals with shorter bony ectotympanic among haplorhines, meaning that an animal with a shorter ectotympanic bone will have a longer cartilaginous tube, and 2) the cartilaginous tube may be one way that an animal maintains flexibility in the range of motion of the auricle and thus has a functional role in platyrrhines that may be under selection. These are both soft-tissue questions and as such do not lend themselves to standard CT methods. In the future, I will be using iodine and other staining protocols to make the cartilaginous tube more visible in CT scans to test these hypotheses. The results of this chapter provide evidence that this important phylogenetic characteristic (bony ear tube length) is significantly affected by, and potentially determined by, general cranial structure. This sets the stage for further exploration of the evolution of the ectotympanic bone.

5. Development of the Ectotympanic Tube

Introduction

Ectotympanic bone morphology is a classic characteristic used to differentiate primates and identify fossil affinities (Saban, 1963; Hershkovitz, 1974; Simons, 1974; Cartmill, 1982; MacPhee and Cartmill, 1986); though the ectotympanic bone morphology has been frequently cited in academic literature, the way in which the ectotympanic bone lengthens within and across taxa is still not well understood. It is likely, based on the previous evidence presented, that the relative length of the ectotympanic bone is more of a structural by-product of cranial shape and that the length of the ectotympanic bone varies more within and between species than previously thought. For example, humans have relatively shorter ectotympanic tubes than other catarrhines analyzed. Additionally, among lorisiforms the ectotympanic bone is longer than previously appreciated. Thus, one question that remains to be answered substantially is whether taxa with elongate ectotympanic bones have attained this state in similar ways. Are the differing shapes of ectotympanic bones an example of heterochrony in which all species pass through the same initial stage, followed by divergence in shape? And if not, is the growth of the ectotympanic bone among tarsiers more similar to that of catarrhines or lorisiforms? In this chapter, the active ectotympanicum growth periods will be identified and qualitatively compared in several taxa of catarrhine, tarsier and lorisiforms.

All mammals possess an ectotympanic bone that provides structural support of the tympanic membrane, which demarcates the lateral wall of the middle ear. Through development the mammal ectotympanic bone is derived from the mandibular division of the first pharyngeal arch, the precursor to the Meckel's cartilage (Maier and Ruf, 2016a). The ectotympanic bone in all primates fuses superiorly to the petrous portion of the temporal bone. In lemuriforms it remains free-floating. Among lorisiforms and

haplorhines, the ring fuses laterally to the petrous plate that forms the floor of the middle ear.

Ectotympanic bone morphology certainly aids in the differentiation of extinct and extant primates (e.g., Rosenberger and Szalay, 1980; Rasmussen, 1986; Kay et al., 1994). It has been shown in previous chapters that while lorisiforms tend to have longer "ectotympanic regions" than previously thought, especially when scaled for endocranial width, this characteristic appears to be largely determined by forces external to the bone itself like cranial base width and basicranial flexion. The geometric morphometric analyses of the auditory regions across primates are complicated by the assumption that landmarks are homologous. The composition of the bony external auditory meatus (EAM) in lemuriforms is derived from the petrosal ossification center and thus lacks strict homology with the EAM landmark in other primates (MacPhee, 1977; Novacek, 1977; MacPhee and Cartmill, 1986). Lemuriforms EAM composition is not in debate; more interesting for the purposes of the current study is the bony composition of the lorisiforms EAM.

Saban (1963) illustrates the variation seen in adult lorisiform EAM composition that is often overlooked in other descriptions of the ectotympanic bone (Piveteau, 1957; Fleagle, 2013). In this series of anatomical drawings, he shows that the ectotympanic bone often is only one contributor to the external auditory meatus. He notes that in some lorisiforms, namely *Loris tardigradus* and *Nycticebus bengalensis,* the external auditory meatus is composed of the ectotympanic bone as well as other ossification centers: the petrous portion of the temporal bone and the post-glenoid tubercle (Figure 5.1). The external auditory meatus of *Loris tardigradus,* in particular, draws a parallel to lemuriform morphology in which the petrosal-derived bulla encapsulates the ectotympanic bone ring completely. In his illustration, the *Loris* ear canal is deflated and the ectotympanic bone is fused to the petrosal floor. The tarsier ectotympanic tube however, is represented as a

single origin bone, derived from the ectotympanic bone like the catarrhine tube, potentially aligning it more strongly with anthropoids (Figure 5.2).

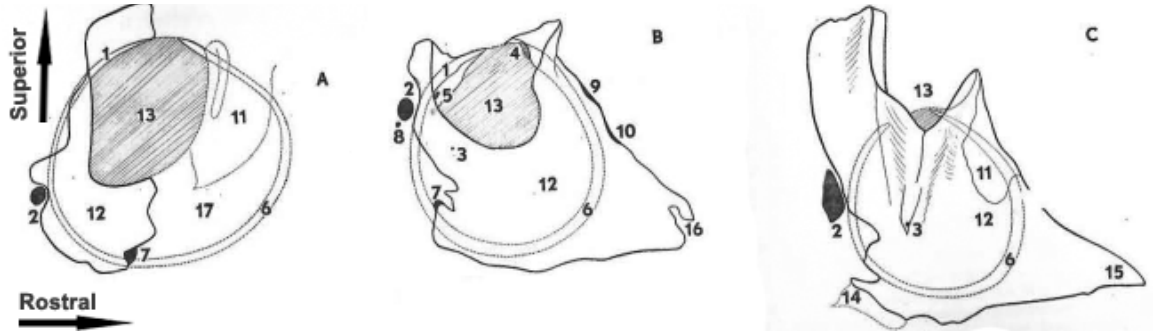

Figure 5.1: Illustrations from Saban (1963) of A. *Loris gracilis (tardigradus),* B. *Perodicticus potto*, and C. *Nycticebus cinereus (bengalensis)*. Based on these drawings, the EAM of these three lorisiforms is composed of the ectotympanic, the post-glenoid tubercle, and the petrous portion of the temporal bone.

1. Tympanic groove; 2. Stylomastoid foramen; 3. Canaliculus of the deep auricular artery; 4. Malleolar gutter; 5. Posterior canal of the chorda tympani; 6. Tympanic ring; 7. Styloid fossa; 8. *Ostium introitum*; 9. Malleolar gutter, external orifice; 10. Groove of the anterior tympanic artery; 11. Post-glenoid process; 12. Ectotympanic/tympanic plate; 13, external auditory meatus; 14, styloid process; 15, tubal process; 16, tubal orifice; 17, petrous.

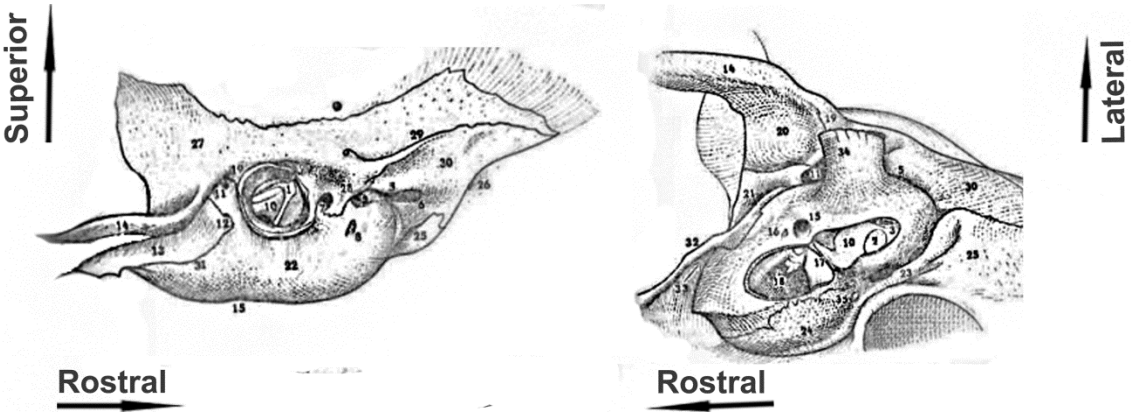

Figure 5.2: Tarsier temporal bone as illustrated by Saban (1963). 1. Malleus; 22. Auditory bulla; 34. Ectotympanic/tympanic plate. The full EAM is derived from the ectotympanic bone, according to these illustrations.

Based on these illustrations, it is possible that the *Loris tardigradus* condition is closer to the ancestral state. In order to answer the question of homology, the origins of the bones that contribute to the EAM must be clarified. Several important studies have described the development of strepsirrhine morphology largely in attempts to address

phylogenetic relationships using the auditory anatomy (Hershkovitz, 1974; Archibald, 1977; MacPhee, 1977, 1979). Conroy (1980) noted the elongation of the ectotympanic ring among lorisiforms that was demonstrated quantitatively in Chapter 3 and 4. He further questioned the homology of this feature with the true ectotympanic tube seen among catarrhines. Conroy suggested that the lorisiform elongate ectotympanic bone may in fact be an expanded, lemur-like, linea semicircularis (the lateral extension of the petrosal plate that forms the auditory bulla in lemuriforms); thus the ectotympanic might be truly intra-bullar. This description is similar to the *Loris* image provided by Saban. He further notes that the growth of the lorisiform and tarsier ectotympanic bones seems to happen very differently than in catarrhines; the *Galago* ectotympanic lengthens in a single sheet, which differs from the catarrhine elongation pattern (discussed below). Following Conroy's findings and Saban's descriptions, it is likely that *some* lorisiforms have what may be defined as an intra-bullar ectotympanic bone. However, the range of variation pointed out by Saban among lorisiforms highlights the need for a re-examination of the growth of the lorisiform, and indeed all primates, ectotympanic morphology using a developmental perspective.

There is a rich history of description of the human ectotympanic bone and postnatal growth and it is perhaps the best documented in the literature of any primate. In their seminal book on juvenile osteology, Scheuer & Black (2000) summarize the ossification of the human ectotympanic tube morphology as follows: 1) the ectotympanic ring forms prenatally, 2) anterior and posterior tubercles begin to expand and lengthen in the inferior and lateral directions, 3) the anterior and posterior tubercles blunt at either end and reach for the midline of the future ectotympanic tube, 4) the anterior and posterior tubercles fuse, leaving a foramen (foramen of Huschke), finally 5) the foramen later fills in (Scheuer and Black (2000) citing: Weaver, 1979; Reinhard and Rösing, 1985; Ars, 1989).

Most growth studies of the human ectotympanic examine the first three to five years of postnatal life (Anson et al., 1955; Weaver, 1979; Ars, 1989). Weaver (1979) proposed a set of developmental stages and found that the development of the ectotympanic plate could be used to estimate the ages of children (Figure 5.3). The Weaver method was based on dry skulls of Native American children with no known age. There are several potential issues with this study, not the least of which is that the lack of known ages introduces potential error. The Weaver study was also based on dry skulls and thus only the external morphology was observable and no direct measurements of the length of the ectotympanic tube could be taken. With the advent of CT technology, it is now possible to assess more thoroughly and accurately ectotympanic plate development among humans. Additionally, there may be significant variation in this characteristic at the population level. Some literature has noted the perpetuation of juvenile morphology in ectotympanic tubes, with patent foramina of Huschke, but the prevalence of this phenomenon varies greatly by population; e.g., 4.6% among modern humans from the Netherlands (Lacout et al., 2005) to 12-20% in modern Japanese crania (Hashimoto et al., 2011). This highlights the need for a re-examination of the growth of the tympanic plate that includes more developmentally advanced and more diverse sample.

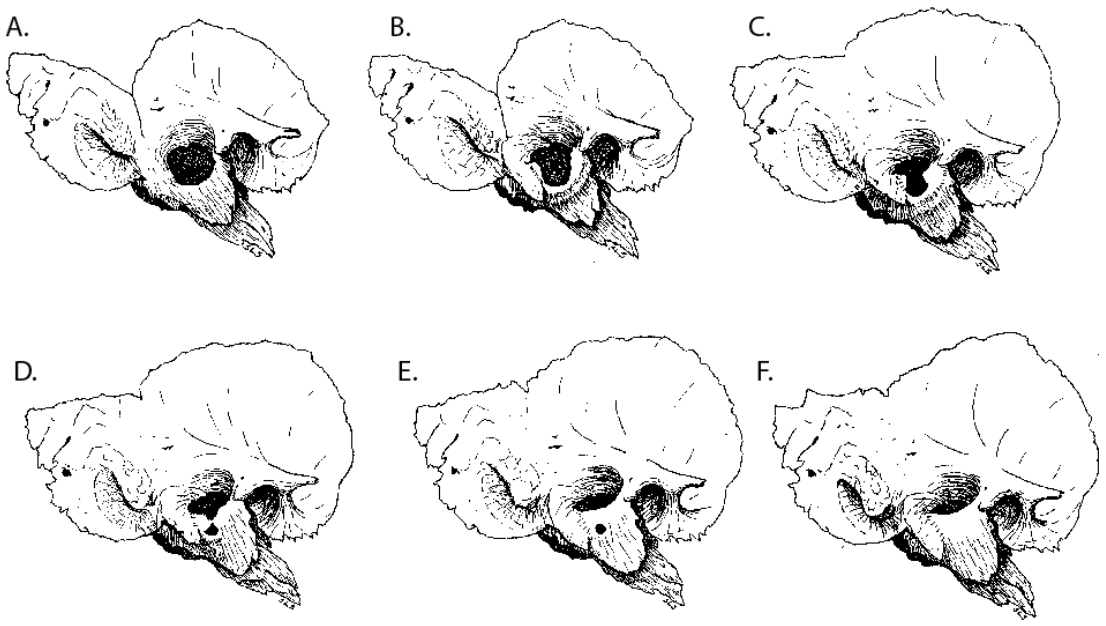

Figure 5.3: All crania were scored non-metrically based on a protocol suggested by Weaver (1979). In general, the individual was given a score of A. If there was only a bony ring, B. If the anterior and posterior tubercles had begun to lengthen, C. If the tubercles had begun to stretch inferiorly, D. If the tubercles met in the midline, E. If the EAM was complete and the foramen of Huschke had begun to fill in, and F. If the foramen had filled in completely and the EAM was smooth.

Catarrhines

Non-human catarrhine ectotympanic growth patterns have not been well documented previously. Though catarrhines are often mentioned in developmental and phylogenetic descriptions (e.g., Saban, 1963; Conroy, 1980; Fleagle, 2013), there are no known studies that quantify the growth of the non-human catarrhine ectotympanic bone. This is possibly because the other catarrhines are assumed to follow roughly the ectotympanic bone growth patterns detailed for humans but it has been shown that the ectotympanic bones of humans are unique. Interestingly, the foramen of Huschke has not been noted in other catarrhines. This indicates that one of the following is true: 1) the tube grows differently in other catarrhine species such that there is no foramen, patent or otherwise, 2) the foramen is less likely to remain open in other primates either because of the rate of growth or growth patterning, or 3) least likely, no one has noticed or written

on the foramen of Huschke's presence in non-human primates. Although the ectotympanic ring/tube dichotomy has long been discussed in the literature, some key questions have been left out.

Questions

1. Can ontogeny resolve the questions surrounding the lorisiform and tarsier ectotympanic bones? Across lorisiforms, is the external auditory meatus derived from the petrosal bone, ectotympanic bone, or some combination of the two?

2. Will an updated sample of known-age modern individuals and new visualization technology alter the developmental models of the human ectotympanic bone illustrated in Scheuer & Black (2000)?

3. Do other catarrhines follow the same or a similar ontogenetic trajectory as humans?

Materials and Methods

Non-Humans

A sample of juvenile non-human primates were assessed using micro-CT scans (Table 5.1). These species were chosen to be as similar as possible to the taxa analyzed in Chapter 4. All animals included in this study exhibit active ossification of the ectotympanic bone, which occurs at younger ages in prosimians than anthropoids. The ages of the strepsirrhines and some catarrhines are largely known as they come from research and zoo populations, access to scans of these animals was graciously provided by VB DeLeon, TD Smith, and CJ Vinyard. Catarrhine scans were obtained from the KUPRI database (the Digital Morphology Museum housed at the Kyoto University Primate Research Institute) and ages were estimated using dental methods.

Table 5.1: Non-Human sample

Genus	Species	N	Age	Scan Parameters	Scan Source
Cercocebus	*torquatus*	1	0.58-1.5**	0.2x0.2x0.2mm	KUPRI
Cercocebus	*galeritus*	1	0.58-1.5**	0.2x0.2x0.2mm	KUPRI
Galago	*senegalensis*	1	0 days	20.5x20.5x 20.5um	VBD
		1	7 days	25x25x25um	VBD
Macaca	*nemestrina*	1	34 days	35x35x35um	VBD
Macaca	*cyclopis*	3	0.5-1.5 years***	0.18x0.18x0.5 mm (2) 0.19x0.19x0.5 mm (1)	KUPRI
Nycticebus	*pygmaeus*	2	Neonatal	20.5x20.5x 20.5um	VBD
Loris	*tardigradus*	1	Late fetal	20.5x20.5x 20.5um	VBD
Papio	*hamadryas*	3	0.55-2.08 years***	0.2x0.2x0.2 mm	KUPRI
Mandrillus	*sphinx*	4	0.24-0.58 years***	0.2x0.2x0.1 mm	KUPRI
Tarsius	*syrichta*	1	0 days	20.5x20.5x 20.5um	VBD
		1	6 days	25x25x25 um	VBD
Trachypithecus	*francoisii*	1	2 days	20.5x20.5x20.5 um	VBD
Colobus	*guereza*	1	0	25x25x25 um	VBD

** Published dental age standards are not available for *Cercocebus*; these ages follow *Mandrillus* standards, based on Setchell and Wickings' (2004) assessment that these two genera are very similar in their growth processes. There is almost certainly some additional error included in this estimate. All of the deciduous dentition has fully erupted but no adult dentition is present in occlusion.

*** Age estimated using standards in Smith et al. (1994), Phillips-Conroy and Jolly (1988), Setchell and Wickings (2004)

Human

To reassess postnatal development of the human ectotympanic bone, a collection of medical CT scans from 49 modern juvenile (mid-fetal to nine years old) human crania was evaluated. Age groups are illustrated in Figure 5.4. The distribution of ages is right-skewed with a density surrounding the early infancy phase. These scans are collected routinely by the medical examiner as a method to supplement routine autopsy. Due to privacy concerns, all measurements and impressions were collected on site at the Office of the Chief Medical Examiner (OCME) in Baltimore, Maryland. Measurements, images, and other data collected were anonymized to protect the privacy of the individuals. Precise ages were provided via the OCME records. The ages

were recorded in months under the age of two and by year over the age of two. Privacy measures were approved in IRB exemption (IRB00129349).

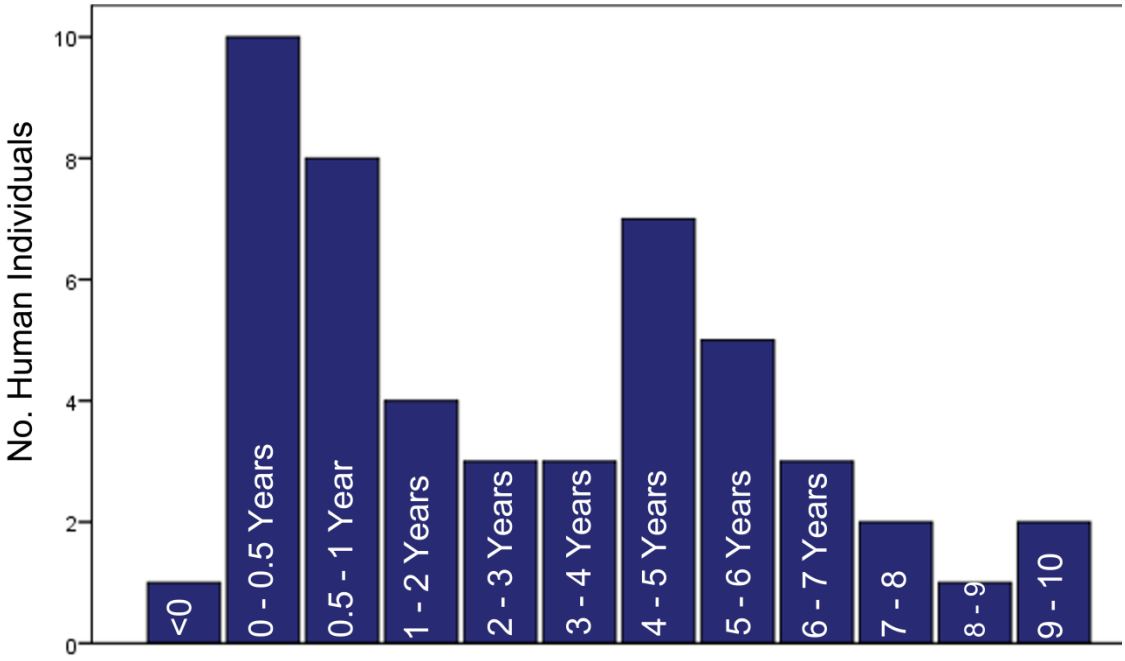

Figure 5.4: Ages of human individuals included in this study.

Three methods were employed to analyze these crania using both non-metric and morphometric approaches. First, the development of the ectotympanic tube in all humans was scored non-metrically using previously published standards (Weaver, 1979). This method was also applied not only to provide a gross idea of how "developed" the ectotympanic tube is on each cranium but also the shape of the ectotympanicum as it grows to compare growth modalities across taxa. A Weaver score was assessed for each individual. For humans, Spearman rank correlations were performed to compare developmental stages and age. Second, the length of the ectotympanic tube was taken along the anterior tubercle, posterior tubercle, and along the midline of the floor of the growing ectotympanic tube (Figure 5.5). When there was a foramen of Huschke, the measurement of "center ectotympanic length" was assessed as the base of the ectotympanic groove, not where the tubercles met. Third, qualitative assessment of all

individuals was used to illustrate and describe ectotympanic bone growth across species.

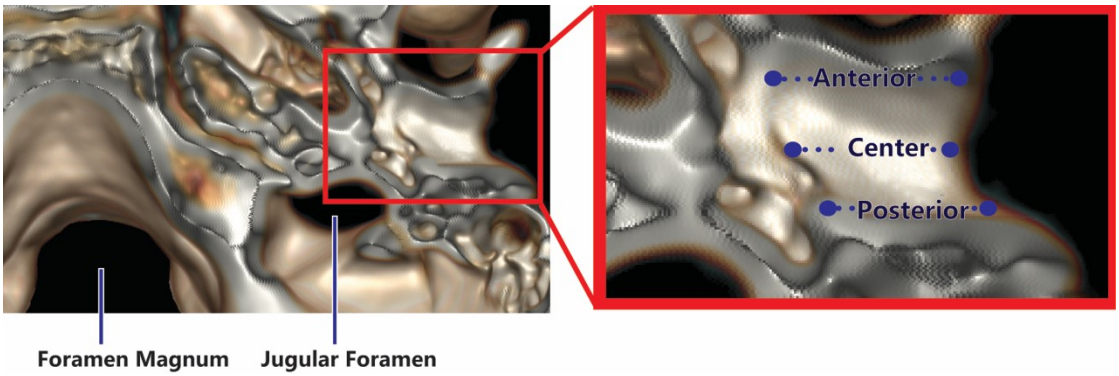

Figure 5.5: Superior view of an axial slice through center of the ectotympanic tube demonstrating the location of three ectotympanic tube lengths (anterior, center and posterior).

Results

Strepsirrhines

In all lorisiforms, and indeed all primates presented here, the ectotympanic ring is formed by birth. The elongation of the ectotympanic bone in lorisiforms occur almost immediately postnatal lorisiforms. Contrasting with the known human growth pattern, the ectotympanic ring lengthens in *Galago* as a single, ragged sheet, rather than the bi-phasic pattern described for humans (Figure 5.6). The *Galago* ectotympanic bone, consistent with Saban's illustrations, forms almost all of the external auditory meatus at birth. The petrosal-ectotympanic suture is still clearly visible at the time of birth, which supports the single bone hypothesis.

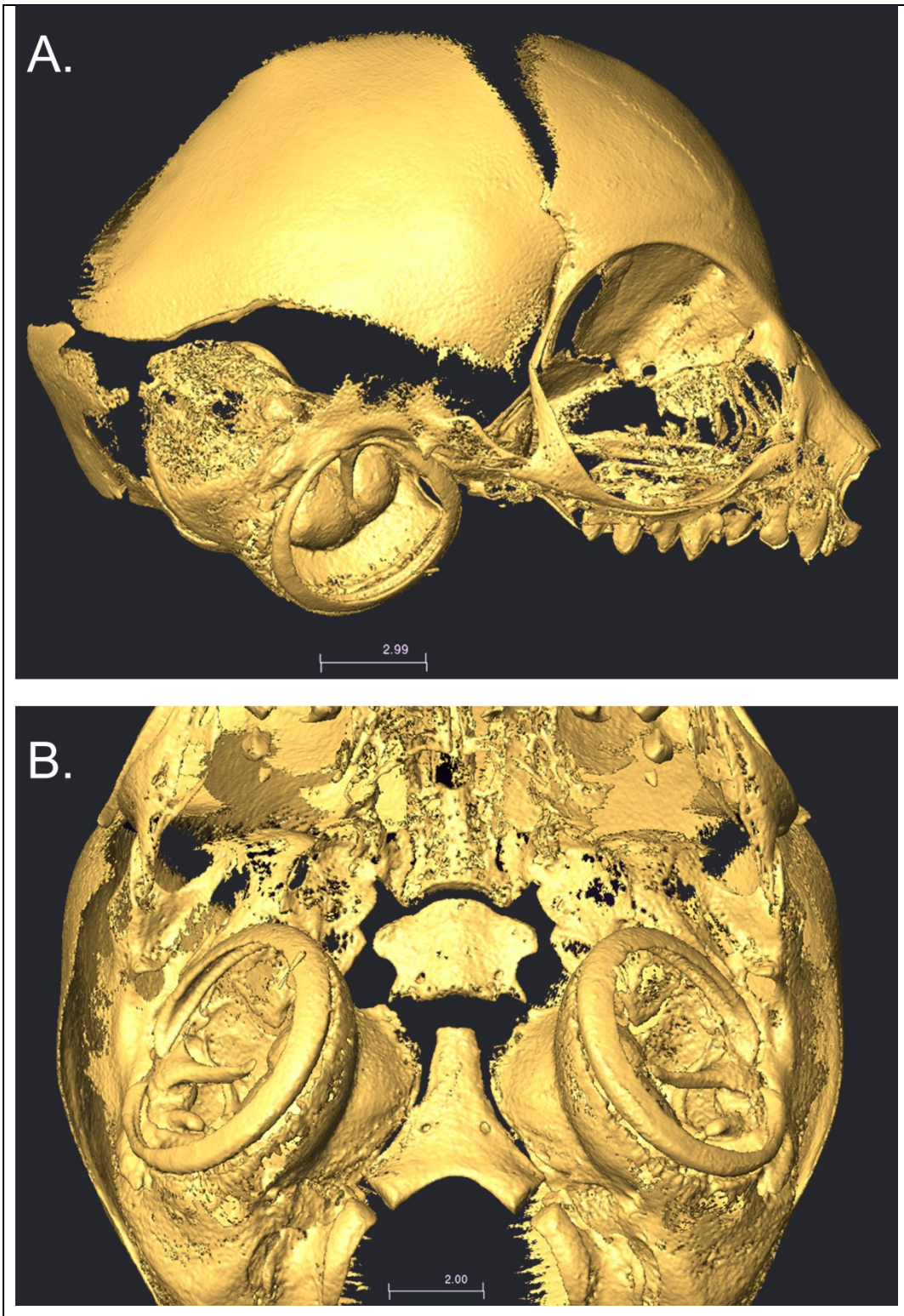

Figure 5.6: *Galago senegalensis,* neonatal. The ectotympanic ring is clearly visible and the petrosal-ectotympanic suture is prominent. The ectotympanic ring is lengthening evenly all the way around the EAM, with the exception of the gap between the anterior and posterior crura.

At birth, *Nycticebus* looks very similar to *Galago*. The EAM is composed solely of the ectotympanic ring at birth. The post-glenoid process and post-glenoid foramen are clearly visible (Figure 4.7). The post-glenoid foramen fills in in adult *Nycticebus*, and the post-glenoid process fuses with the ectotympanic to become part of the EAM (Saban, 1963).

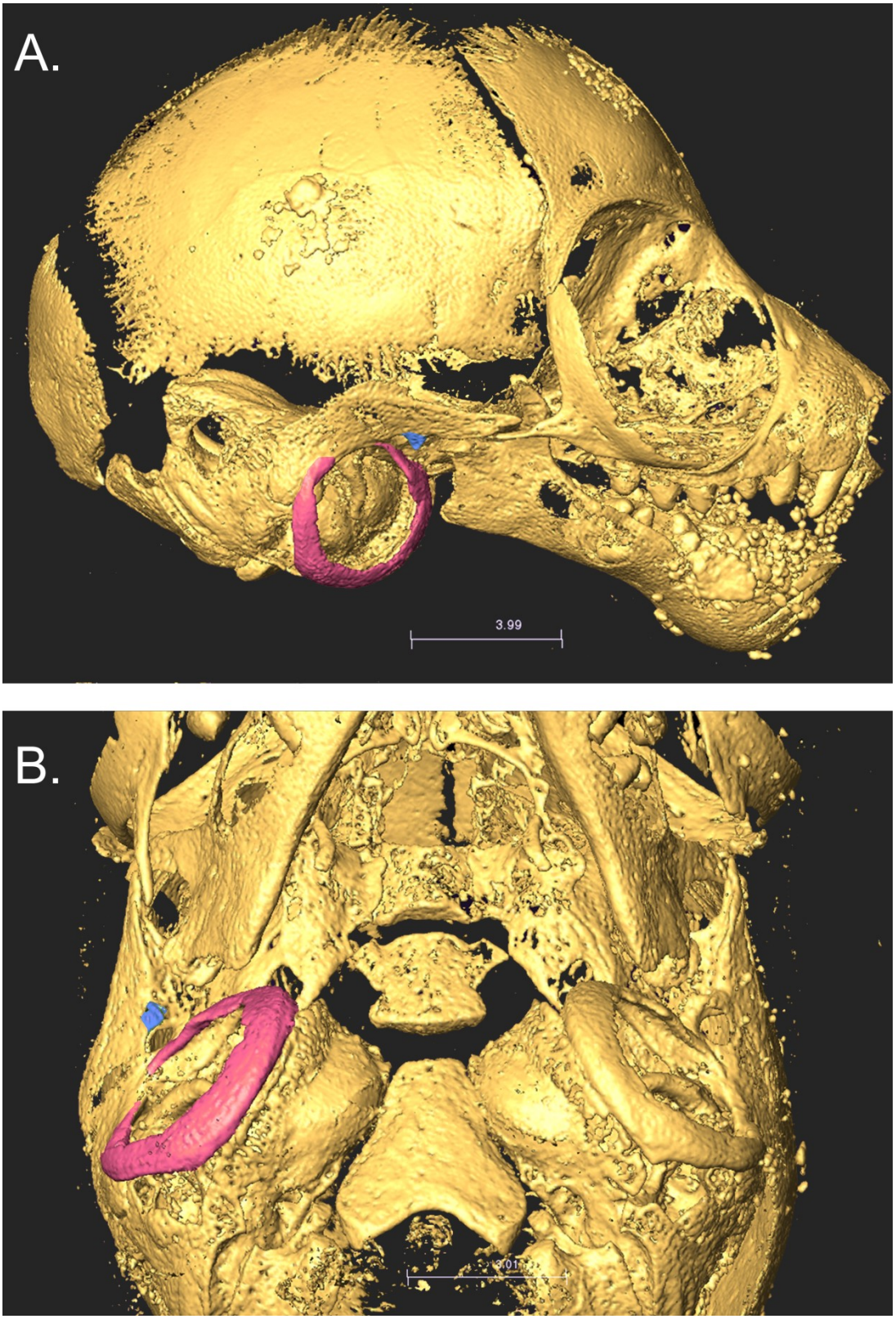

Figure 5.7: *Nycticebus tardigradus*, neonatal. Pink is highlighting the ectotympanic ring; blue is showing the post-glenoid tubercle.

Consistent with Saban's interpretation of *Loris* ear morphology, the *Loris tardigradus* stands out as unusual (Figure 5.8 and 5.9). An ectotympanic ring is visible in the neonate, within a nearly complete petrosal derived EAM. The *Loris* is the only example shown here of what Conroy described (Conroy, 1980). At this point in development, the ectotympanic bone is not contributing to the EAM as was shown in Saban's illustration (See Figure 5.1). Saban indicated the ectotympanic ring elongates in the posterior aspect to fill in the posterior EAM.

In the neonate *Loris*, the post-glenoid process is elongating and growing toward the petrosal bulla but not yet contributing to the EAM. It is likely that the posterior ectotympanic bone will lengthen eventually to form part of the EAM and it is assumed that the post-glenoid process will likely shift posteriorly to become the anterior wall of the EAM in a fashion similar to the *Nycticebus* ear. At birth, however, the post-glenoid process in both species has not been incorporated into the EAM. Thus, the post-glenoid process is incorporated into the EAM in both *Loris* and *Nycticebus* but in both species the post-glenoid process is incorporated secondarily, and remodels the original ectotympanic ring.

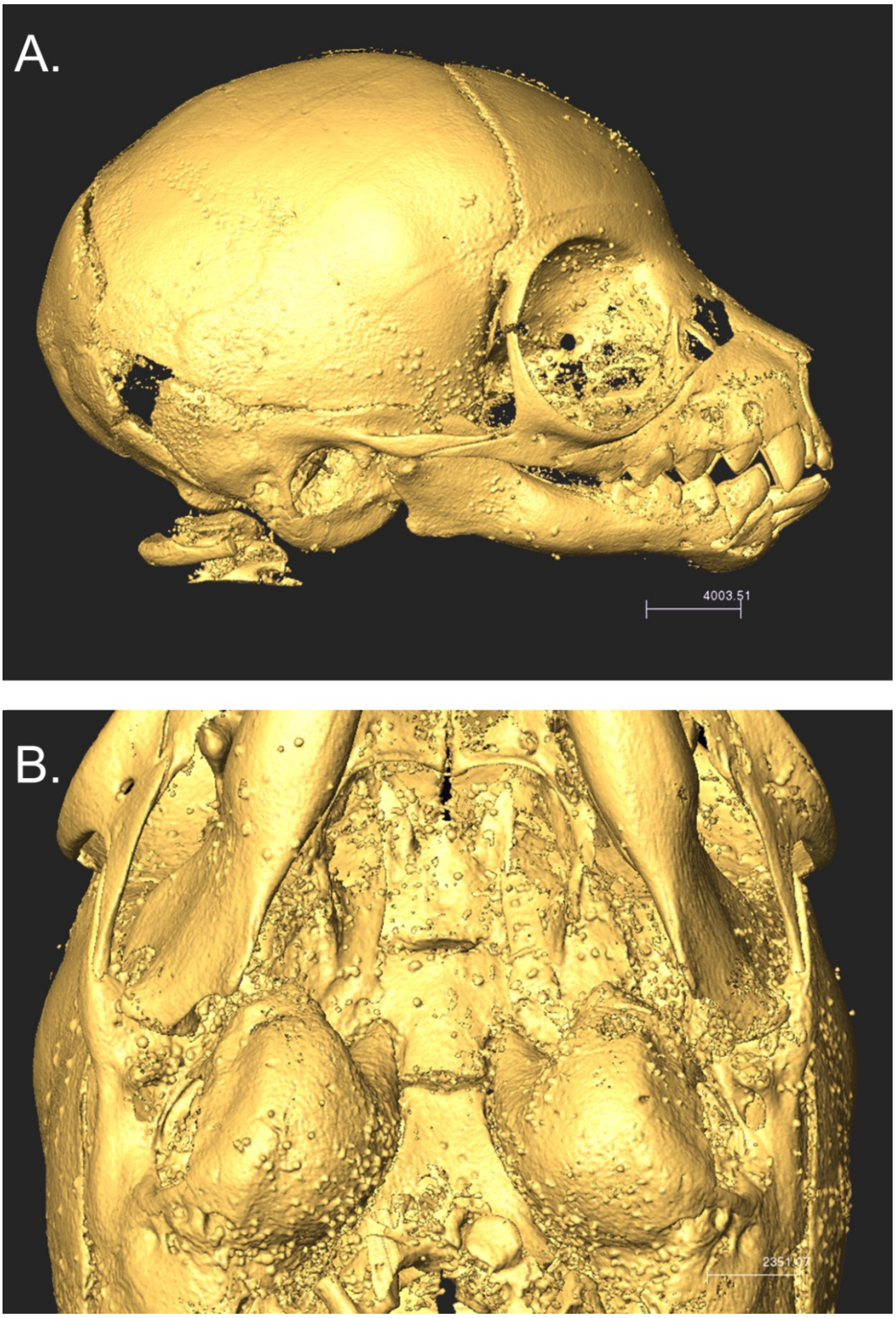

Figure 5.8: *Loris tardigradus*, neonatal. There is no petrosal-ectotympanic suture, the auditory bulla (petrosal derived) has overgrown the ectotympanic ring.

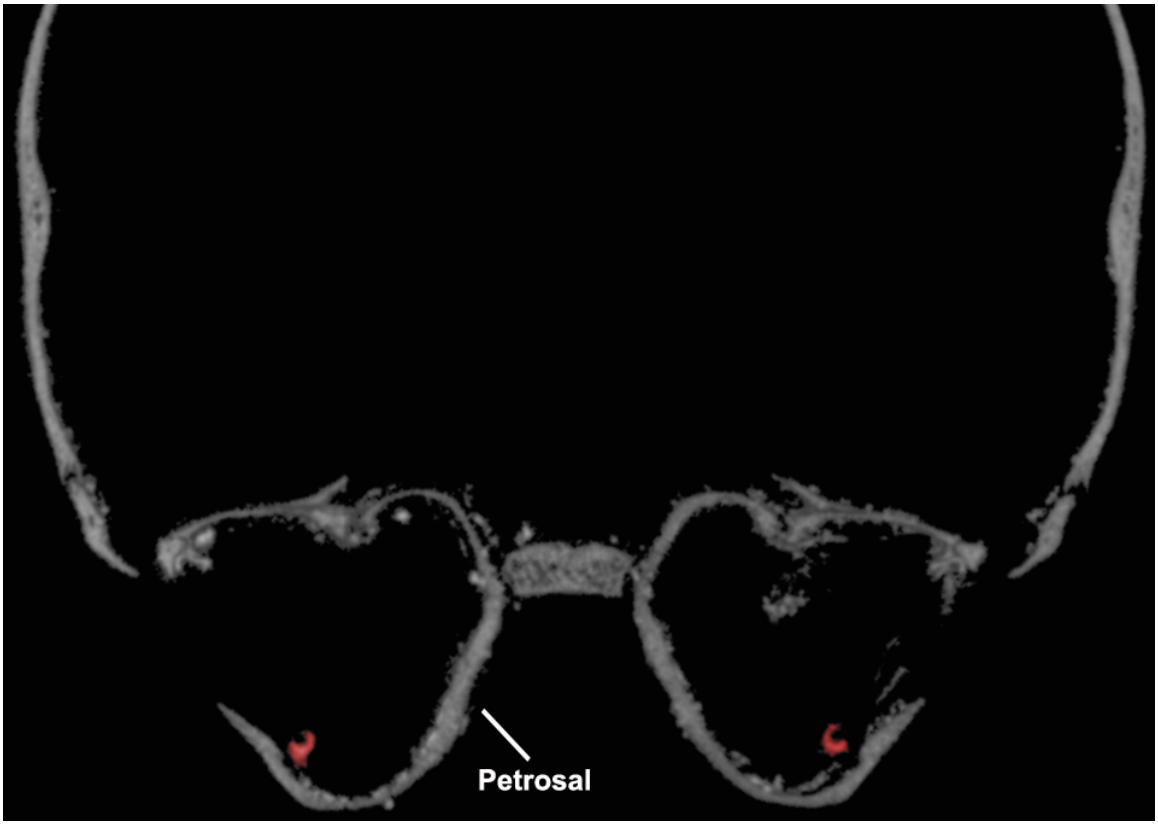

Figure 5.9: Coronal slice though EAM of *Loris tardigradus*. The ectotympanic ring is highlighted in pink.

At birth, *Tarsius* has a complete ring of bone at the EAM derived completely from the ectotympanic bone (Figure 5.10). This is similar to *Galago* and *Nycticebus.* At this point, the tarsier ectotympanic bone does not appear to be developing tubercles similar to catarrhine growth patterns.

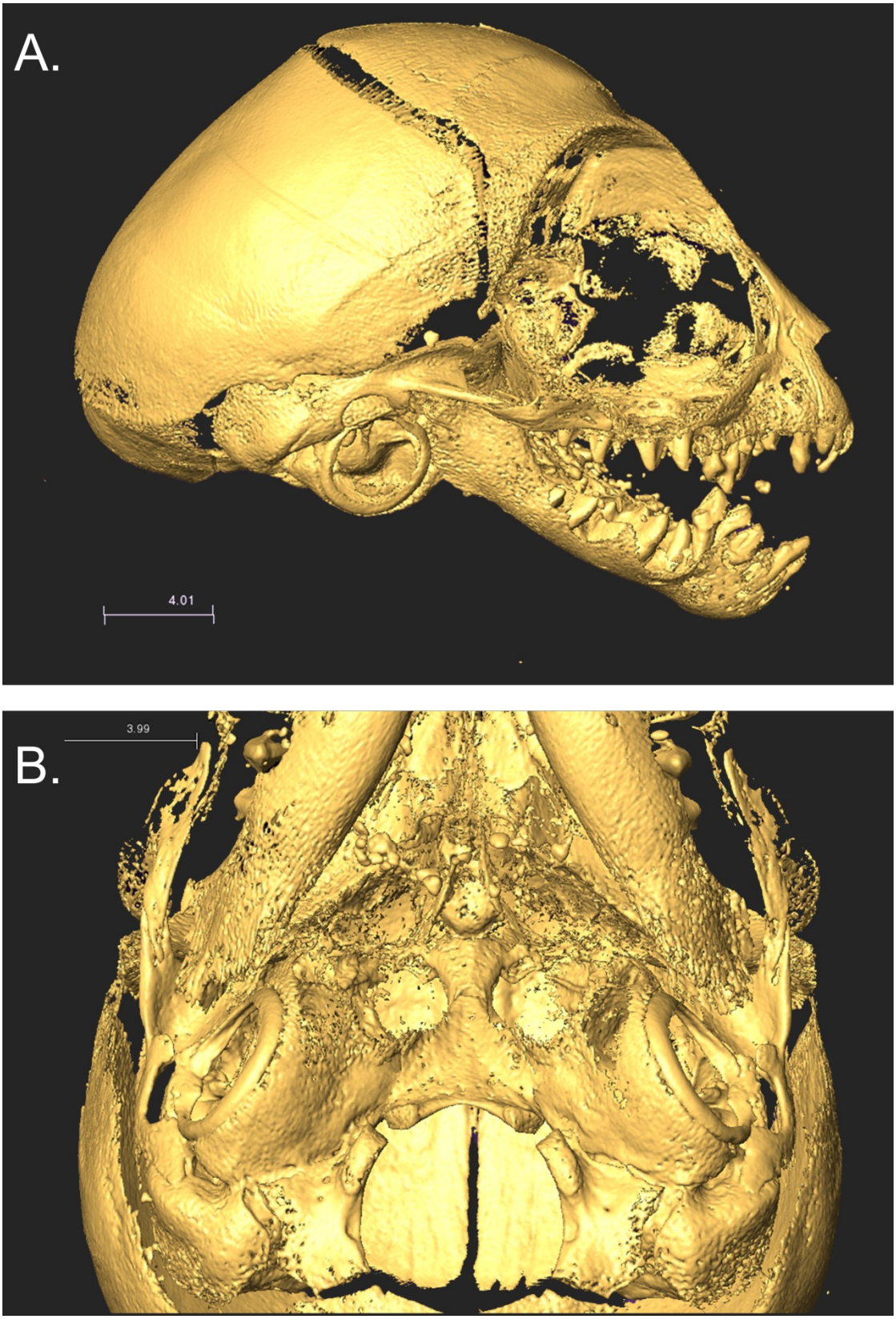

Figure 5.10: *Tarsius syrichta,* neonatal. The petrosal-ectotympanic suture is clearly visible; the ectotympanic bone has not lengthened in any significant way.

Humans

Pronounced anterior and posterior tympanic tubercles are present as early as one month postnatal in humans (Figure 5.11). The tube continues to ossify, remaining roughened and ragged for some time, and generally smoothing out by age six. The ectotympanic tube undergoes a period of rapid ossification between ages one and two. In addition to the ossification of the ectotympanic tube, the tympanic ring shifts orientation, due to pneumatization of the middle ear and the relatively slow growth of the roof of the future ectotympanic tube. Using this modern United States sample, non-metric developmental scores using Weaver (1979) stages correlate significantly with age (Figure 5.12).

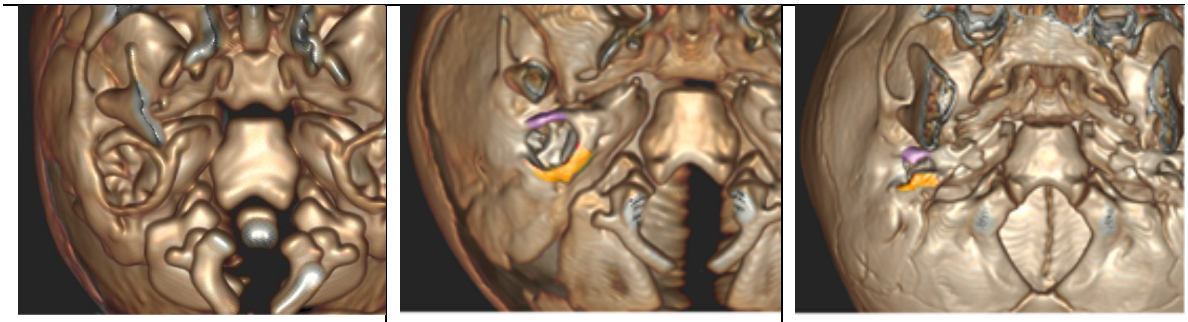

Figure 5.11: The inferior ectotympanic tube expands laterally along with the braincase and mastoid process. Images were obtained from the Baltimore OCME, A: 25 week old fetus; B: 1 month old; C: a 9 month old. Purple = anterior tubercle; orange = posterior tubercle.

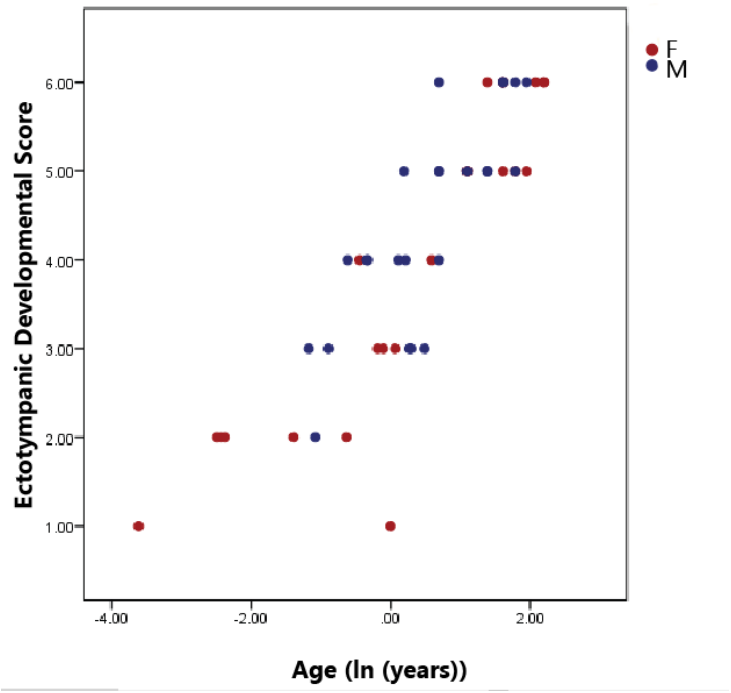

Figure 5.12: Log age v. non-metric developmental score. Spearman rank results indicate the two are highly correlated (correlation coefficient= 0.88, $p<0.001$).

The lengths of the developing areas of the ectotympanic were isolated and measured separately (Figure 5.13). Results indicate that all the areas increase at the same rate until age 2.5 in humans. The center of the ectotympanic generally catches up to the anterior and posterior tubercles by that point and fills out. The anterior and posterior tubercles slow in growth between ages of 2.5 and 7.5. The posterior tubercle generally outpaces the anterior tubercle throughout growth. There is a second growth period late in childhood, 7.5 to 9 years, and it may continue into adolescence.

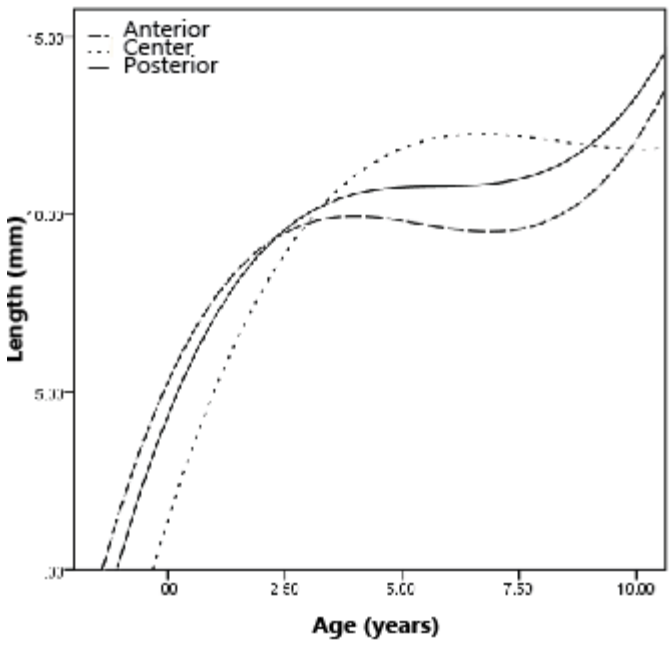

Figure 5.13: Age versus length of the ectotympanic tube at the anterior tubercle, center, and posterior tubercles. The anterior and posterior tubercles undergo rapid ossification between ages 0 and 2. The center ectotympanic largely ossifies between ages 2 and 6.

Non-Human Catarrhine

The non-human catarrhine ectotympanic bone growth variation has not been documented formally before. The youngest catarrhines studied, *Trachypithecus* and *Colobus*, both have a definitive ectotympanic ring at the time of birth (Figure 5.14 and 5.15). The ectotympanic bone is lengthening at this point, but in a single sheet rather than with tubercles.

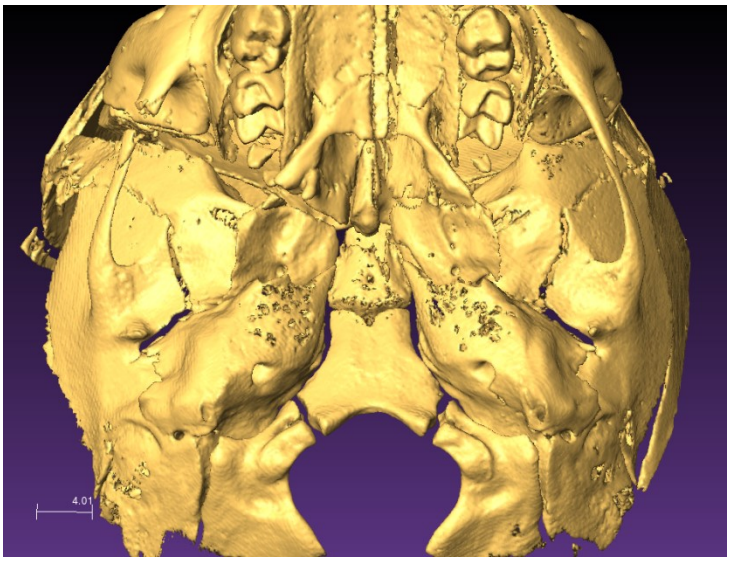

Figure 5.14: *Trachypithecus francoisii,* age 2 days postnatal. Note the lengthening ectotympanic bone but the lack of definitive tubercles at the anterior or posterior margins.

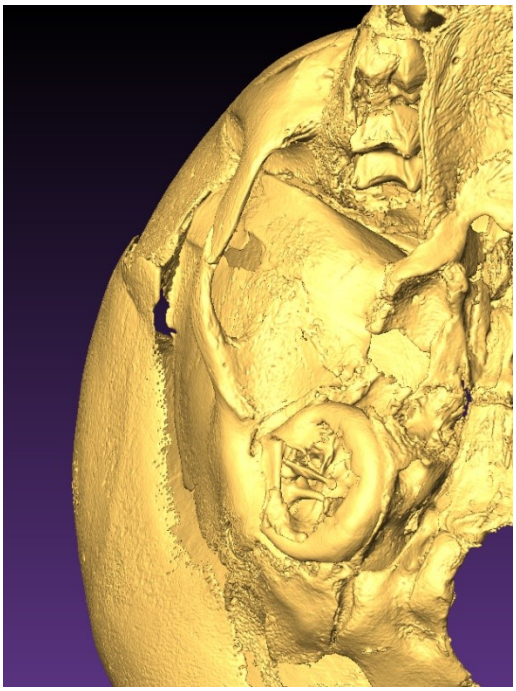

Figure 5.15: Neonatal *Colobus guereza* (Postnatal day 0). There are no definitive tubercles and the bone is lengthening in one uniform sheet.

Slightly later in development, the two *Cercocebus* studied have two tubercles at the anterior and posterior sides of the tube but they demonstrate a much shallower ectotympanic groove (or the angle between the anterior and posterior tubercles) than humans, meaning that the center of the ectotympanic plate is growing more in step with the anterior and posterior tubercles (Figures 5.16-5.17).

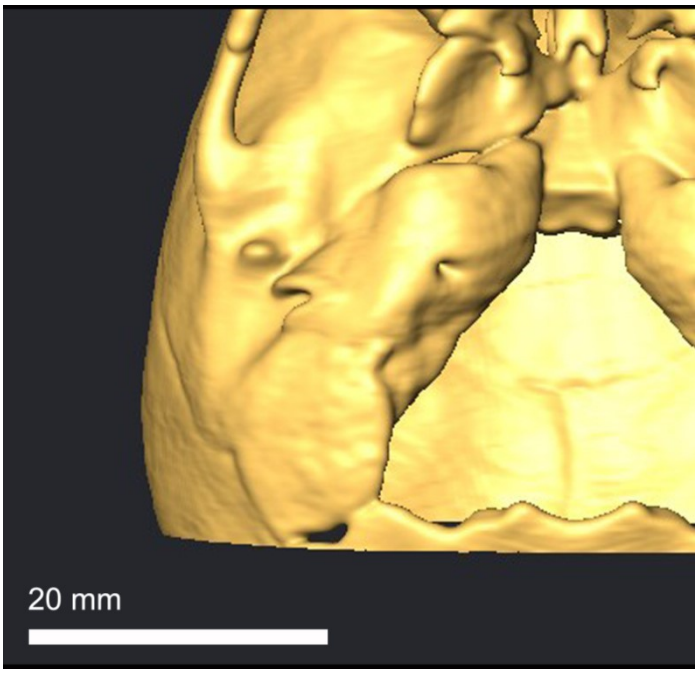

Figure 5.16: *Cercocebus torquatus.* The *Cercocebus* ectotympanic bone growth grows similarly to that of the macaque but the ectotympanic groove is shallower.

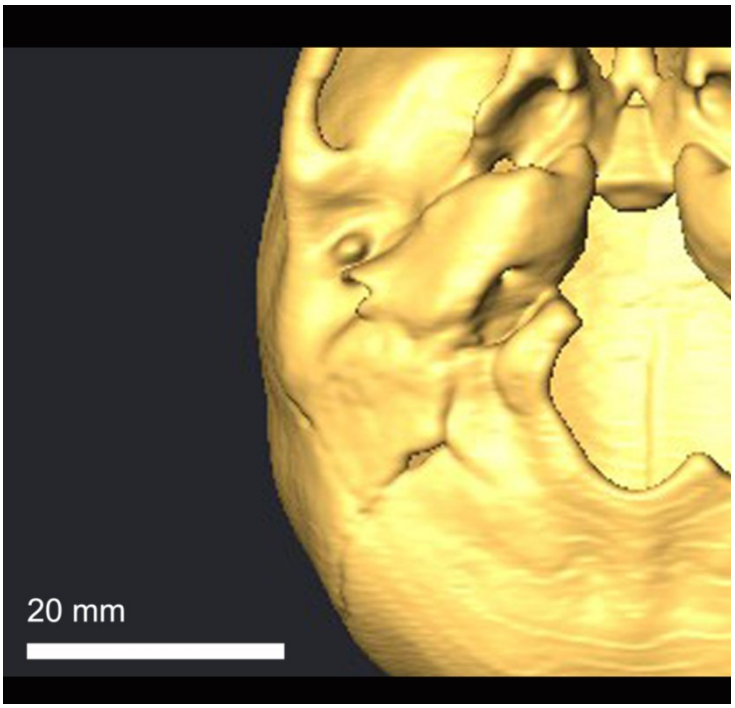

Figure 5.17: *Cercocebus galeritus.* This *Cercocebus* is the same approximate age as that in Fig. 5.16, but slightly further in development. There is no evidence of a foramen of Huschke.

Much more pronounced are the anterior and posterior tubercles seen in the macaques. The tubercles are present in the earliest macaques studied, 34 days postnatal (Figure 5.18).

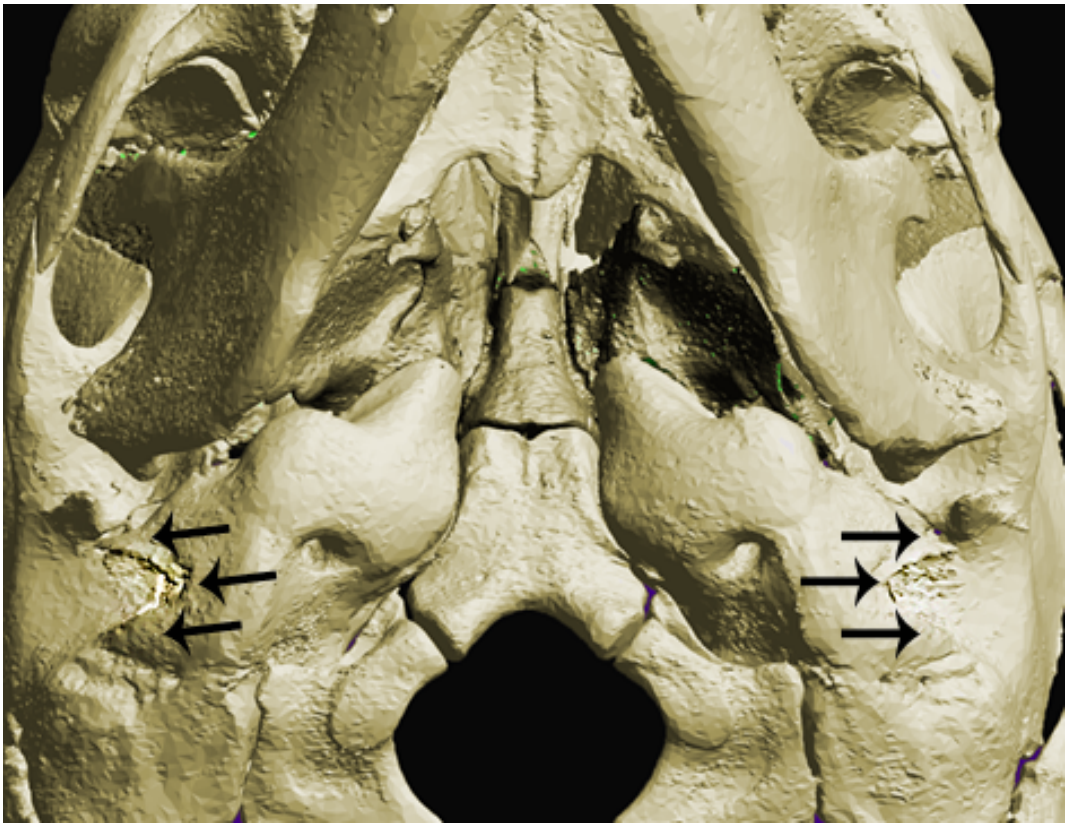

Figure 5.18: *Macaca nemestrina* 34 days postnatal. Note the deep, V-shaped ectotympanic groove indicated with the arrows.

All the catarrhines shown here are in active ossification. The ages of many of the non-human catarrhines are less certain and based on dental aging methods. Rapid ossification of the ectotympanic tube continues through eruption of most or all deciduous dentition but completes prior to eruption of any adult dentition. The three older macaques seen in Figure 5.19 are roughly the equivalent of Weaver's stages 3 and 4.

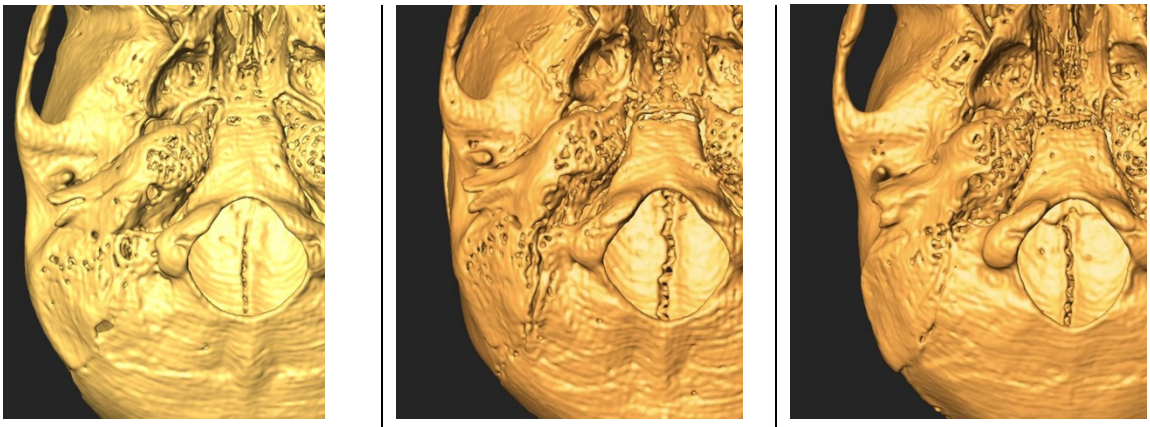

Figure 5.19: *Macaca cyclopis* developing ectotympanic tube. All of these macaques are approximately the same age, ~0.5-1.5 years, Table 5.1.

The ectotympanic groove is generally sharper among non-human catarrhines than in humans. This ectotympanic groove is generally more of a V shape than a U shape (Figure 5.20). No foramina of Huschke were noted among the species examined here. The ectotympanic groove gradually fills in medial to lateral in all the non-human catarrhines analyzed. The *Mandrillus* developing ectotympanic was the most "human-like", with more rounded tubercles anteriorly and posteriorly (Figure 5.21). No mandrills studied, however, exhibited the human condition of lateral tubercles that meet leaving a foramen.

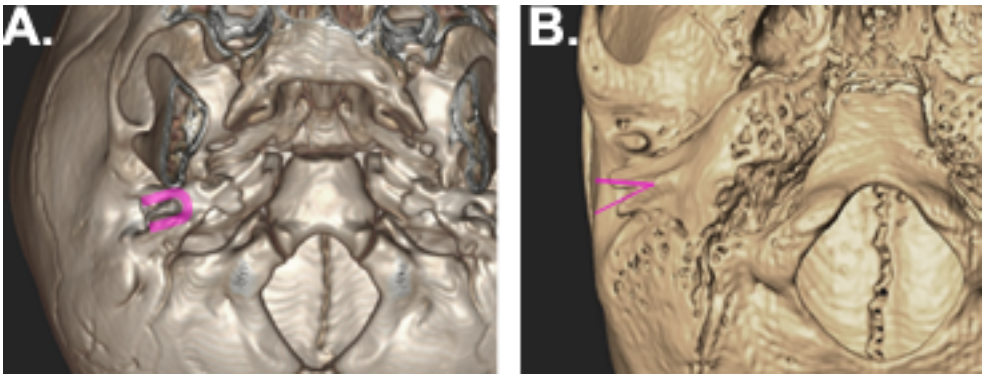

Figure 5.20: Ectotympanic groove highlighted in pink in A. human and B. macaque at Weaver developmental score 4

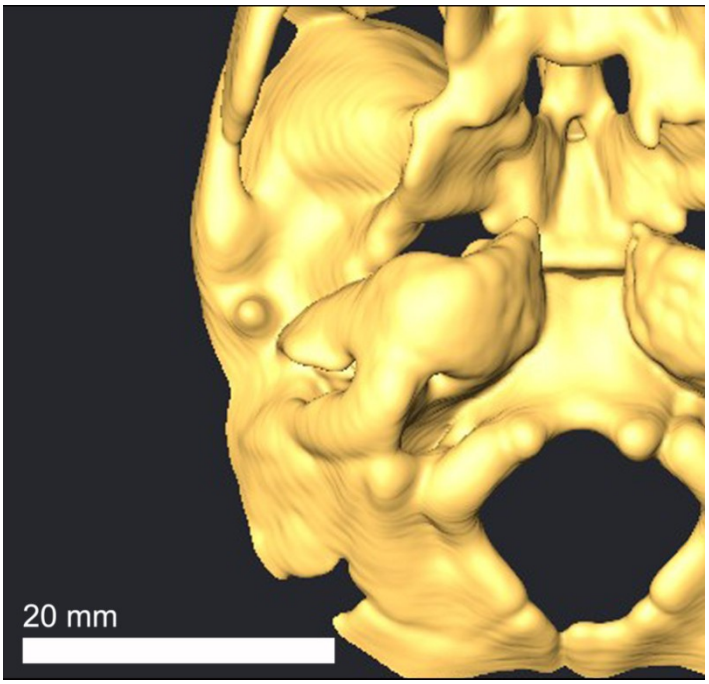

Figure 5.21: *Mandrillus sphinx.* This mandrill is slightly younger than the other catarrhines presented, the anterior and posterior tubercles have fully formed and a deep ectotympanic groove is evident.

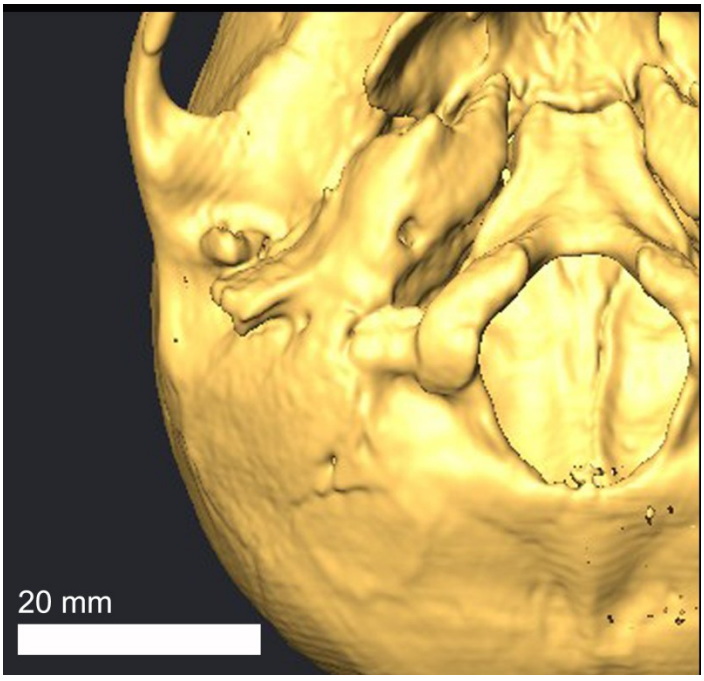

Figure 5.22: *Papio hamadryas.* This baboon has a fully formed ectotympanic tube, again with no foramen of Huschke.

Discussion

Strepsirrhines

The developmental processes shown here among the lorisiforms broadly support Saban's interpretation of the adult morphology but are contrary to the accepted model of primate ectotympanic evolution presented in other texts, particularly those used for introductory courses and broad-stroke primate evolution studies (e.g., Piveteau, 1957; Fleagle, 2013). The accepted wisdom that the lorisiform ectotympanic ring has fused to the lateral bulla is likely true, but the degree to which the ectotympanic bone contributes to the EAM varies quite a bit in many of the species shown here. It has been shown that the ectotympanic bone, while it may contribute to the EAM in the *Loris* adult it likely does so in a secondary way as the result of remodeling of the lemur-like, petrosal-derived EAM. At birth in the genus *Loris*, most of the ectotympanic ring is still intra-bullar, and is not yet fused to the bulla floor.

Additionally, Saban proposed that part of the EAM in *Nycticebus* and *Loris* is composed — at least in part — of the post-glenoid process. It is shown here that in both *Nycticebus* and *Loris* at birth, the post-glenoid processes are separated from the EAM — a configuration that looks very similar to that of lemuriforms (Figure 5.7). Therefore, the incorporation of the post-glenoid process into the EAM structure in both of these lorisiform species is a post-natal occurrence; this could be a mechanical response to the loading of the temporomandibular joint in these two genera.

Particularly compelling evidence for the early presence of the post-glenoid tubercle and lemuriform-style ear morphology in the neonatal *Loris* is the clear presence of the post-glenoid foramen (Figure 5.8). The post-glenoid foramen is variably present across the primate tree and often present among very young primates, but among adult primates it is most common among lemuriforms (Boyd, 1929; Wysocki, 2002). This also provides support for the supposition that the ancestral condition for lorisiforms is likely an

ectotympanic-derived EAM and the post-glenoid process is incorporated in some genera secondarily.

The partial incorporation of the ectotympanic bone into the EAM among lorisiforms complicates the potential for use of this characteristic in the fossil record, as it is not as cut-and-dry as the ectotympanic bones fuse to the lateral petrosal. A driving question behind this dissertation, particularly of Chapter 4, was why there are so few fossil incidences of "intermediate" ectotympanic bones. It is argued here that there are many intermediate examples that have been overlooked, like *Loris*. These results also provide support for the conclusions set forth in Chapters 3 and 4. The species in which the ectotympanic ring is most lateral and comprises most of the EAM are the species that have been noted for wide brains and crania, e.g., *Galago* and *Tarsius*.

Human

In general, ectotympanic bone development correlates unsurprisingly with age. When comparing the present results to the Weaver (1979) results, we see a broadly similar pattern. Most ectotympanic growth occurs in infancy and the anterior and posterior tubercles do outpace the center of the ectotympanic tube; this does not differ significantly from Weaver's original findings. Some important results not captured in the Weaver study, however, are that, in general, the posterior tubercle is longer than the anterior and that the tubercles grow beyond age five. No foramina of Huschke were found over the age of five. Given the evidence of patent foramina in other populations, particularly archaeological ones, it is suggested that modern incidences of this phenomenon are population dependent and that the abnormal persistence of the foramen may be diet and health dependent. The speed of foramen closure and the developmental timing of this closure (around the time of weaning) indicate that failure to close could be a sign of poor health and diet in a population. An additional consideration

in the present study is that these are juveniles that were autopsied, meaning they may have been victims of violence, malnutrition, and/or infectious disease. Their growth may not have been “normal” and that must be considered when asking questions about timing of growth processes.

Non-human Catarrhine

None of the non-human catarrhines examined here displayed evidence of a foramen of Huschke. While the absence of evidence is not evidence of absence, the shape of the developing non-human catarrhine tube does not appear to lend itself to the formation of such a foramen. However, the sample sizes are small and not all age groups were considered for all species, making it difficult to make conclusions on this front. Regardless, this is the first analysis of the ectotympanic tube growth across non-human catarrhines and provides a basis on which future analyses can be built. Non-human catarrhines, like humans, develop large anterior and posterior tubercles and the center of the ectotympanic plate “catches up” later. The gross morphology of the ectotympanic tubercles, however, is dissimilar from humans in overall shape. Whereas human tubercles are blunted and bulbous at the lateral tips, the non-human catarrhine tubercles are smooth and sharp and these tips do not extend inferiorly in the way that human tubercles do. The lack of blunting among non-human catarrhines is likely why they do not exhibit the foramen of Huschke. The other possibility, though not tested here, is that the human ectotympanic plate is thicker and shorter than in other catarrhines and the short, thick ectotympanic tube morphology is predisposed to prematurely meeting before the center of the ectotympanic can catch up.

Non-human catarrhines develop the ectotympanic plate earlier than humans do, which is consistent with many biological processes and life histories (Clutton-Brock and Harvey, 1980). Broadly, rapid ectotympanic growth occurs near the time of weaning in

most species. At the time of weaning, however, many processes are co-occurring including the eruption of the first permanent molar (Smith, 1991), a burst in brain growth as the diet begins to change (Harvey and Clutton-Brock, 1985), and the mandible begins to be mechanically loaded in earnest. The temporomandibular joint is immediately adjacent to the ectotympanic region. One of the functional hypotheses for the ossification of the ectotympanic cartilage is to provide an additional barrier to dampen the noise produced during mastication (Packer and Sarmiento, 1984). If that functional hypothesis holds true, then it does indeed make sense that rapid ossification would occur as that joint begins to be loaded. However, given previous results, it is contended that it is much more likely that the reason we see this rapid period of ectotympanic bone growth when we do is that the brain is growing so rapidly, particularly in the lateral direction, during infancy.

Conclusion

Can ontogeny resolve the questions surrounding the lorisiform and tarsier ectotympanic bones? Across lorisiforms, is the external auditory meatus derived from the petrosal bone, ectotympanic bone, or some combination of the two?

It was shown in previous chapters that the lorisiform ectotympanic bone was longer than expected given the ring-versus-tube dichotomy. The lorisiform and tarsier ectotympanic bones both tend to lengthen in a single sheet, rather than dividing up into tubercles. Saban's illustrations prove to be quite accurate, and there is very significant variation within the lorisiform external auditory meatus makeup, and at birth we can see the developing contributions from both the post-glenoid tubercle in *Loris* and *Nycticebus* as well as the differentiation between the petrosal bulla and ectotympanic bone in the *Loris.*

Will an updated sample of known-age modern individuals and new visualization technology alter the developmental models of the human ectotympanic bone illustrated in Scheuer & Black (2000)?

Weaver's model works fairly well for this sample of modern human children. His self-critique remains valid: that this methodology has limited applicability for age estimation of forensic or archaeological human remains. He also underestimated the time in which growth occurs; here we saw continual active growth until age nine. In previous chapters, it was hypothesized and shown that among adults the most important factor in length of an ectotympanic tube is the relative width of the cranial base. The pattern observed in the adult humans and other primates bears out when observing the juveniles; juveniles with wide crania tend to have long ectotympanic bones.

Do other catarrhines follow the same or a similar ontogenetic trajectory as humans?

The non-human catarrhine ectotympanic bones broadly follow the pattern observed in humans with the notable exception of the foramen of Huschke. Most of the lengthening of the ectotympanic bone across species tends to occur around the time of weaning but that likely has more to do with brain growth than mechanical loadings caused by mastication.

6. Conclusions and Future Directions

These three chapters taken together address the core of how and why the ectotympanic tube varies and have potential for interpretations of the ear tube in phylogenetic analysis. Phylogenetic analysis has changed greatly in recent years, incorporating molecular methods and thus building phylogenies has become a compromise between molecular and morphological methods (Hillis, 1987; Meyer and Zardoya, 2003; Delsuc et al., 2005; Perelman et al., 2011). Morphological characteristics remain useful and broadly applied, particularly in the fields of paleobiology and paleoanthropology where DNA is rarely available. When choosing a character for these kinds of analyses, one frequent filter applied is the preference for “discrete” characters, rather than continuous ones (Baum, 1988; Thiele, 1993). This is not only for the ease of analysis, but also discrete characters are assumed to be generally more independent than continuous ones. However, biology tends to be so complicated that these types of discrete characters are rare and perhaps that is one reason the ectotympanic bone/ring dichotomy is so attractive. Not only is it an easy way to illustrate primate diversity but it seems so strictly phylogenetic at a glance. However, it is shown here that the morphology of the ectotympanic bone is not nearly as cut-and-dry as previously assumed.

Ectotympanic bone length is likely an evolutionary byproduct of overall cranial shape driven by brain shape. While the fact that the ectotympanic bone is evidently not binary somewhat discounts its applicability as a discrete character in phylogenetic analysis, this knowledge increases the potential for analyses of overall cranial structures and the interplay between soft and hard tissues in the primate cranium. The lateral aspect of the ectotympanic tube does not directly attach to muscles and but it is still being affected by soft tissues in interesting ways and it should be considered when evaluating the overall shape of the cranial base.

This dissertation has clarified some of the uncertainty surrounding the ectotympanic bone, particularly those specific to the lorisiform primates. These neonatal observations provide a strong argument for treating the ectotympanic bone as a continuous character. It has been shown that the lorisiform ectotympanic bone makes up a varying amount of the external auditory meatus, and this is mostly affected by post-natal changes. At birth, all primates studied here exhibited a fully formed ectotympanic ring and this provides support that among lorisiforms, this is the ancestral condition.

The tarsier condition has long been of interest to understanding how the ectotympanic bone varies across phylogeny. Furthermore, the elongation of the ectotympanic bone in this taxon has been cited as an example of convergent evolution with haplorhines. In many ways, the tarsier is similar to the lorisiforms condition and it is suggested here that the tarsier has a lorisiform cranial base arrangement at birth, but that hypertrophy of the brain in certain regions is the proximate cause of its unusual ectotympanic bone condition. This tarsiiform condition is certainly unusual but would be expected based on other aspects of its basicranial anatomy; the tarsier ectotympanic bone is laterally displaced, but looks nearly identical to that of the *Galago* at birth. The strikingly large eyeballs of the tarsier might constrain growth on the ectotympanic bone's medial edge. The morphology of the temporal lobe of the brain certainly places pressures on the lateral limit of the ectotympanic, and the documented extreme brachycephaly and anthropoid brain proportions (Allen, 2014) are likely contributing to the relative length of the ectotympanic bone.

Based on these analyses, platyrrhines tend to be unusual in their extremely short ectotympanic bones; it is certainly possible that they are demonstrating a derived condition. However, based on the suggestions here, a contributing factor may be a relatively narrow, long cranium. This taxon is in need of further study, particularly in the relationship between the cartilage morphology and the bone. Coleman and Ross (2004)

and Coleman's subsequent publications (Coleman, 2007, 2009; Coleman and Colbert, 2010) began the important work of describing and analyzing the potential relationships between anatomy and auditory performance in primates but his studies were focused on the soft tissues that are observable from the outside and on bony anatomy. Plates of cartilage certainly fill some or all of the space between the ectotympanic bone and the platyrrhine pinna, but the morphology and the cross-species diversity of these internal cartilaginous structures have not been shown previously. They must be better understood in order to fully understand the pressures on the auditory complex in platyrrhines. Until recently, these soft tissue structures had to be studied through anatomical dissection, which is both a costly and destructive method. However, with the advent of staining protocols paired with micro-CT scans, the soft tissues will become much more accessible in future years.

In this dissertation, it was shown that, in agreement with previous assessments, the fossil taxa *Aegyptopithecus zeuxis* and *Pliopithecus vindobonensis* both fall in between the catarrhine and platyrrhine conditions. In many respects, the ectotympanic bones of both taxa are much closer to the platyrrhine condition than the catarrhine. While this does corroborate the findings of the earliest descriptions of these fossils, other results presented here suggest that this is likely an artifact of cranial shape that in some ways make the short length of the ectotympanic bone more interesting. The present conclusions support previous research that shows both that the endocranial volume and brain proportions of *A. zeuxis* fall intermediately between haplorhines and strepsirrhines (Allen, 2014).

The chapters presented in this dissertation provide a clearer view of the many complex factors affecting the primate ectotympanic tube and provide context for the apparent variation in adult, extant primates. Ectotympanic tube morphology is strongly

associated with many aspects of the cranial base and soft tissue structures including brain morphologies and masticatory systems through development and evolution.

Future Directions

To further demonstrate the relationship between soft tissue structures and ectotympanic shape, in the future I will be employing iodine and osmium staining protocols to visualize soft tissues of the ear region. These methods will solve several of the methodological problems of working solely with micro-CT data. Iodine allows for the direct visualization of the brain (e.g., Gignac and Kley, 2014; Balanoff et al., 2016) and the comparison of regional brain morphology to search for the suspected scaling relationships with the ectotympanic bone length. Further, iodine staining may potentially allow for the observation of the auricular muscles to test for the suspected relationship between the soft tissue ear canal and mobility in the pinna.

References

Adams DC, Collyer ML, Kaliontzopoulou A, Sherratt E. 2017. Geomorph: Software for geometric morphometric analyses. R package version 3.0. 5.

Alba DM, Almécija S, Demiguel D, Fortuny J, Ríos MPDL, Pina M, Robles JM, Moyà-solà S. 2015. Miocene small-bodied ape from Eurasia sheds light on hominoid evolution. Science 350:528.

Allen K. 2014. Endocranial volume and shape variation in early anthropoid evolution. Doctoral Dissertation. Duke University.

Allen KL, Kay RF. 2012. Dietary quality and encephalization in platyrrhine primates. Proc R Soc B Biol Sci 279:715–721.

Allin EF. 1986. The auditory apparatus of advanced mammal-like reptiles and early mammals. In: Hotton N, MacLea P, Roth J, Roth E, editors. The ecology and biology of mammal-like reptiles. Washington, DC: Smithsonian Institution Press. p 283–294.

Allin EF, Hopson JA. 1992. Evolution of the auditory system in Synapsida ("mammal-like reptiles" and primitive mammals) as seen in the fossil record. In: Webster D, Fay R, Popper A, editors. The evolutionary biology of hearing. New York: Springer. p 587–614.

Anderson JE. 1960. The development of the tympanic plate. Natl Museum Canada Bull 180:143–153.

Andresen PR, Nielsen M. 2001. Non-rigid registration by geometry-constrained diffusion. Med Image Anal 5:81–88.

Andrews P., Harrison T., Delson E, Bernor RL., Martin L. 1996. Distribution and biochronology of European and southwest Asian Miocene catarrhines. In: Bernor PL, Fahlbusch V., Mittmann H-W, editors. European and Southwest Asian Miocene Catarrhines. New York: Columbia University Press. p 168–207.

Ankel-Simons F, Fleagle JG, Chatrath PS. 1998. Femoral anatomy of *Aegyptopithecus zeuxis*, an early oligocene anthropoid. Am J Phys Anthropol 106:413–424.

Anson BJ, Bast TH., Richany SF. 1955. The fetal and early postnatal development of the tympanic ring and related structures in man. Ann Otol Rhinol Laryngol 64:802–822.

Anson BJ, Donaldson JA. 1981. Surgical anatomy of the temporal bone and ear, 3rd Edition. Philadelphia: WB Saunders Company.

Archibald JD. 1977. Ectotympanic bone and internal carotid circulation of eutherians in reference to anthropoid origins. J Hum Evol 6:609–622.

Arias-Martorell J, Alba DM, Potau JM, Bello-Hellegouarch G, Pérez-Pérez A. 2015. Morphological affinities of the proximal humerus of *Epipliopithecus vindobonensis* and *Pliopithecus antiquus*: Suspensory inferences based on a 3D geometric

morphometrics approach. J Hum Evol 80:83–95.

Ars B. 1989. Organogenesis of the middle ear structures. J Laryngol Otol 103:16–21.

Balanoff AM, Bever GS, Colbert MW, Clarke JA, Field DJ, Gignac PM, Ksepka DT, Ridgely RC, Smith NA, Torres CR, Walsh S, Witmer LM. 2016. Best practices for digitally constructing endocranial casts: examples from birds and their dinosaurian relatives. J Anat 229:173–190.

Bast TH. 1930. Ossification of otic capsule in human fetuses. Contrib Embryol 121:53–82.

Bastir M, Rosas A. 2009. Mosaic evolution of the basicranium in *Homo* and its relation to modular development. Evol Biol 36:57–70.

Bastir M, Rosas A, Lieberman DE, O'Higgins P. 2008. Middle cranial fossa anatomy and the origin of modern humans. Anat Rec 291:130–140.

Baum BR. 1988. A simple procedure for establishing discrete characters from measurement data, applicable to cladistics. Taxon 37:63–70.

Beard KC, Krishtalka L, Stucky RK. 1991. First skulls of the early Eocene primate *Shoshonius cooperi* and the anthropoid-tarsier dichotomy. Nature 349:64.

Beard KC, MacPhee RDE. 1994. Cranial anatomy of *Shoshonius* and the antiquity of Anthropoidea. In: Anthropoid origins. Springer. p 55–97.

Begun DR. 2002. The Pliopithecoidea. In: Hartwig W, editor. Primate Fossil Record. Cambridge University Press, Cambridge. p 221–240.

Biegert J. 1963. The evaluation of characteristics of the skull, hands and feet for primate taxonomy. In: Washburn SL, editor. Classification and human evolution. Vol. 37. Chicago: Aldine. p 116–145.

Bloch JI, Silcox MT. 2001. New basicrania of paleocene-eocene Ignacius: Re-evaluation of the plesiadapiform-dermopteran link. Am J Phys Anthropol 116:184–198.

Bookstein FL. 1997. Morphometric tools for landmark data: geometry and biology. Cambridge: Cambridge University Press.

Boyd GI. 1929. The emissary foramina of the cranium in man and the anthropoids. J Anat 65:108–121.

Burger BJ. 2010. Skull of the Eocene primate *Omomys carteri* from Western North America. Paleontol Contrib:1–19.

Byrne R, Whiten A. 1989. Machiavellian intelligence: social expertise and the evolution of intellect in monkeys, apes, and humans. Oxford, UK: Oxford University Press.

Cartmill M. 1982. Assessing tarsier affinities: Is anatomical description phylogenetically neutral? Geobios Mem Spec 6:279–287.

Cartmill M, Kay RF. 1978. Craniodental morphology, tarsier affinities, and primate suborders. Recent Adv Primatol 3:205–214.

Cartmill M, MacPhee RDE. 1980. Tupaiid affinities: the evidence of the carotid arteries and cranial skeleton. In: Comparative biology and evolutionary relationships of tree shrews. Springer. p 95–132.

Cartmill M, MacPhee RDE, Simons EL. 1981. Anatomy of the temporal bone in early anthropoids, with remarks on the problem of anthropoid origins. Am J Phys Anthropol 56:1–21.

Clutton-Brock TH, Harvey PH. 1980. Primates, brains and ecology. J Zool 190:309–323.

Coleman MN. 2007. The functional morphology and evolution of the primate auditory system. Doctoral Dissertation. State University of New York at Stony Brook.

Coleman MN. 2009. What do primates hear? A meta-analysis of all known nonhuman primate behavioral audiograms. Int J Primatol 30:55–91.

Coleman MN, Colbert MW. 2010. Correlations between auditory structures and hearing sensitivity in non-human primates. J Morphol 271:511–532.

Coleman MN, Kay RF, Colbert MW. 2010. Auditory morphology and hearing sensitivity in fossil new world monkeys. Anat Rec 293:1711–1721.

Coleman MN, Ross CF. 2004. Primate auditory diversity and its influence on hearing performance. Anat Rec - Part A Discov Mol Cell Evol Biol 281:1123–1137.

Conroy GC. 1980. Ontogeny, auditory structures, and primate evolution. Am J Phys Anthropol 52:443–451.

Daegling DJ. 1989. Biomechanics of cross-sectional size and shape in the hominoid mandibular corpus. Am J Phys Anthropol 80:91–106.

Daegling DJ. 2001. Biomechanical scaling of the hominoid mandibular symphysis. J Morphol 250:12–23.

Darwin C. 1859. On the Origin of Species by Means of Natural Selection, or Preservation of Favored Races in the Struggle for Life. London: John Murray.

Dean MC, Wood BA. 1982. Basicranial anatomy of Plio-Pleistocene hominids from East and South Africa. Am J Phys Anthropol 59:157–174.

DeLeon VB, Richtsmeier JT. 2009. Fluctuating asymmetry and developmental instability in sagittal craniosynostosis. Cleft Palate-Craniofacial J 46:187–196.

DeLeon VB, Smith TD, Rosenberger AL. 2016. Ontogeny of the postorbital region in tarsiers and other primates. Anat Rec 299:1631–1645.

Delson E, Rosenberger L. 1980. Phyletic perspectives on platyrrhine origins and anthropoid relationships. In: Evolutionary biology of the new world monkeys and

continental drift. . p 445–458.

Delsuc F, Brinkmann H, Philippe H. 2005. Phylogenomics and the reconstruction of the tree of life. Nat Rev Genet 6:361.

Dryden IL, Mardia K V. 1998. Statistical shape analysis. Chinchester: Wiley.

Dumont ER. 1995. Enamel thickness and dietary adaptation among extant primates and chiropterans. Am Soc Mammal 76:1127–1136.

Dunbar RIM. 1998. The social brain hypothesis. Evol Anthropol 6:178–190.

Edinger T. 1948. Paleoneurology versus comparative brain anatomy. Stereotact Funct Neurosurg 9:5–24.

Falk D. 1980. Hominid brain evolution: The approach from paleoneurology. Am J Phys Anthropol 23:93–107.

Fish JL, Lockwood CA. 2003. Dietary constraints on encephalization in primates. Am J Phys Anthropol 120:171–181.

Fleagle JG. 2013. Primate adaptation and evolution. San Diego: Academic Press.

Fleischer G. 1978. Evolutionary principles of the mammalian middle ear. Anat Embryol Cell Biol 55:1–70.

Forster A. 1925. L'inclinaison du tympan chez les mammifères supérieurs et chez l'homme. Arch Anat Histol Embryol 4:295–321.

Gignac PM, Kley NJ. 2014. Iodine-enhanced micro-CT imaging: Methodological refinements for the study of the soft-tissue anatomy of post-embryonic vertebrates. J Exp Zool Part B Mol Dev Evol 322:166–176.

Gilbert SF. 2000. Osteogenesis: the development of bones. In: Gilbert SF, editor. Developmental biology. 6th ed. Sunderland, MA: Sinauer Associates.

Gilroy AM, MacPherson BR eds. 2016. Atlas of Anatomy. 3rd ed. New York.

Gingerich PD. 1973. Anatomy of the temporal bone in the Oligocene Anthropoid *Apidium* and the Origin of Anthropoidea. Folia Primatol 19:329–337.

Gingerich PD. 1980. Eocene Adapidae, paleobiogeography, and the origin of South American Platyrrhini. In: Ciochon; RL, Chiarelli AB, editors. Evolutionary biology of the New World monkeys and continental drift. Springer. p 123–138.

Gingerich PD. 1981. Early cenozoic omomyidae and the evolutionary history of tarsiiform primates. J Hum Evol 10:345–374.

Gingerich PD, Smith BH. 1982. Allometric scaling in the dentition of primates and insectivores. Am J Phys Anthropol 58:81–100.

Gould SJ. 1977. Ontogeny and phylogeny. Cambridge, MA: Harvard University Press.

Gregory W. 1920. On the structure and relations of Notharctus, an American Eocene primate. Mem Am Mus Nat Hist N Ser 3.

Groves CP. 1970. *Gigantopithecus* and the Mountain Gorilla. Nature 227:520–521.

Haeckel E. 1866. Generelle morphologie der organismen, 2 Vols.–I. Allgemeine Anatomie der Organismen; II: Allgemeine Entwicklungsgeschichte der Organismen.

Hallgrimsson B, Willmore K, Dorval C, Cooper DML, Hallgrímsson B. 2004. Craniofacial variability and modularity in macaques and mice. J Exp Zool 302B:207–225.

Harris JD. 1943. The auditory acuity of preadolescent monkeys. J Comp Psychol 35:255.

Harrison T. 2005. The zoogeographic and phylogenetic relationships of early catarrhine primates in Asia. Anthropol Sci 113:43–51.

Harrison T, Delson E, Jian G. 1991. A new species of *Pliopithecus* from the middle Miocene of China and its implications for early catarrhine zoogeography. J Hum Evol 21:329–361.

Harvey PH, Clutton-Brock TH. 1985. Life History Variation in Primates. Evolution (N Y) 39:559–581.

Hashimoto T, Ojiri H, Kawai Y. 2011. The foramen of Huschke: Age and gender specific features after childhood. Int J Oral Maxillofac Surg 40:743–746.

Heffner RS. 2004. Primate hearing from a mammalian perspective. Anat Rec 281:1111–1122.

Hershkovitz P. 1974. The ectotympanic bone and origin of higher primates. Folia Primatol 22:237–242.

Hillis DM. 1987. Molecular versus morphological approaches to systematics. Ann Rev Ecol Syst 18:23–42.

Himalstein MR. 1959. Mastoid pneumatization: a case with interesting developmental and phylogenetic aspects. Laryngoscope 69:561–570.

Holloway RL. 1992. The failure of the gyrification index (GI) to account for volumetric reorganization in the evolution of the human brain. J Hum Evol 22:163–170.

Holloway RL, Broadfield DC, Yuan MS. 2005. Hominid endocasts: some general notes. Hum Foss Rec:283–294.

Hürzeler J. 1948. Zur stammesgeschichte der necrolemuriden. Schweiz Palaeont Abh 6:1–48.

Jackson LL, Heffner RS, Heffner HE. 1999. Free-field audiogram of the Japanese macaque (*Macaca fuscata*). J Acoust Soc Am 106:3017–3023.

Jurda M, Urbanová P, Králík M. 2015. The post-mortem pressure distortion of human

crania uncovered in an early Medieval pohansko (Czech Republic) graveyard. Int J Osteoarchaeol 25:539–549.

Kalinka AT, Varga KM, Gerrard DT, Preibisch S, Corcoran DL, Jarrells J, Ohler U, Bergman CM, Tomancak P. 2010. Gene expression divergence recapitulates the developmental hourglass model. Nature 468:811–814.

Kawasaki K, Richtsmeier JT. 2017. Association of the chondrocranium and dermatocranium in early skull development. In: Percival CJ., Richtsmeier JT, editors. Building bones: Early bone development informing anthropological inquiry. Cambridge, UK: Cambridge University Press. p 52–78.

Kay RF, Ross C, Williams BA. 1994. Anthropoid Origins. Science (80) 275:797–804.

Kay RF, Williams BA, Ross CF, Takai M, Shigehara N. 2004. Anthropoid origins: a phylogenetic analysis. Anthr Orig:91–135.

Keith A. 1903. The extent to which the posterior segments of the body have been transmuted and suppressed in the evolution of man and allied primates. J Anat Physiol 37:18.

Keith A. 1923. Hunterian lectures on man's posture: Its evolution and disorders: Given at the royal college of surgeons of england. Br Med J 1:669.

Kelley J, Plavcan JM. 1998. A simulation test of hominoid species number at Lufeng, China: Implications for the use of the coefficient of variation in paleotaxonomy. J Hum Evol 35:577–596.

Kelley J, Xu QH. 1991. Extreme sexual dimorphism in a Miocene hominoid. Nature 352:151–153.

Kimbel WH. 1986. Calvarial morphology of *Australopithecus afarensis*: a comparative phylogenetic study. Doctoral Dissertation. Kent State University.

Kirk EC, Daghighi P, Macrini TE, Bhullar BAS, Rowe TB. 2014. Cranial anatomy of the duchesnean primate *Rooneyia viejaensis*: New insights from high resolution computed tomography. J Hum Evol 74:82–95.

Klaauw CJ van der. 1931. The auditory bulla in some fossil mammals: with a general introduction to this region of the skull. Bull AMNH 62.

Klingenberg CP. 2011. MorphoJ: an integrated software package for geometric morphometrics. Mol Ecol Resour 11:353–357.

Klingenberg CP. 2016. Size, shape, and form: concepts of allometry in geometric morphometrics. Dev Genes Evol 226:113–137.

Klingenberg CP, Barluenga M, Meyer A. 2002. Shape analysis of symmetric structures: Quantifying variation among individuals and asymmetry. Evolution (N Y) 56:1909–1920.

Kobrak HG. 1948. Construction material of the sound conduction system of the human ear. J Acoust Soc Am 20:125–130.

Krogman WM. 1932. The morphological characters of the Australian skull. J Anat 66:399.

Lacout A, Marsot-Dupuch K, Smoker WRK, Lasjaunias P. 2005. Foramen tympanicum, or foramen of Huschke: Pathologic cases and anatomic CT study. Am J Neuroradiol 26:1317–1323.

Lambert JE, Chapman CA, Wrangham RW, Conklin-Brittain N Lou. 2004. Hardness of cercopithecine foods: Implications for the critical function of enamel thickness in exploiting fallback foods. Am J Phys Anthropol 125:363–368.

Larsen WJ, Sherman LS, Potter SS, Scott WJ. 1993. Human embryology. New York: Churchill Livingstone.

Laughlin WS, Jørgensen JB. 1956. Isolate variation in Greenlandic Eskimo crania. Hum Hered 6:3–12.

Lieberman DE. 1998. Sphenoid shortening and the evolution of modern human cranial shape. Nature 393:158–162.

Lieberman DE, Mcbratney BM, Krovitz G, Harpending HC. 2002. The evolution and development of cranial form in *Homo sapiens*. PNAS 99:1134–1139.

Lieberman DE, Pearson OM, Mowbray KM. 2000. Basicranial influence on overall cranial shape. J Hum Evol 38:291–315.

Lockwood CA, Lynch JM, Kimbel WH. 2002. Quantifying temporal bone morphology of great apes and humans: an approach using geometric morphometrics. J Anat 201:447–464.

Lombard RE, Bolt JR. 1979. Evolution of the tetrapod ear: an analysis and reinterpretation. Biol J Linn Soc 11:19–76.

Lombard RE, Hetherington TE. 1993. Structural basis of hearing and sound transmission. In: Hanken J, Hall B, editors. The Skull. Vol. 3: Functional and Evolutionary Mechanisms. Vol. 3. Chicago: The University of Chicago Press Chicago, Illinois. p 241–302.

Lonsbury-Martin BL, Martin GK. 1981. Effects of moderately intense sound on auditory sensitivity in rhesus monkeys: behavioral and neural observations. J Neurophysiol 46:563–586.

Luckett WP. 1976. Cladistic relationships among primate higher categories: Evidence of the fetal membranes and placenta. Folia Primatol 25:245–276.

Luo Z-X, Schultz JA, Ekdale EG. 2016. Evolution of the middle and inner ears of mammaliaforms: The approach to mammals. In: Clack JA, Fay RR, Popper AN, editors. Evolution of the Vertebrate Ear. Vol. 139–174. Cham, Switzerland: Springer

International Publishing.

MacPhee RDE, Novacek MJ., Storch G. 1988. Basicranial morphology of early tertiary erinaceomorphs and the origin of primates. Am Museum Novit 2921:1–42.

MacPhee RDE. 1977. Ontogeny of the ectotympanic-petrosal plate relationship in strepsirrhine prosimians. Folia Primatol 27:245–283.

MacPhee RDE. 1979. Entotympanics, ontogeny and primates. Folia Primatol 31:23–47.

MacPhee RDE. 1981. Auditory regions of primates and eutherian insectivores: morphology, ontogeny, and character analysis. Contrib primatol 18:1–282.

MacPhee RDE, Cartmill M. 1986. Basicranial structures and primate systematics. In: Swindler D, Erwin J, editors. Comparative Primate Biology. Vol. 1: Systematics, Evolution and Anatomy. New York: AR Liss. p 219–275.

Maier W. 2013. The entotympanic in late fetal artiodactyla (Mammalia). J Morphol 274:926–939.

Maier W, Ruf I. 2016a. Evolution of the mammalian middle ear: A historical review. J Anat 228:270–283.

Maier W, Ruf I. 2016b. The anterior process of the malleus in Cetartiodactyla. J Anat 49:313–323.

Manley GA. 2000. Cochlear mechanisms from a phylogenetic viewpoint. Proc Natl Acad Sci 97:11736–11743.

Marino L, Marino L. 2002. Convergence of complex cognitive abilities in cetaceans and primates. Hum Soc Inst Sci Policy Anim Stud Repos 59:21–32.

Martin RD. 1990. Primate origins and evolution. Boca Raton: Chapman and Hall.

McCarthy RC. 2001. Anthropoid cranial base architecture and scaling relationships. J Hum Evol 40:41–66.

McGraw WS, Pampush JD, Daegling DJ. 2012. Brief communication: Enamel thickness and durophagy in mangabeys revisited. Am J Phys Anthropol 147:326–333.

Meng J, Hu Y, Li C. 2003. The Osteology of Rhombomylus (Mammalia , Glires): Implications for Phylogeny and Evolution of Glires. Bull Am MUSEUM Nat Hist 275:1–81.

Meyer A, Zardoya R. 2003. Recent advances in the (molecular) phylogeny of vertebrates. Annu Rev Ecol Evol Syst 34:311–338.

Miller ER, Gunnell GF, Martin RD. 2005. Deep time and the search for anthropoid origins. Yearb Phys Anthropol 48:60–95.

Milton K. 1988. Foraging behaviour and the evolution of primate intelligence.

Milton K. 2006. Diet and Primate Evolution. Sci Am sp 16:22–29.

Mitteroecker P, Bookstein F. 2008. The evolutionary role of modularity and integration in the hominoid cranium. Evolution (N Y) 62:943–958.

Mitteroecker P, Gunz P, Bernhard M, Schaefer K, Bookstein FL. 2004. Comparison of cranial ontogenetic trajectories among great apes and humans. J Hum Evol 46:679–698.

Moss ML. 1958. The pathogenesis of artificial cranial deformation. Am J Phys Anthropol 16:269–286.

Napier JR, Napier PH. 1967. A handbook of living primates: morphology, ecology and behaviour of nonhuman primates. New York: Academic Press.

Neubauer S, Gunz P, Hublin JJ. 2010. Endocranial shape changes during growth in chimpanzees and humans: A morphometric analysis of unique and shared aspects. J Hum Evol 59:555–566.

Novacek MJ. 1977. Aspects of the problem of variation, origin and evolution of the eutherian auditory bulla. Mamm Rev 7:131–149.

Novacek MJ. 1992. Mammalian phytogeny: Shaking the tree. Nature 356:121–125.

Olson EC, Miller RL. 1999. Morphological integration. University of Chicago Press.

Packer DJ, Sarmiento EE. 1984. External and Middle Ear Characteristics of Primates , With Reference to Tarsier-Anthropoid Affinities. Am Museum Novit:1–23.

Pampush JD, Duque AC, Burrows BR, Daegling DJ, Kenney WF, McGraw WS. 2013. Homoplasy and thick enamel in primates. J Hum Evol 64:216–224.

Perelman P, Johnson WE, Roos C, Seuánez HN, Horvath JE, Moreira MAM, Kessing B, Pontius J, Roelke M, Rumpler Y, Schneider MPC, Silva A, O'Brien SJ, Pecon-Slattery J. 2011. A molecular phylogeny of living primates. PLoS Genet 7:1–17.

Perry JMG, Hartstone-Rose A, Logan RL. 2011. The Jaw Adductor Resultant and Estimated Bite Force in Primates. Anat Res Int 2011:1–11.

Phillips-Conroy JE, Jolly CJ. 1988. Dental eruption schedules of wild and captive baboons. Am J Primatol 15:17–29.

Piveteau J. 1957. Traite de Paleontologie, Vol. 7: Primates, Paleontologie Humaine. Paris: Masson.

Preuss TM. 2000. What's human about the human brain. In: Gazzaniga MS, editor. The New Cognitive Neurosciences. Vol. 2. Champaign, IL: Cambridge Massachusetts: MIT Press. p 1219–1234.

R Core Team. 2013. R: A language and environment for statistical computing.

Ramsier M a., Cunningham AJ, Moritz GL, Finneran JJ, Williams C V., Ong PS, Gursky-

Doyen SL, Dominy NJ. 2012a. Primate communication in the pure ultrasound. Biol Lett 8:508–511.

Ramsier MA. 2010. The Evolutionary Ecology of Primate Auditory Sensitivity.

Ramsier MA, Cunningham AJ, Finneran JJ, Dominy NJ. 2012b. Social drive and the evolution of primate hearing. Philos Trans R Soc B Biol Sci 367:1860–1868.

Rasmussen DT. 1986. Anthropoid origins: a possible solution to the Adapidae-Omomyidae paradox. J Hum Evol 15:1–12.

Reinhard R, Rösing FW. 1985. Ein Literaturüberblick über Definitionen diskreter Merkmale/anatomischer Varianten am Schädel de Mensen. Selbstverlag der Autoren.

Rezaian J, Namavar MR., Nasab HV, Nobari ARH., Abedollahi A. 2015. Foramen tympanicum or foramen of huschke: A bioarchaeological study on human skeletons from an iron age cemetery at tabriz kabud mosque zone. Iran J Med Sci 40:367–371.

Richtsmeier JT, Aldridge K, Deleon VB, Kane AA, Marsh JL, Yan P, Theodore M, Iii C. 2009. Phenotypic integration of neurocranium and brain. J Exp Zool B Mol Dev Evol 2006:360–378.

Rilling JK, Insel TR. 1999. The primate neocortex in comparative perspective using magnetic resonance imaging. J Hum Evol 37:191–223.

Rilling JK, Seligman RA. 2002. A quantitative morphometric comparative analysis of the primate temporal lobe. J Hum Evol 42:505–533.

Rodríguez-Vázquez JF, Mérida-Velasco JR, Verdugo-López S, Sánchez-Montesinos I, Mérida-Velasco JA. 2006. Morphogenesis of the second pharyngeal arch cartilage (Reichert's cartilage) in human embryos. J Anat 208:179–189.

Rodriguez-Vazquez JF, Murakami G, Verdugo-Lopez S, Abe S, Fujimiya M. 2011. Closure of the middle ear with special reference to the development of the tegmen tympani of the temporal bone. J Anat 218:690–698.

Rohlf FJ. 1990. Morphometrics. Annu Rev Ecol Syst 21:299–316.

Rohlf FJ, Slice D. 1990. Extensions of the Procrustes method for the optimal superimposition of landmarks. Syst Biol 39:40–59.

Rosenberger AL. 1985. In Favor of the Necrolemur-Tarsier Hypothesis. Folia Primatol 45:179–194.

Rosenberger AL, Szalay FS. 1980. On the tarsiiform origins of Anthropoidea. In: Ciochon RL., Chiarelli AB, editors. Evolutionary biology of the New World monkeys and continental drift. Boston: Springer. p 139–157.

Ross CF. 2000. Into the light: The origin of anthropoidea. Annu Rev Anthropol 29:147–

194.

Ross CF., Ravosa M. 1993. Basicranial flexion , relative brain size , and facial kyphosis in nonhuman primates. Am J Phys Anthr 324:305–324.

Rossie JB, Ni X, Beard KC. 2006. Cranial remains of an Eocene tarsier. Proc Natl Acad Sci U S A 103:4381–4385.

RStudio. 2015. RStudio: Integrated development for R. RStudio, Inc.

Saban R. 1963. Contribution à l'etude de l'os temporal des primates: description chez l'homme et les prosimiens: anatomie comparée et phylogénie. Mem Mus natl Hist nat A:1–378.

Saban R. 1964. Sur la pneumatisation de l'os temporal des primates adultes et son developpement ontogenique chez le genre *Alouatta* (Platyrhinien). Morph Jb 106:569–593.

Sai X, Ladher RK. 2015. Early steps in inner ear development : induction and morphogenesis of the otic placode. 6:1–8.

Scheuer L;, Black SM. 2000. Developmental Juvenile Osteology. San Diego, CA: Elsevier Academic Press.

Seidler H, Falk D, Stringer C, Wilfing H, Müller GB, Zur Nedden D, Weber GW, Reicheis W, Arsuaga JL. 1997. A comparative study of stereolithographically modelled skulls of Petralona and Broken Hill: Implications for future studies of middle Pleistocene hominid evolution. J Hum Evol 33:691–703.

Seiffert ER, Perry JMG, Simons EL, Boyer DM. 2009. Convergent evolution of anthropoid-like adaptations in Eocene adapiform primates. Nature 461:1118.

Seiffert ER, Simons EL, Fleagle JG, Godinot M. 2010. Paleogene anthropoids. Cenozoic Mamm Africa Berkeley Univ Calif Press p:369–391.

Semendeferi K, Damasio H. 2000. The brain and its main anatomical subdivisions in living hominoids using magnetic resonance imaging. J Hum Evol 38:317–332.

Semendeferi K, Damasio H, Frank R, Van Hoesen GW. 1997. The evolution of the frontal lobes: A volumetric analysis based on three-dimensional reconstructions of magnetic resonance scans of human and ape brains. J Hum Evol 32:375–388.

Setchell JM, Wickings EJ. 2004. Sequences and timing of dental eruption in semi-free-ranging mandrills (*Mandrillus sphinx*). Folia Primatol 75:121–132.

Shapiro R, Robinson F. 1981. The embryogenesis of the human skull: an anatomic and radiographic atlas. J Anat 133:103.

Sherwood RJ, Ward SC. 1989. Development of temporal bone pneumatization in the African great apes. Am J Phys Anthropol 78:301.

Shoshani J, Groves CP, Simons EL, Gunnell GF. 1996. Primate phylogeny:

Morphological vs molecular results. Mol Phylogenet Evol 5:102–154.

Simons EL. 1961. Notes on Eocene tarsioids and a revision of some Necrolemurinae. Bull Brit Mus Nat Hist, Geol 5:43–69.

Simons EL. 1972. Primate evolution: an introduction to man's place in nature. Science 177:601–602.

Simons EL. 1974. Notes on early Tertiary prosimians. In: Martin RD, Doyle GA, Walker AC, editors. Prosimian biology. Duckworth, London. p 415–433.

Simons EL, Rasmussen DT. 1989. Cranial morphology of *Aegyptopithecus* and *Tarsius* and the question of the tarsier-anthropoidean clade. Am J Phys Anthropol 79:1–23.

Simons EL, Seiffert ER, Ryan TM, Attia Y. 2007. A remarkable female cranium of the early Oligocene anthropoid *Aegyptopithecus zeuxis* (Catarrhini, Propliopithecidae). Proc Natl Acad Sci U S A 104:8731–8736.

Smith BH. 1991. Age of weaning approximates age of emergence of the first permanent molar in nonhuman primates. Am J Phys Anthr Suppl 12:163–164.

Smith BH, Crummett TL, Brandt KL. 1994. Ages of eruption of primate teeth: A compendium for aging individuals and comparing life histories. Yearb Phys Anthropol 37:177–231.

Smith GE. 1928. Endocranial cast obtained from the Rhodesian skull. In: Pyecraft WP., Smith GE., Yersley M., Carter JT., Smith RA., Hopwood AT., Bate DMA., Swinton WE, editors. Rhodesian Man and Associated Remains. London: British Museum (Natural History).

Smith KK. 1996. Integration of craniofacial structures during development in mammals. Integr Comp Biol 36:70–79.

Smith RJ, Jungers WL. 1997. Body mass in comparative primatology. J Hum Evol 32:523–559.

Smith TD, DeLeon VB, Rosenberger AL. 2013. At birth, tarsiers lack a postorbital bar or septum. Anat Rec 296:365–377.

Sperber GH. 1989. Craniofacial embryology. London: Wright.

Spoor CF. 1993. The human bony labyrinth: a morphometric description. In: The comparative morphology and phylogeny of the human bony labyrinth. Unpublished PhD dissertation.

Spoor F. 1997. Basicranial architecture and relative brain size of Sts 5 (*Australopithecus africanus*) and other Plio-Pleistocene hominids. S Afr J Sci 93:182–186.

Spoor F, O'higgins P, Dean C, Lieberman DE. 1999. Anterior sphenoid in modern humans. Nature 397:572.

Squyres N, DeLeon VB. 2015. Clavicular curvature and locomotion in anthropoid

primates: A 3D geometric morphometric analysis. Am J Phys Anthropol 158:257–268.

Starck D. 1967. Le crane des mammiferes. In: Traite de zoologie V. 16. Paris: Masson. p 405–549.

Stebbins WC. 1975. Hearing of the anthropoid primates: a behavioral analysis. Nerv Syst 3:113–124.

Strait DS. 1999. The scaling of basicranial flexion and length. J Hum Evol 37:701–719.

Szalay F rederick S, Rosenberger AL, Dagosto M. 1987. Diagnosis and differentation of the order primates. Yearb Phys Anthropol 30:75–105.

Szalay FS. 1972. Cranial morphology of the early Tertiary *Phenacolemur* and its bearing on primate phylogeny. Am J Phys Anthropol 36:59–75.

Szalay FS. 1977. Constructing primate phylogenies: A search for testable hypotheses with maximum empirical content. J Hum Evol 6:3–18.

Tallman M, Amenta N, Delson E, Frost SR, Ghosh D, Klukkert ZS, Morrow A, Sawyer GJ. 2014. Evaluation of a new method of fossil retrodeformation by algorithmic symmetrization : Crania of Papionins (Primates, Cercopithecidae) as a test case. PloS one, 9(7), e100833

Taylor AB. 2002. Masticatory form and function in the African apes. Am J Phys Anthropol 117:133–156.

Taylor AB. 2005. A comparative analysis of temporomandibular joint morphology in the African apes. J Hum Evol 48:555–574.

Taylor AB. 2006. Diet and mandibular morphology in African apes. Int J Primatol 27:181–201.

Taylor AB, Vinyard CJ. 2013. The relationships among jaw-muscle fiber architecture, jaw morphology, and feeding behavior in extant apes and modern humans. Am J Phys Anthropol 151:120–134.

Terhune CE. 2009. Scaling relationships in the anthropoid temporomandibular joint. Am J Phys Anthropol 48:254.

Terhune CE, Kimbel WH, Lockwood CA. 2007. Variation and diversity in *Homo erectus*: a 3D geometric morphometric analysis of the temporal bone. J Hum Evol 53:41–60.

Thiele K. 1993. The holy grail of the perfect character: The cladistic treatment of morphometric data. Cladistics 9:275–304.

Turner JS. 1990. The ear and auditory system. In: Walker HK., Hall WD., Hurst JW, editors. Clinical Methods: The History, Physical, and Laboratory Examinations. 3rd ed. Boston: Butterworths. p 609–611.

Vogel ER, van Woerden JT, Lucas PW, Utami Atmoko SS, van Schaik CP, Dominy NJ.

2008. Functional ecology and evolution of hominoid molar enamel thickness: *Pan troglodytes schweinfurthii* and *Pongo pygmaeus wurmbii*. J Hum Evol 55:60–74.

Walker AC, Leakey RE. 1988. The evolution of *Australopithecus boisei*. In: Grine FE, editor. Evolutionary history of the “Robust” Australopithecines. New York: Aldine de Gruyter. p 247–258.

Waller BM, Parr LA, Gothard KM, Burrows AM, Fuglevand AJ. 2008. Mapping the contribution of single muscles to facial movements in the rhesus macaque. Physiol Behav 95:93–100.

Warwick R, Williams PL, Gray H. 1973. Gray’s anatomy. Harlow, UK: Longman.

Weaver DS. 1979. Application of the likelihood ratio test to age estimation using the infant and child temporal bone. Am J Phys Anthropol 50:263–9.

Weidenreich F. 1941. The brain and its role in the phylogenetic transformation of the human skull. Trans Am Philos Soc 31:320–442.

West CD. 1985. The relationship of the spiral turns of the cochlea and the length of the basilar membrane to the range of audible frequencies in ground dwelling mammals. J Acoust Soc Am 77:1091–1101.

Wible JR. 1993. Cranial circulation and relationships of the *Colugo Cynocephalus* (Dermoptera, Mammalia). Am Museum Novit:27.

Wible JR, Martin JR. 1993. Ontogeny of the tympanic floor and roof in archontans. In: Primates and their relatives in phylogenetic perspective. Springer. p 111–148.

Wiley D, Amenta N, Alcantara D, Ghosh D, Kil Y. 2005. Evolutionary Morphing. In: Proceedings of IEEE Visualization Conference. p 1–8.

Wunderly J, Wood-Jones F. 1933. The non-metrical morphological characters of the Tasmanian skull. J Anat 67:583.

Wysocki J. 2002. Morphology of the temporal canal and postglenoid foramen with reference to the size of the jugular foramen in man and selected species of animals. Folia Morphol (Warsz) 61:199–208.

Zalmout IS, Sanders WJ, MacLatchy LM, Gunnell GF, Al-Mufarreh YA, Ali MA, Nasser AAH, Al-Masari AM, Al-Sobhi SA, Nadhra AO, Matari AH, Wilson JA, Gingerich PD. 2010. New Oligocene primate from Saudi Arabia and the divergence of apes and old world monkeys. Nature 466:360–364.

Zapfe H. 1958. The Skeleton of *Pliopithecus (Epipliopithecus*). Am J Phys Anthropol 16:441–457.

Zapfe H. 1960. A new fossil anthropoid from the Miocene of Austria. Curr Anthropol 1:428–429.

Zelditch ML, Swiderski DL, Sheets HD. 2012. Geometric morphometrics for biologists: a

primer. Cambridge, UK: Academic Press.

Zumpano MP, Richtsmeier JT. 2003. Growth-related shape changes in the fetal craniofacial complex of humans (*Homo sapiens*) and pigtailed macaques (*Macaca nemestrina*): A 3D-CT comparative analysis. Am J Phys Anthropol 120:339–351.

Zwislocki JJ. 1965. Analysis of some auditory characteristics. In: Luce R, Bush R, Galanter E, editors. Handbook of Mathematical Psychology. New York: Wiley. p 1–98.

A. Appendix

Table A.1: Macaque CT Scan Parameters

Specimen No.	Species	Sex	Voxel size (mm)
1400	*M. fascicularis*	F	0.21x0.21x0.2
1481	*M. fascicularis*	F	0.23x0.23x0.2
1828	*M. fascicularis*	F	0.22x0.22x0.2
3618	*M. fascicularis*	F	0.21x0.21x0.2
3637	*M. fascicularis*	F	0.20x0.20x0.2
995	*M. fascicularis*	M	0.24x0.24x0.2
3046	*M. fascicularis*	M	0.23x0.23x0.2
4477	*M. fascicularis*	M	0.25x0.25x0.2
4478	*M. fascicularis*	M	0.24x0.24x0.2
5225	*M. fascicularis*	M	0.24x0.24x0.2
6680	*M. fascicularis*	M	0.25x0.25x0.2
02_20	*M. fuscata*	F	0.26x0.26x0.2
03_17	*M. fuscata*	F	0.26x0.26x0.2
03_18	*M. fuscata*	F	0.26x0.26x0.2
03_22	*M. fuscata*	F	0.26x0.26x0.2
04_15	*M. fuscata*	F	0.27x0.27x0.2
04_85	*M. fuscata*	F	0.28x0.28x0.2
04_89	*M. fuscata*	F	0.27x0.27x0.2
05_23	*M. fuscata*	F	0.27x0.27x0.2
06_35	*M. fuscata*	F	0.26x0.26x0.2
5859	*M. fuscata*	F	0.24x0.24x0.2
5867	*M. fuscata*	F	0.25x0.25x0.2
6142	*M. fuscata*	F	0.25x0.25x0.2
6168	*M. fuscata*	F	0.26x0.26x0.2
6242	*M. fuscata*	F	0.24x0.24x0.2
6497	*M. fuscata*	F	0.24x0.24x0.2
6809	*M. fuscata*	F	0.25x0.25x0.2
8896	*M. fuscata*	F	0.23x0.23x0.2
H19_079	*M. fuscata*	F	0.24x0.24x0.2
03_10	*M. fuscata*	M	0.31x0.31x0.2
04_14	*M. fuscata*	M	0.31x0.31x0.2
05_16	*M. fuscata*	M	0.30x0.30x0.2
05_17	*M. fuscata*	M	0.30x0.30x0.2
05_43	*M. fuscata*	M	0.30x0.30x0.2
06_23	*M. fuscata*	M	0.31x0.31x0.2
06_59	*M. fuscata*	M	0.30x0.30x0.2
06_60	*M. fuscata*	M	0.30x0.30x0.2
86_3Y	*M. fuscata*	M	0.25x0.25x0.2
5866	*M. fuscata*	M	0.27x0.27x0.2

5868	*M. fuscata*	M	0.29x0.29x0.2
6162	*M. fuscata*	M	0.30x0.30x0.2
6470	*M. fuscata*	M	0.28x0.28x0.2
6474	*M. fuscata*	M	0.27x0.27x0.2
6498	*M. fuscata*	M	0.26x0.26x0.2
6503	*M. fuscata*	M	0.27x0.27x0.2
6504	*M. fuscata*	M	0.26x0.26x0.2
6833	*M. fuscata*	M	0.27x0.27x0.2
H20_117	*M. fuscata*	M	0.29x0.29x0.2
H22_170	*M. fuscata*	M	0.27x0.27x0.2
H23_077	*M. fuscata*	M	0.28x0.28x0.2
1478	*M. mulatta*	F	0.23x0.23x0.2
2205	*M. mulatta*	F	0.26x0.26x0.2
2504	*M. mulatta*	F	0.24x0.24x0.2
2751	*M. mulatta*	F	0.23x0.23x0.2
3027	*M. mulatta*	F	0.25x0.25x0.2
Mm1701	*M. mulatta*	F	0.23x0.23x0.2
218	*M. mulatta*	M	0.25x0.25x0.2
223	*M. mulatta*	M	0.27x0.27x0.2
224	*M. mulatta*	M	0.27x0.27x0.2
580	*M. mulatta*	M	0.27x0.27x0.2
2200	*M. mulatta*	M	0.24x0.24x0.2
3523	*M. mulatta*	M	0.27x0.27x0.2
4408	*M. mulatta*	M	0.27x0.27x0.2
Mm1715	*M. mulatta*	M	0.25x0.25x0.2
2847	*M. nemestrina*	F	0.27x0.27x0.2
3054	*M. nemestrina*	F	0.16x0.16x0.2
3647	*M. nemestrina*	F	0.18x0.18x0.2
3650	*M. nemestrina*	F	0.30x0.30x0.2
1104	*M. nemestrina*	M	0.26x0.26x0.2
2454	*M. nemestrina*	M	0.20x0.20x0.20
1849	*M. nemestrina*	M	0.32x0.32x0.2
2110	*M. nemestrina*	M	0.30x0.30x0.2
2299	*M. nemestrina*	M	0.35x0.35x0.2
4225	*M. nemestrina*	M	0.32x0.32x0.2

Table A.2: Morton Sample Ancestries and Sexes as noted in the ORSA Database

Collection ID	Sex	Continent	Notes on Ancestry
674	?	Arctic	Greenland
1198	?	Africa	Egypt
422	F	Africa	Native American?
100	F	South America	Peru
241	F	Australia	African?
98	F	North America	White
90	F	South America	Peru
74	F	North America	White
423	F	Africa	Mozambique
646	F	Africa	Liberia
818	F	Africa	Egypt
902	F	Africa	Native American
900	F	North America	Black
914	F	Africa	Native African
913	F	Africa	Native African
1204	F	Africa	Egypt
1249	F	Europe	Sweden
1002	F	Central America	Mexico
1332	F	Asia	India
24	F	North America	US White
1064	F	Europe	German White
41	F	Asia	Malaysia
668	F	Asia	Japan
673	F	Asia	Japan
547	F	Asia	India
1247	F	Europe	Sweden
1107	F	Africa	South Africa
910	F	Africa	Native African
1190	F	Europe	German White
14	F	North America	White
407	F	North America	Native American
1907	F	Central America	Panama
1532	F	Europe	Sweden
1544	F	Europe	Sweden
0411 0430	M	Asia	Malaysia
424	M	Asia	Malaysia
426	M	Asia	China
94	M	Asia	China
58	M	Europe	German White
67	M	South America	Peru
20	M	Asia	India
647	M	Africa	Liberia
645	M	Africa	Liberia
546	M	Asia	Malaysia
901	M	Africa	Native American
917	M	Africa	Native African
912	M	Africa	Native African
808	M	Africa	Egypt
820	M	Africa	Egypt
1307	M	Africa	Madagascar
1306	M	Africa	Madagascar
1289	M	Australian	Native New Holland
1100	M	Africa	North African
1261	M	Australian	Native New Holland
926	M	Africa	Native African
1336	M	Asia	China
764	M	Africa	Egypt

1537	M	Europe	Finland
240	M	Australian	Native Australian
413	M	Asia	India
49	M	Asia	India
45	M	North America	White US
57	M	Europe	Ireland
3	M	Asia	China
543	M	Asia	Malaysia
1191	M	Europe	Germany
761	M	Africa	Egypt
1327	M	Australia	Native Australian
434	M	Europe	Netherlands
2006	M	North America	Black
1195	M	Africa	Egypt
421	M	Africa	West Africa
1187	M	Europe	Germany
59	M	Europe	Scotland
1973	M	North America	Black
2144	M	Asia	India
1527	M	Asia	Vietnam
1541	M	Europe	Finland
1545	M	Europe	Finland
1546	M	Europe	Finland

Table A.3: Correlations of macaque ectotympanic length with measures of cranial base width.

Correlations

		Ectotympanic (mm)	IAM-IAM (mm)	EAM-EAM (mm)
Ectotympanic (mm)	Pearson Correlation	1	.40**	0.82**
	Sig. (2-tailed)		0.00	0.00
	N	74	73	73
IAM-IAM (mm)	Pearson Correlation	0.40**	1	0.77**
	Sig. (2-tailed)	0.00		0.00
	N	73	73	73
EAM-EAM (mm)	Pearson Correlation	0.82**	0.77**	1
	Sig. (2-tailed)	0.00	0.00	
	N	73	73	73

**. Correlation is significant at the 0.01 level (2-tailed).

Table A.4: Correlations of human ectotympanic length with measures of cranial width

Correlations

		Ectotympanic (mm)	EAM-EAM (mm)	IAM-IAM (mm)	Euryon-Euryon (mm)
Ectotympanic (mm)	Pearson Correlation	1	0.75**	0.15	0.35**
	Sig. (2-tailed)		0.00	0.21	0.003
	N	71	71	71	71
EAM-EAM (mm)	Pearson Correlation	0.75**	1	0.61**	0.66**
	Sig. (2-tailed)	0.00		0.00	0.00
	N	71	71	71	71
IAM-IAM (mm)	Pearson Correlation	0.15	0.61**	1	0.62**
	Sig. (2-tailed)	0.21	0.00		0.00
	N	71	71	71	71
Euryon-Euryon (mm)	Pearson Correlation	0.35**	0.66**	0.62**	1
	Sig. (2-tailed)	.003	0.00	0.00	
	N	71	71	71	71

**. Correlation is significant at the 0.01 level (2-tailed).

Ellen Elise Irwin Fricano

1830 E Monument St., Suite 307A, Center for Functional Anatomy and Evolution, Johns Hopkins University, Baltimore, MD, 21224, P: 650-380-4956, E: efricano@jhmi.edu

EDUCATION

Ph.D. Candidate Functional Anatomy and Evolution	2018	Johns Hopkins University
M.S. Biological & Forensic Anthropology	2013	Mercyhurst University
B.A. Anthropology	2010	University of Illinois at Urbana Champaign

OTHER EXPERIENCE

Mercyhurst University	Forensic Anthropologist 1, level 2: assist with forensic recoveries and skeletal analysis, and graduate assistant for the Department of Applied Forensic Sciences	2012
	Forensic anthropologist 1, level 1: assisted with forensic recoveries and skeletal analysis.	2011
Ohio State University	Research Assistant to Dr. Samuel Stout, Department of Anthropology.	2010
University of Illinois	Research Assistant to Dr. Charles Roseman and Dr. John Polk, Department of Anthropology.	
	Senior capstone project completed with Dr. Laura Shackleford, Department of Anthropology. Title: "Analysis of Trauma of Human Bones based on Robusticity: Preservation of Neanderthal versus Human Remains."	2009
Illinois Transportation Archaeological Research Program	Archaeological field and lab technician.	2008

RECENT GRANTS AND HONORS

The Research Triangle Nanotechnology Network Kickstarter Grant 2017

PUBLICATIONS

Journal articles

Fricano EEI, Perry JMG. *In Press.* Maximum Bony Gape among Primates. Anatomical Record.

Conference presentations

Fricano EEI, DeLeon VB. 2017. Growth of the Catarrhine Ectotympanic Tube. Am J Phys Anthropol Am J Phys Anthropol 162 Suppl (S64): 1–423.

Fricano EE, DeLeon VB. 2016. Scaling of the Ectotympanic Tube and Tympanic Membrane Diameter among Catarrhine Primates. The FASEB Journal, 30(1 Supplement): 779-4.

Powell EEI, Perry JMG. 2015. Functional Implications of Maximum Bony Gape in Non-Human Primates 156 (S60): 65–334.

Powell EEI, Roth MH, Garvin HM. 2013. Environmental Plasticity of Intralimb Indices. Am J Phys Anthropol 150 (S56): 9–52.

Powell EEI, Ousley SD, Tuamsuk, P. 2013. Sex Estimation in a Modern Thai Sample using Nonmetric Traits of the Innominate. Proc Am Acad Foren Sci 19: 1-608.

TEACHING EXPERIENCE

Johns Hopkins University	Human Anatomy, School of Medicine, substitute and grader	2017
	Human Anatomy, School of Medicine, substitute and grader	2016
	Physical Medicine and Rehabilitation, Prosector	
	Human Origins (290), Teaching Assistant	
	Human Anatomy, School of Medicine, Instructor	2015
	Introduction to the Human Body, Teaching Assistant	
	Introduction to the Human Skeleton (365), Teaching Assistant	
	Human Anatomy, School of Medicine, Prosector	2014
	Introduction to the Human Body, Teaching Assistant	
	Human Gross Anatomy (375), Teaching Assistant	
Duke University TIP	Introduction to Anthropology, Instructor	2013

Mercyhurst University	Modification of the Human Skeleton, Guest/Substitute Lecturer	
	Human Osteology and Lab (326/327), Teaching assistant	2012
	Forensic Archaeology and Lab (510/511), Teaching Assistant	
	Skeletal Biology and Lab (333/334), Teaching Assistant	
	Paleoanthropology (270), Teaching Assistant	

GUEST LECTURES

Diversity of Living Anthropoids	Johns Hopkins University	2016
Dental Anatomy as Applied to Osteology	Johns Hopkins University	2015
Anatomy of the Ear and Larynx	Johns Hopkins University	2014
Assorted lectures and labs in “Modification of the Human Skeleton”	Mercyhurst University	2013

PROFESSIONAL SERVICE

AAPA Student Liaison to the Executive Committee	2017-2018
AAPA Committee on Diversity Mentor	2014-2018
Graduate Student Association, Johns Hopkins University	2015-2016